Superconducting RF Cavity Basics

Rongli Geng

USPAS Course:

SRF Technology: Practices and Hands-On Measurements

January 2015

Suggested Literatures

- H.Padamsee, J. Knobloch, T. Hays
  " RF Superconductivity for Accelerators", John Wiley&Sons, Inc; ISBN 0-471-15432-6

- Proceedings of the Workshops on RF Superconductivity 1981 – 2014
  - Available online from www.jacow.org up to 2013

- A.W.Chao, M. Tigner
  "Handbook of Accelerator Physics and Engineering", World Scientific PublishingCo, P.O.Box 128, Farrer Road, Singapore, ISBN 9810235003

Outline

- General introduction and fundamentals
  - Timeline leading to SRF based accelerators
  - Cavity fundamentals
  - Losses in normal conductor and superconductor
  - Critical field
- Limit to SRF cavity performance
  - Gradient limit
  - Q_0 limit
  - Gradient progress and SRF based accelerators
- SRF cavity fabrication and processing

General Introduction and Fundamentals

Milestones that led to accelerators based on SRF

Superconductivity

<u>1908:</u> Heike Kamerlingh Onnes (Holland)
Liquefied Helium for the first time.

<u>1911:</u> Heike Kamerlingh Onnes
Discovered Superconductivity.

<u>1928-34:</u> Walther Meissner (Germany)
Discovered Superconductivity of Ta, V, Ti and Nb.

RF Acceleration

<u>1924:</u> Gustaf Ising (Sweden)
The First Publication on RF Acceleration
Arkiv för Matematik, Astronomi och Fysik.

<u>1928:</u> Rolf Wideröe (Norway, Germany)
Built the first RF Accelerator,
Arch. für Elektrotechnik 21, vol.18.

<u>1947:</u> Luis Alvarez (USA)
Built first DTL (32 MeV protons).

<u>1947:</u> W. Hansen (USA)
Built first 6 MeV e-accelerator, Mark I
(TW- structure).

1961: W. Fairbank (Stanford Univ.)

Presented the first proposal for a superconducting accelerator for electrons

A. Banford and G. Stafford (Rutherford Appleton Lab.)

Presented the first proposal for a superconducting accelerator for protons

1964: W. Fairbank, A. Schwettman, P. Wilson (Stanford Univ.)

First acceleration of electrons with sc lead cavity

1970: J. Turneaure (Stanford Univ.)

E_{peak} =70 MV/m and Q~10^{10} in 8.5 GHz cavity !

1968-1981: M. McAshan, A. Schwettman, T. Smith, J. Turneaure, P. Wilson (Stanford Univ.)

Developed and Constructed the Superconducting Accelerator SCA

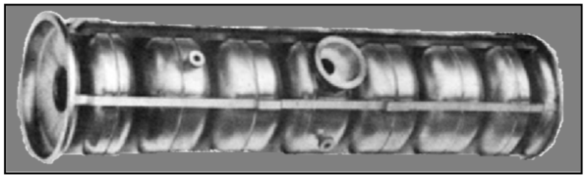

Since then, many sc accelerators were built and we are constructing and making plans for many new facilities.

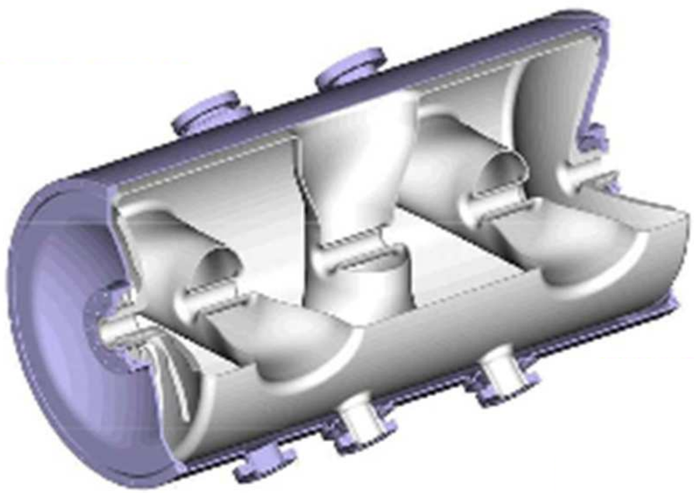

RF Resonator/Cavity

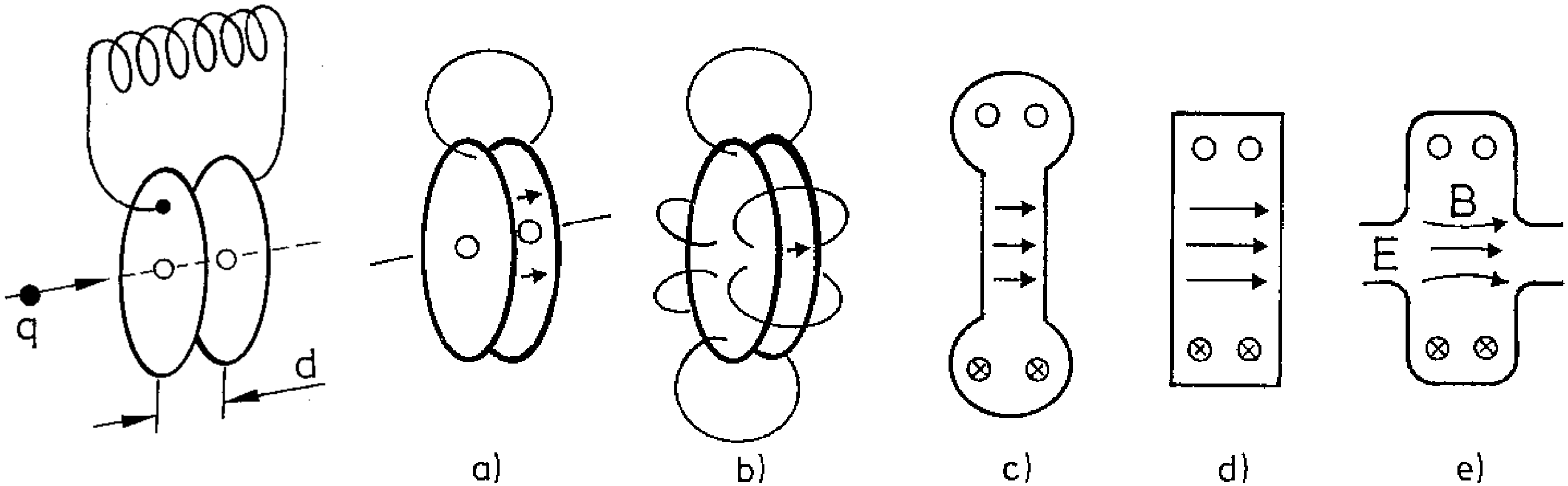

$$\nu_0 = \frac{1}{2\pi\sqrt{LC}}$$

"Pillbox cavity"
$\nu_0 = 2.405\, c\, /(2*\pi*radius)$

Cavity Modes

- **Fields in the cavity are solutions to the wave equation**

$$\left(\nabla^2 - \frac{1}{c^2}\frac{\partial^2}{\partial t^2}\right)\begin{Bmatrix}\mathbf{E}\\ \mathbf{H}\end{Bmatrix} = 0$$

- **Subject to the boundary conditions**

$$\hat{n}\times\mathbf{E} = 0, \quad \hat{n}\cdot\mathbf{H} = 0$$

- **Solutions are two families of modes with different eigenfrequencies**
  - TE modes have only transverse electric fields
  - TM modes have only transverse magnetic fields (but longitudinal component for **E**)
- **TM modes are needed for acceleration. Choose the one with the lowest frequency (TM_{010})**
- **For pillbox (no beam tubes) solution is:**

$$E_z = E_0 J_0\left(\frac{2.405\rho}{R}\right) e^{-i\omega t}$$

$$H_\phi = -i\frac{E_0}{\eta} J_1\left(\frac{2.405\rho}{R}\right) e^{-i\omega t}$$

$$\omega_{010} = \frac{2.405c}{R} \qquad \eta = \sqrt{\frac{\mu_0}{\epsilon_0}}$$

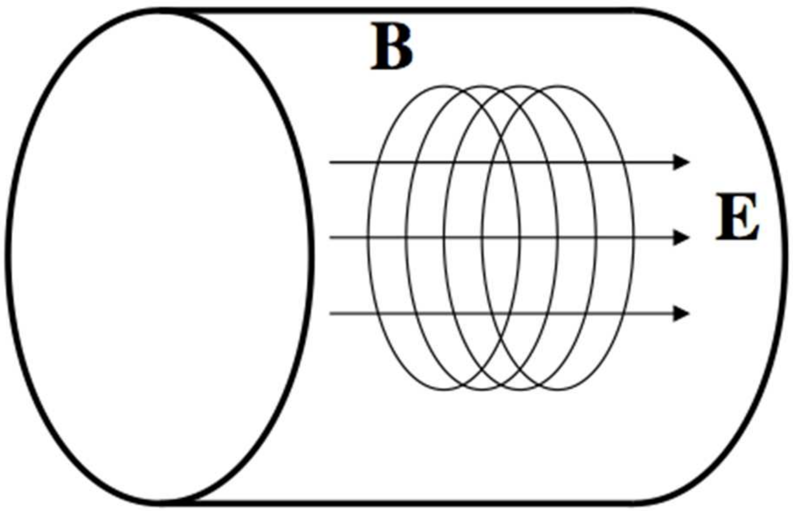

- **Note that the frequency scales inversely with the linear dimension of the cavity (call this „*a*")**

Cavity Fundamentals

- **Optimizing Cavity Length**

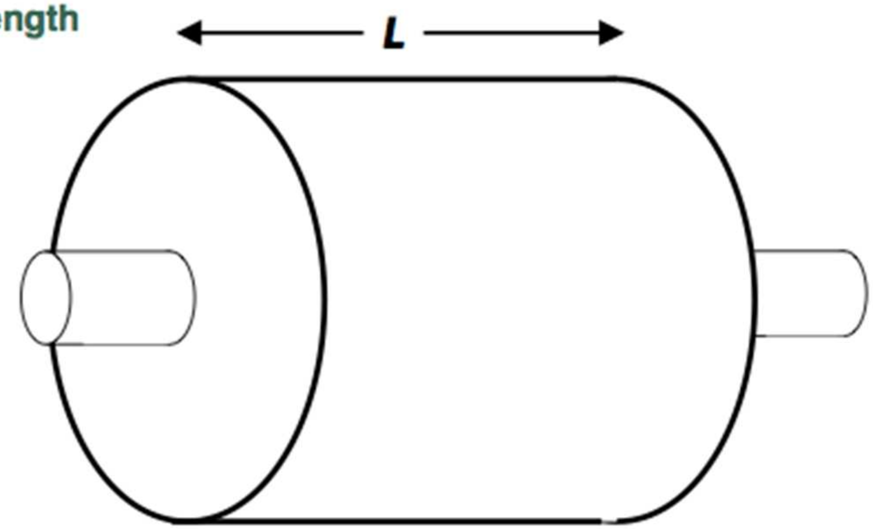

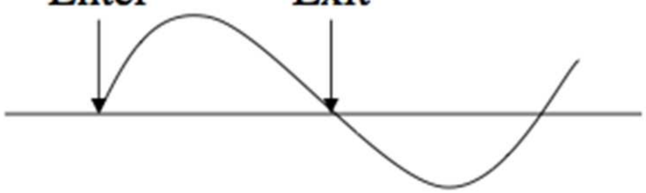

$$T_{\text{transit}} = \frac{L_{\text{acc}}}{\beta c} = \frac{T_{RF}}{2} \quad \Rightarrow L_{\text{acc}} = \frac{\beta c T_{RF}}{2}$$

E.g.: For 1.5 GHz cavity and speed of light electrons (ß = 1), L_{acc} = 10 cm

Accelerating Voltage/Field (β=1)

- How much energy gain can we expect?
- Integrate the E-field at the particle position as it traverses the cavity:

$$V_c = \left| \int_0^d E_z(\rho = 0, z) e^{i\omega_0 z/c} dz \right|$$ (assume speed of light electrons)

$$L_{acc} = \frac{cT_{RF}}{2}$$

- For the pillbox cavity this is $V_c = E_0 \left| \int_0^L \exp\left(\frac{i\omega_0 z}{c}\right) dz \right| = LE_0 \frac{\sin\left(\frac{\omega_0 L}{2c}\right)}{\frac{\omega_0 L}{2c}} = \frac{2}{\pi} E_0 L$

- We can define the accelerating field as $E_{acc} = \frac{V_c}{L} = \frac{2}{\pi} E_0$

Active acceleration gap = half wavelength

Transit time factor

Accelerating Voltage/Field(β<1)

Energy gain: $$\Delta W_p = q\int_{-L/2}^{L/2} E_z(z_p,t)dz_p$$

In a resonator $E_z(r,z,t)=E_z(r,z)\cos(\omega t+\varphi)$. (For simplicity, we assume to be on axis so that $r=0$, and $E_z(0,z) \equiv E_z(z)$).

A particle with velocity βc, which crosses $z=0$ when $t=0$, sees a field $E_z(z)\cos(\omega z/\beta c+\varphi)$.

Transit time factor: $$T(\beta) = \frac{\int_{-L/2}^{L/2} E_z(z)\cos\left(\frac{\omega z}{\beta c}\right)dz}{\int_{-L/2}^{L/2} E_z(z)dz}$$

Avg. accelerating field: $$E_a = \frac{1}{L}\int_{-L/2}^{L/2} E_z(z)dz$$

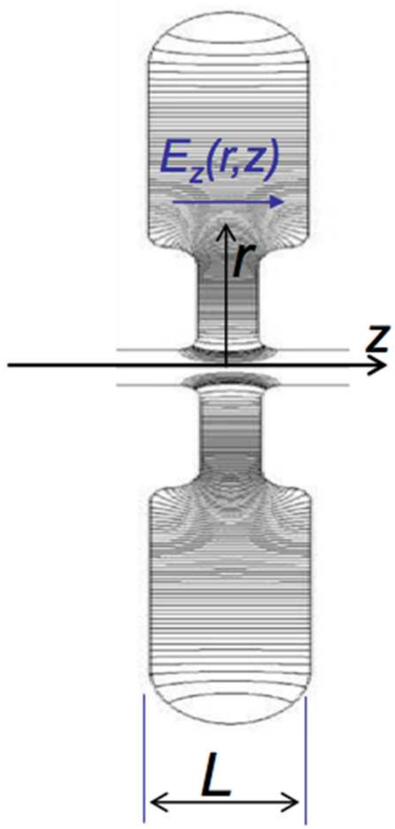

We obtain a simple espression for the energy gain

$$\Delta W_p = qE_a LT(\beta)\cos\varphi$$

Note: choice of active acceleration gap may vary

Peak Surface Electric Field

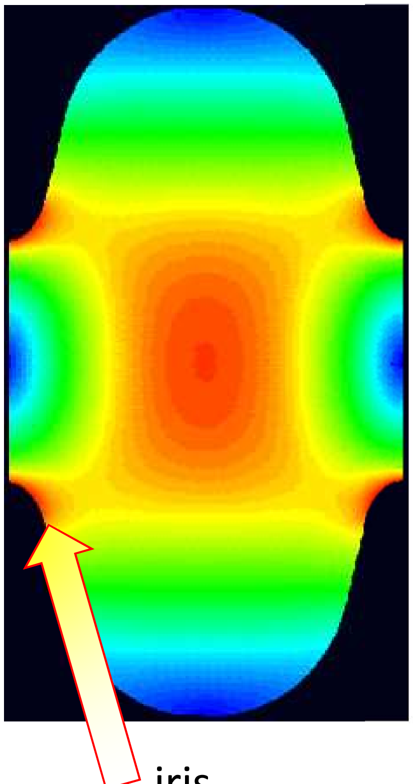

Elliptical cavity
TM-class
Epk/Eacc ~ 2

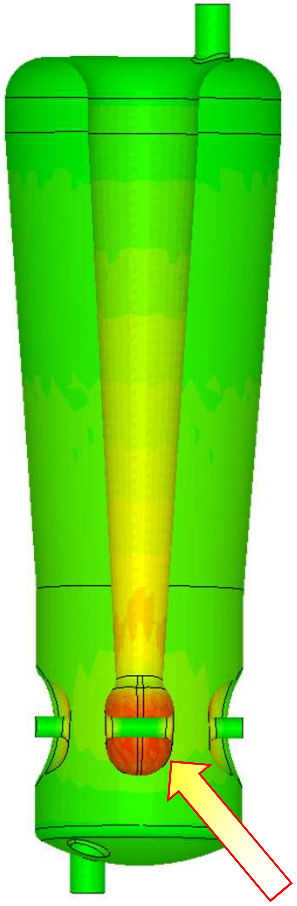

Half-Wave Cavity, TEM class
Epk/Eacc ~ 3-6

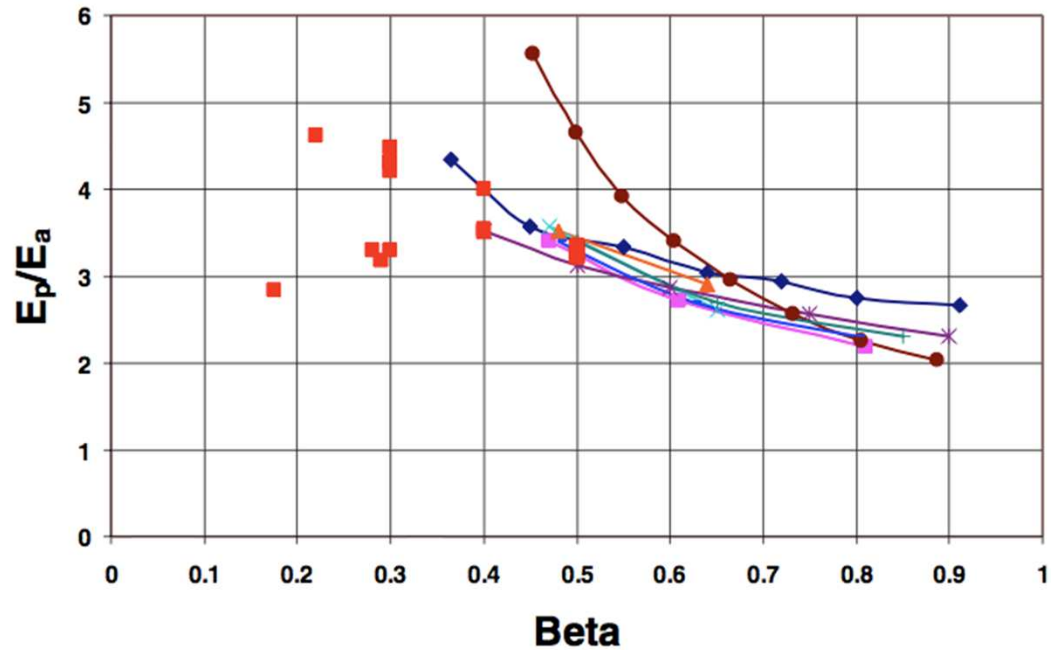

Figure 11: Ratio of peak surface to accelerating field. Data points joined by lines are for TM structures, isolated points (red squares) are for $\lambda/2$ structures.

Peak Surface Magnetic Field

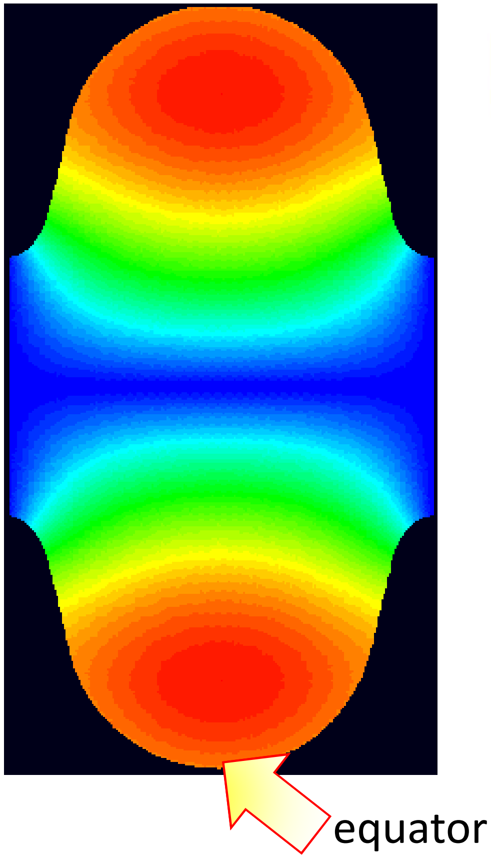

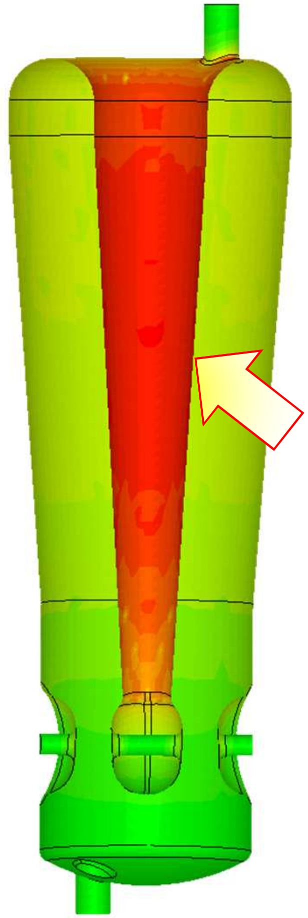

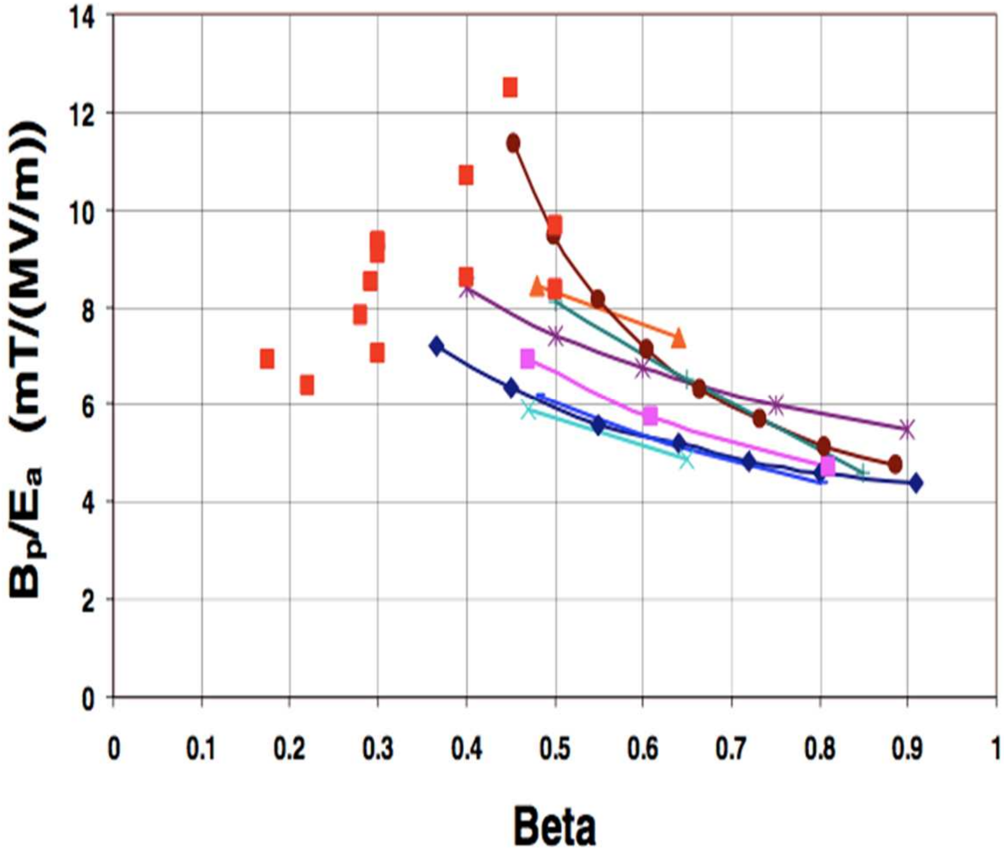

Elliptical cavity
TM-class
Bpk/Eacc ~ 4 mT/(MV/m)

Half-Wave Cavity, TEM class
Bpk/Eacc ~ 6-12 mT/(MV/m)

Figure of Merit

Surface current ($\propto$ H) results in power dissipation proportional to the surface resistance (R_s)

$$\frac{\mathrm{dP_c}}{\mathrm{ds}} = \frac{1}{2} R_s |H|^2$$

Total power dissipation in cavity wall $P_c = \frac{1}{2} \int_S R_s |\mathbf{H}|^2 \, \mathrm{d}s$

Stored energy in cavity $U = \frac{1}{2} \mu_0 \int_V |\mathbf{H}|^2 \, \mathrm{d}v$

Cavity quality factor $Q_0 = \frac{\omega_0 U}{P_c} = \frac{\omega_0 \mu_0}{R_s} \frac{\int_V |\mathbf{H}|^2 \, \mathrm{d}v}{\int_S |\mathbf{H}|^2 \, \mathrm{d}v}$

= 10^4 for n.c.
= 10^{10} for s.c.

Measure of how lossy the cavity material is

Figure of Merit

$$Q_0 = \frac{\omega_0 U}{P_c} = \frac{\omega_0 \mu_0}{R_s} \frac{\int_V |\mathbf{H}|^2 \, \mathrm{d}v}{\int_S |\mathbf{H}|^2 \, \mathrm{d}v} = \frac{G}{R_s}$$

$$G = \omega_0 \mu_0 \frac{\int_V |\mathbf{H}|^2 \, \mathrm{d}v}{\int_S |\mathbf{H}|^2 \, \mathrm{d}v}$$

G is independent of size and material of cavity

G is only dependent of cavity shape ➔ Geometry factor

For pill-box cavity, G = 257 Ω

Figure of Merit

Shunt impedance $$R_a = \frac{V_c^2}{P_c}$$ → To get maximum acceleration, maximize shunt impedance

Measure of how much acceleration one gets for a given power dissipation

$$\frac{R_a}{Q_0} = \frac{V_c^2}{\omega_0 U}$$

independent of size and material of cavity
only dependent of cavity shape

For pill-box cavity, $\frac{R_a}{Q_0} = 196\ \Omega$

Figure of Merit

Accelerator operation requirement

Cavity material

$$P_c = \frac{V_c^{\,2}}{R_a} = \frac{V_c^{\,2}}{\frac{R_a}{Q_0}\cdot Q_0} = \frac{V_c^{\,2}}{\frac{R_a}{Q_0}\cdot G}\cdot R_s$$

Cavity geometry

For copper cavities, power dissipation is a constraint, cavity design is driven by this fact

For SRF cavities, power dissipation is minimal,
This enables cavity design for specific applications

Features of SRF Cavity

- Low power dissipation
  - allows high gradient in CW or long-pulsed operation
    - Less number of cells
      - Less disruption to beam
    - Shorter linac and tunnel length
      - Cost saving
  - allows cavity design with large beam tube
    - Many benefits (next slide)

Features of SRF Cavity

Large beam tube & Fewer cells

- Reduces the interaction of the beam with the cavity (scales as size^3) →
- The beam quality is better preserved (important for, e.g., FELs).
- HOMs are removed easily → better beam stability → more current accelerated (important for, e.g., B-factories)
- Reduce the amount of beam scraping → less activation in, e.g., proton machines (important for, e.g., SNS, Neutrino factory)

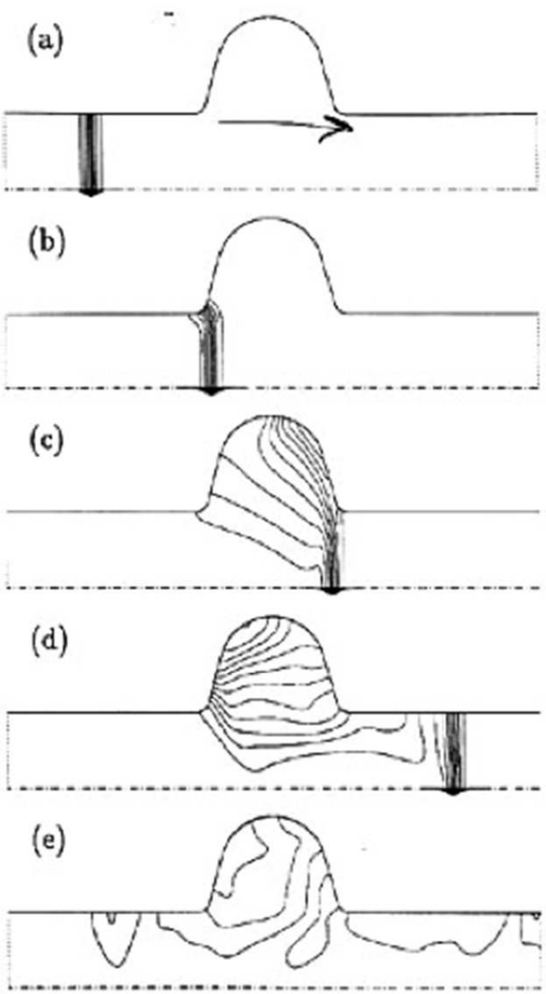

Large aperture of SRF cavity relaxes wakefields

RF Losses in Normal Conductor

- For simplicity, use nearly-free electron model
- Losses given by Ohm's law $j = \sigma E = \frac{n_e e^2 \tau}{m_e} E$
  - τ is scattering time
  - Electron gains energy between scattering $\Delta v = \frac{-eE\tau}{m_e}$
- In a cavity, RF magnetic field drives an oscillating current in cavity wall
  - From Maxwell equation

$$\nabla \times B = \mu j + \mu\varepsilon \frac{\partial E}{\partial t} \qquad \nabla \times E = -\frac{\partial B}{\partial t}$$

RF Losses in Normal Conductor

- Combine three equations and note the harmonic time dependence $e^{i\omega t}$

$$\nabla \times \mathrm{B} = \mu j + \mu\varepsilon \frac{\partial \mathrm{E}}{\partial t} \qquad j = \sigma \mathrm{E} \qquad \nabla \times \mathrm{E} = -\frac{\partial \mathrm{B}}{\partial t}$$

$$-\nabla^2 \mathrm{B} = \mu\sigma\nabla \times \mathrm{E} - \mu\varepsilon \frac{\partial^2 \mathrm{B}}{\partial t^2} = -\mu\sigma \frac{\partial \mathrm{B}}{\partial t} - \mu\varepsilon \frac{\partial^2 \mathrm{B}}{\partial t^2} = -i\mu\sigma\omega \mathrm{B} + \cancel{\mu\varepsilon\omega^2}\mathrm{B}$$

cavity at RF frequency $\sigma >> \varepsilon\omega$

RF Losses in Normal Conductor

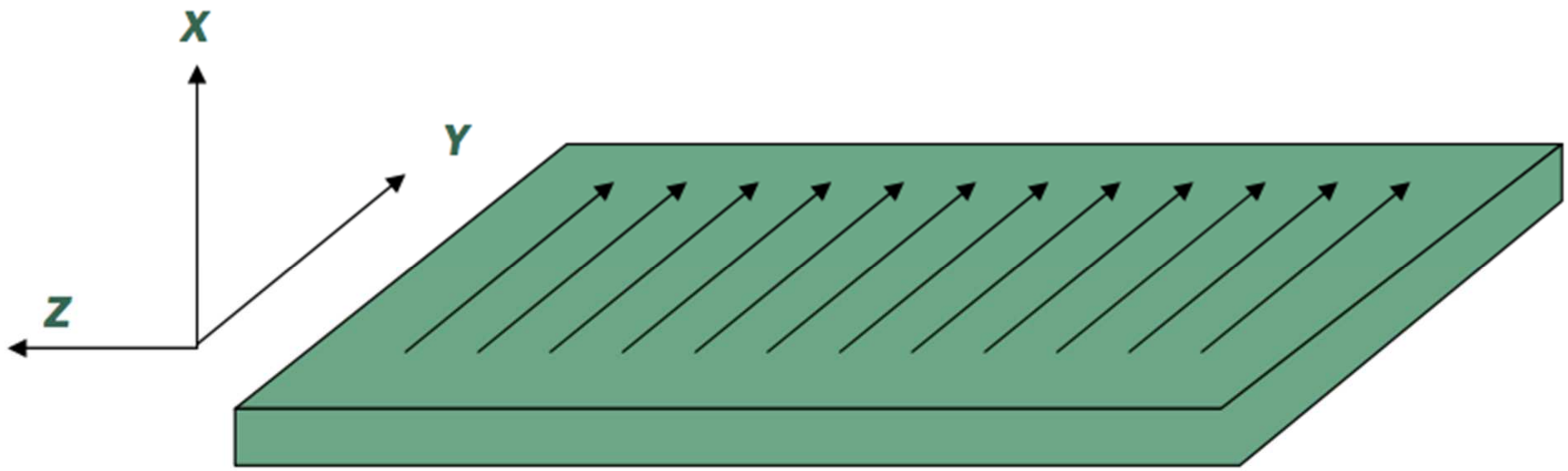

Now solve an one dimensional problem at surface of a conductor
A uniform magnetic field in y direction

$$\nabla^2 \mathrm{B} - i\mu\sigma\omega \mathrm{B} = 0 \quad \rightarrow \quad H_y = H_0 e^{-\frac{1+i}{\delta}x}$$

The field decays into the conductor over skin depth

$$\delta = \frac{1}{\sqrt{\pi f \mu \sigma}}$$

RF Losses in Normal Conductor

From Maxwell $E_z = -\frac{1+i}{\sigma\delta} H_y$

A small tangential electric field exists and decays into the conductor

Power loss per unit area

$$P'_{loss} = \frac{1}{2}\int_0^{\infty} j_z^* \mathrm{E}_z dx = \frac{1}{2}\int_0^{\infty} \sigma |\mathrm{E}_z|^2 dx = \frac{1}{2\sigma\delta} H_0^2 = \frac{1}{2} R_s H_0^2$$

Surface resistance $\boxed{R_s = \frac{1}{\sigma\delta} = \sqrt{\frac{\pi f \mu}{\sigma}}}$

Copper σ = 5.8×10^7 A/Vm, μ_0 = 1.26×10^{-6} Vs/Am
at 1.3 GHz, δ = 1.8 μm, R_s = 9 mΩ, Q_0 = 2.9×10^4 for pill box cavity

Homework: skin depth, surface resistance for cooper at 650 MHz

RF Losses in Normal Conductor

Surface impedance $$Z_s = \frac{E_z}{H_y} = \frac{1+i}{\sigma\delta} = (1+i)\sqrt{\frac{\pi f \mu}{\sigma}} = \sqrt{\frac{\omega\mu}{\sigma}} e^{i\frac{\pi}{4}}$$

Surface resistance is just the real part of the surface impedance

An Intuitive Model of Surface Resistance

Consider a square sheet of metal and calculate its resistance to a transverse current flow:

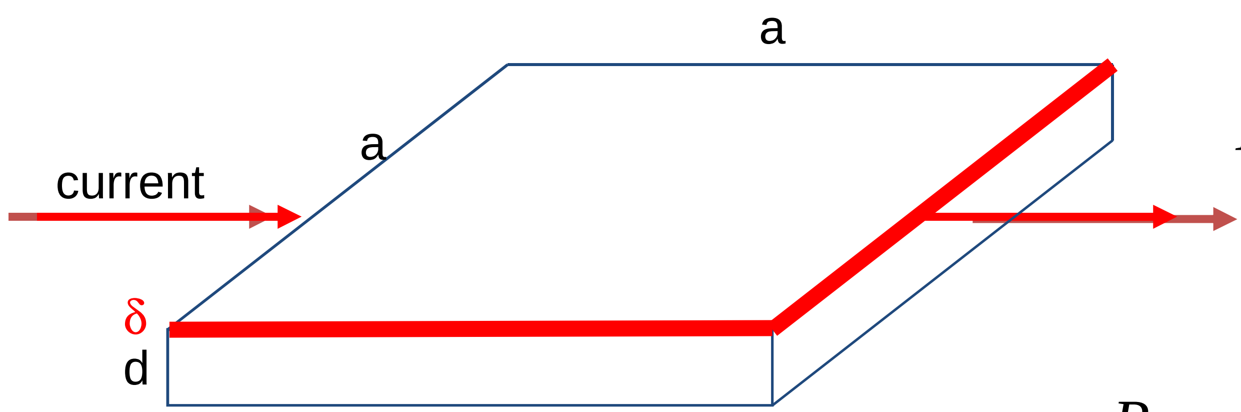

$$R = \frac{\rho \cancel{a}}{d\,\cancel{a}} = \frac{\rho}{d}$$

$$R_s = \sqrt{\frac{\mu_0 \omega}{2\sigma}} = \frac{1}{\sigma\delta} = \frac{\rho}{\delta}$$

The surface resistance R_s is the resistance that a square piece of conductor opposes to the flow of the currents induced by the RF wave, within a layer δ

Superconductivity – Zero DC Resistance

Heike Kammerlingh-Onnes, 1911, discovery of SC in mercury

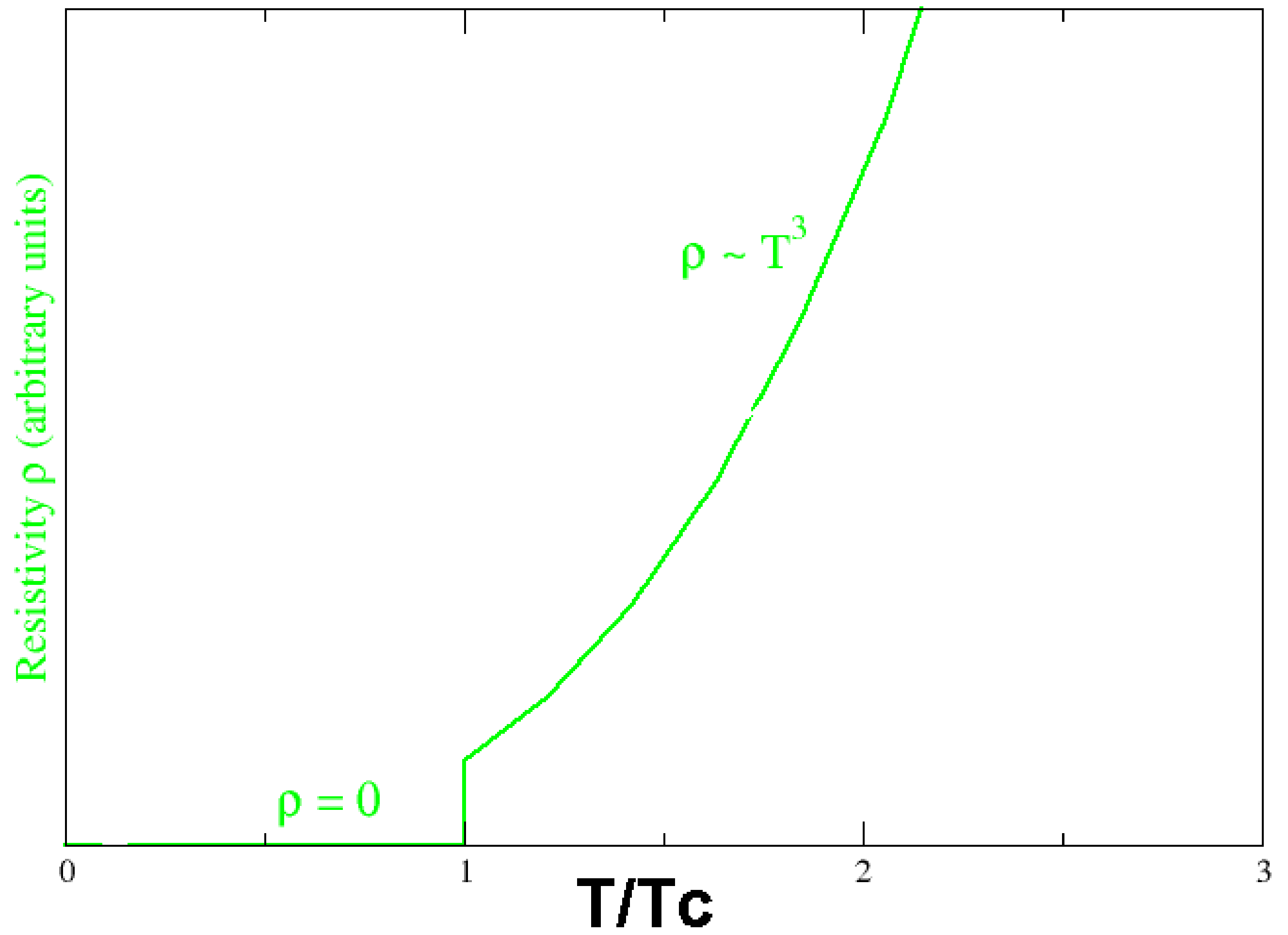

Superconductivity – Meissner Effect

Magnetic field is expelled from a superconductor

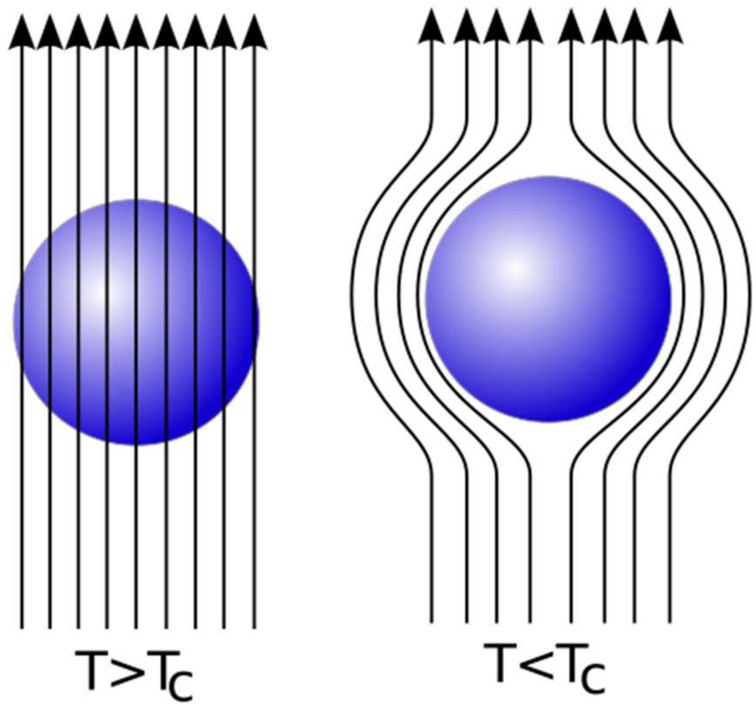

Complete magnetic shielding by circulating surface supercurrents

Energy Gap and Two-Fluid Model

Energy Gap

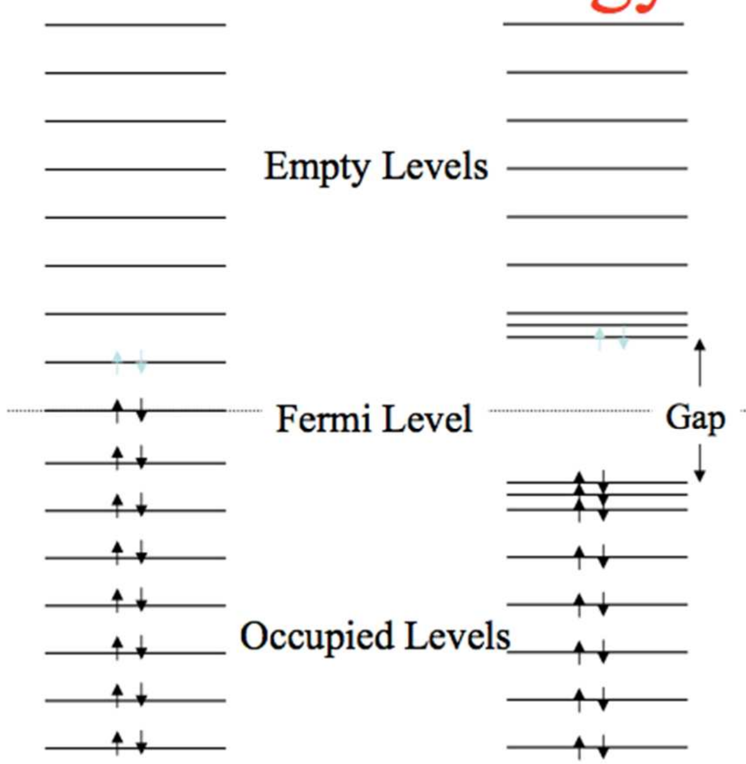

Normal conductor

Superconductor
(electrons condense into Cooper pairs)

At $T > 0$K, some "normal" electrons not yet condensed into pairs

$$\boxed{n_{\text{normal}} \propto \exp\left(-\frac{\Delta}{k_B T}\right)}$$

13

- Two fluid model
  - SC electrons
    - Cooper pairs
    - Below Tc, Cooper pairs are formed with an energy gap 2Δ
  - Normal electrons
- DC case
  - Cooper pairs short out field
  - Normal electrons not accelerated
  - SC is Lossless even at T > 0 K

Losses in Superconductor

- Now look at the RF case
- Cooper pairs have inertia
  - They can not follow the AC field instantly
    - Thus do not shield AC field perfectly
    - A residual field remains
    - The normal electrons are accelerated
      - Thus dissipate power
- Scaling of RF surface resistance
  - The faster the field oscillates the less perfect the shielding
    - RF surface resistance increases with frequency
  - The more normal electrons, the lossier the material
    - RF surface resistance deceases with temperature below Tc

London Penetration Depth

For "superconducting " electrons, there is no scattering $j_s = -n_s ev$

$$m_e \frac{\partial v}{\partial t} = -e\mathrm{E} \quad \Rightarrow \quad \frac{\partial j_s}{\partial t} = \frac{n_s e^2}{m_e}\mathrm{E}$$

First London equation

Note the harmonic time dependence $e^{i\omega t}$ $\quad j_s = -i\frac{n_s e^2}{m_e \omega}\mathrm{E}$

or $j_s = \frac{-i}{\omega \mu_0 \lambda_L^2}\mathrm{E}$ $\qquad \sigma_s = \frac{n_s e^2}{m_e \omega}$ acts as AC conductivity of SC fluid

where $\lambda_L = \sqrt{\frac{m_e}{\mu_0 n_s e^2}}$ is the London penetration depth

Losses in Superconductor

Add currents due to two fluids to get total current $j = j_n + j_s = (\sigma_n - i\sigma_s)\mathrm{E}$

The treatment of a superconductor is the same as before,

Just replace σ_n with $\sigma_n - i\sigma_s$

Surface impedance $\sqrt{\frac{\omega\mu}{\sigma}e^{i\frac{\pi}{4}}} \Rightarrow \sqrt{\frac{\omega\mu}{\sigma_n - i\sigma_s}e^{i\frac{\pi}{4}}}$

Penetration depth $\delta = \frac{1}{\sqrt{\pi f\mu\sigma}} \Rightarrow \delta = \frac{1}{\sqrt{\pi f\mu(\sigma_n - i\sigma_s)}}$

note $H_y = H_0 e^{-\frac{1+i}{\delta}x}$ $\quad \sigma_n = \frac{n_n e^2\tau}{m_e} \quad \sigma_s = \frac{n_s e^2}{m_e\omega}$

Losses in Superconductor

Note 1/ω is of order 100 ps, whereas for normal electrons τ is of order few 10 fs

Also $n_s >> n_n$ for $T << T_c$, therefore $\sigma_s >> \sigma_n$

As a result one finds $\delta \approx (1+i)\lambda_L(1 - i\frac{\sigma_n}{2\sigma_s})$

$$H_y = H_0 e^{-\frac{x}{\lambda_L}} e^{-ix\frac{\sigma_n}{2\sigma_s\lambda_L}}$$

The magnetic field decays rapidly over the London penetration depth

Surface Impedance of Superconductor

Surface impedance $$Z_s \approx \sqrt{\frac{\omega\mu}{\sigma_s}}\left(i + \frac{\sigma_n}{2\sigma_s}\right) = R_s + iX_s$$

Surface resistance $$R_s = \frac{1}{2}\sigma_n \omega^2 \mu_0^2 \lambda_L^3$$

Niobium λ_L=36 nm

For comparison, for copper the skin depth is 1.8 μm at 1.3 GHz

The field penetrates over a much shorter distance than for a normal conductor

Temperature Scaling of Surface Resistance

$$R_s = \frac{1}{2}\sigma_n \omega^2 \mu_0^2 \lambda_L^3$$

- The surface resistance is proportional to the conductivity of the normal fluid!
  - Explanation: for residual field not shielded by cooper pairs, more normal current flow, more dissipation $P_{diss} \propto \sigma_n \mathrm{E}^2$
- Below T_c, electrons condense into cooper pairs
  - For the normal fluid $n_n \propto e^{-\frac{\Delta}{k_B T}} \approx e^{-\frac{1.86 T_c}{T}}$
  - Conductivity $\sigma_n \propto l e^{-\frac{1.86 T_c}{T}}$
    - Mean free path of normal electron: l
- Hence superconductor surface resistance $R_s \propto \omega^2 \lambda_L^3 l e^{-\frac{1.86 T_c}{T}}$

Losses in Superconductor

$$R_s \propto \omega^2 \lambda_L^3 l e^{-\frac{1.86 T_c}{T}}$$

- Increases quadratically with frequency
  – Use lower frequency
- Decreases exponentially with temperature
  – Work at temperature well below T_c
- Increases with increasing material purity
  – Use lower purity material

Impact of Purity to R_s of Superconductor

$$R_s \propto \omega^2 \lambda_L^3 l e^{-\frac{1.86 T_c}{T}}$$

- Surface resistance decreases as the mean free path decreases (less pure)
- This is only valid as long as the coherence length is much less than the mean free path $\xi_0 << l$
- Otherwise the first London equation breaks down
- In this case λ_L must be replaced by $\Lambda_L = \lambda_L \sqrt{1 + \frac{\xi_0}{l}}$
- And thus the surface resistance increases with $l \leq \xi_0 = 64\, nm$

Losses in Superconductor

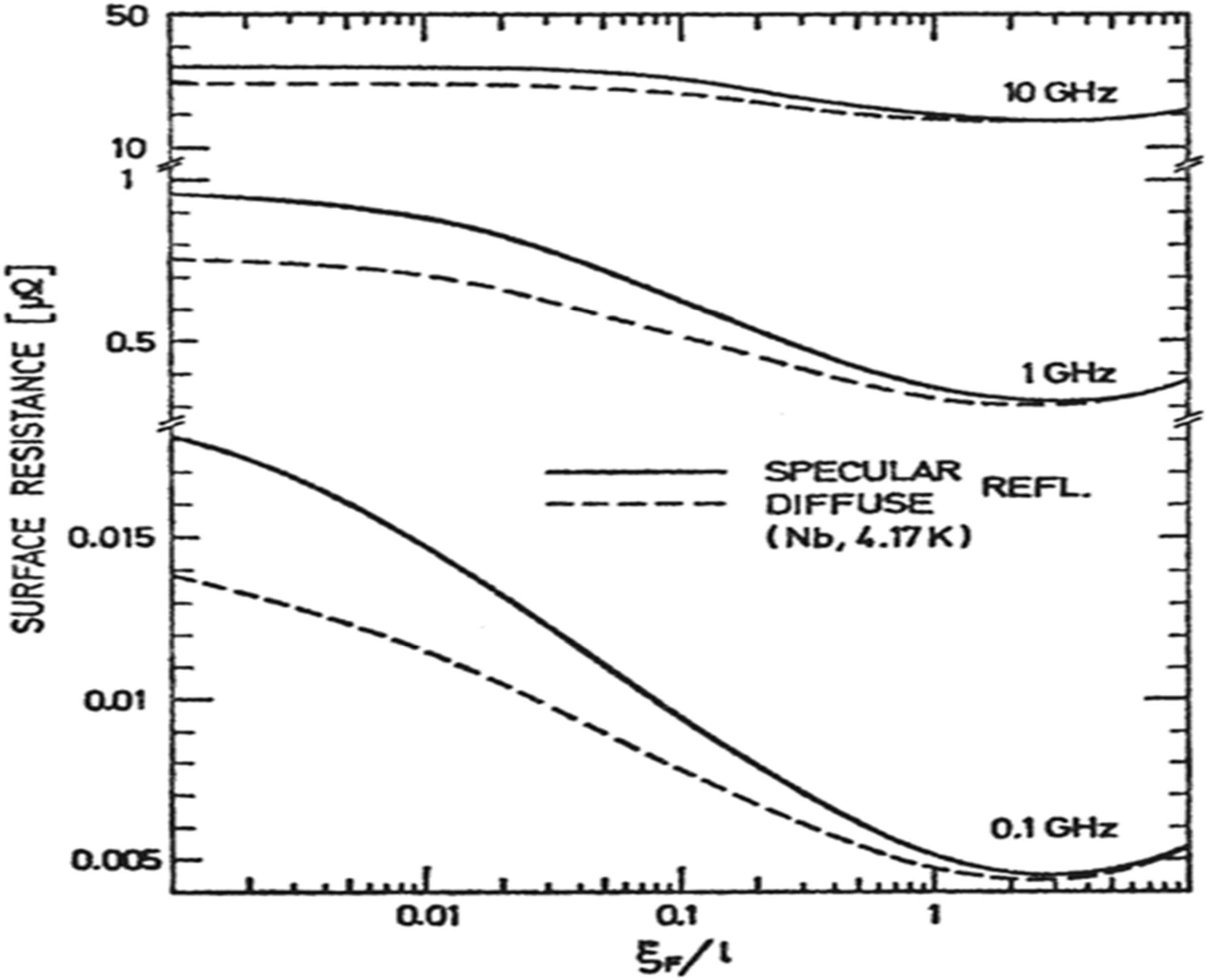

Halbritter's theoretical predictions

Losses in Superconductor

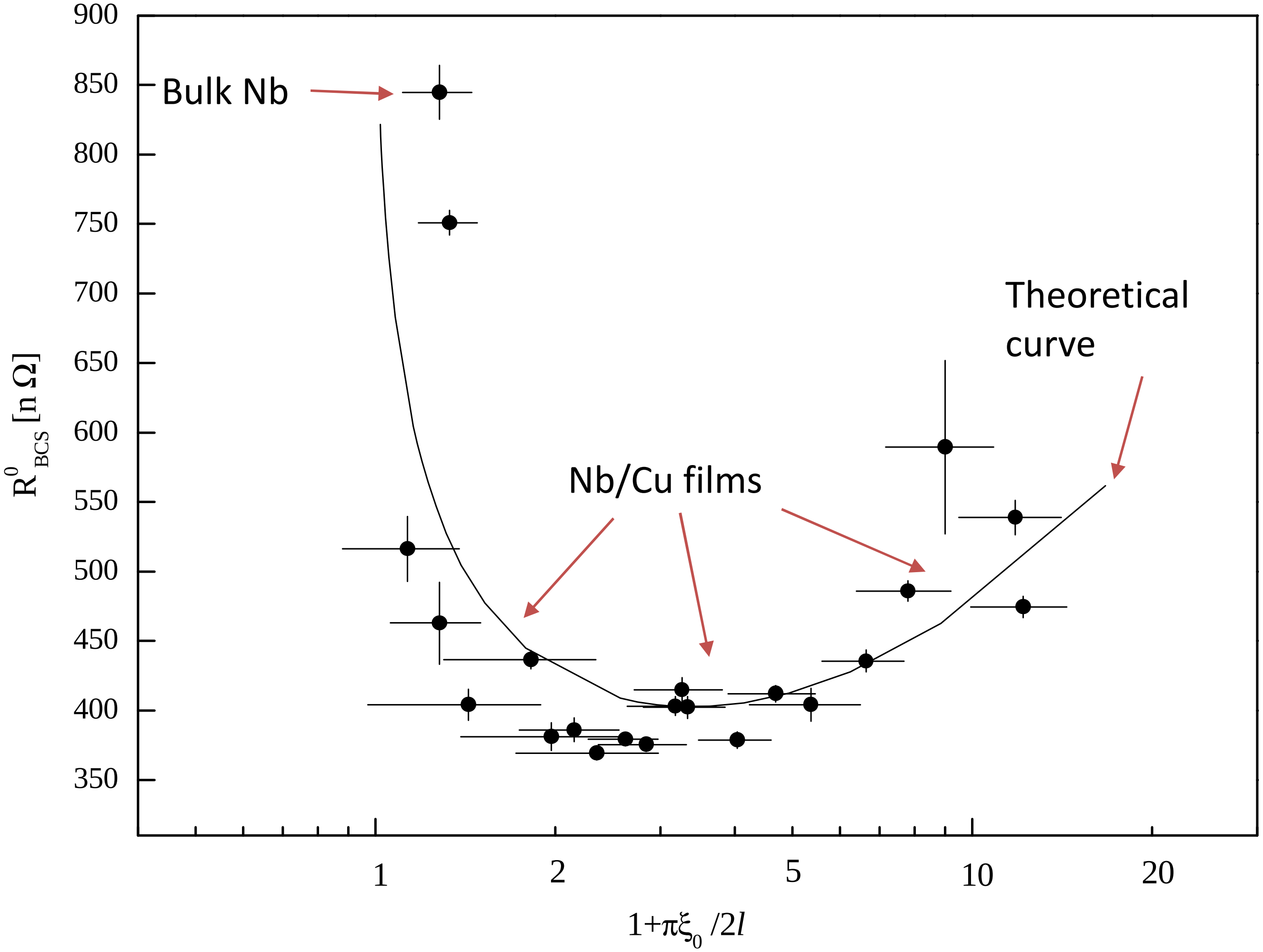

Compilation of results from several Nb/Cu and Nb bulk 1.5 GHz RF cavities

C. Benvenuti et. al, Physica C 316 (1999)

Losses in Superconductor

- Mattis and Bardeen developed theory based on BCS Mattis & Bardeen, Phys. Rev. 111 (1958) 412
- An approximate expression for Niobium

$$R_{BCS} = 3 \times 10^{-4}\,\Omega\left(\frac{f}{1500\,MHz}\right)^2\left(\frac{1}{T}\right)e^{-\frac{17.67}{T}}$$

- A program written by J. Halbritter to calculate surface resistance under wide range of conditions
- Note: calculations only for $H_{RF} << H_c$

Losses in Superconductor: measurements

Exponential drop

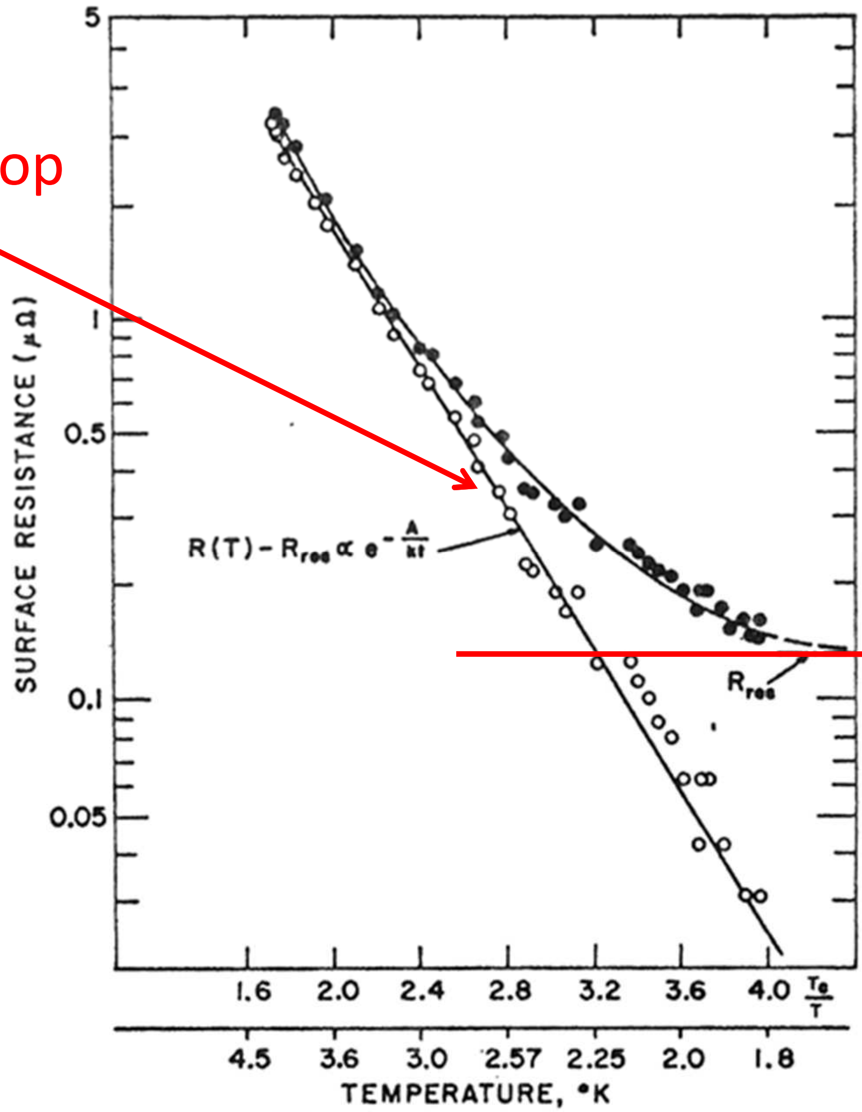

Limited by a temperature term: residual resistance

Type-I and Type-II Superconductor

- Two types of superconductors defined by Ginsburg-Landau

$$\kappa = \lambda(T) / \xi(T)$$

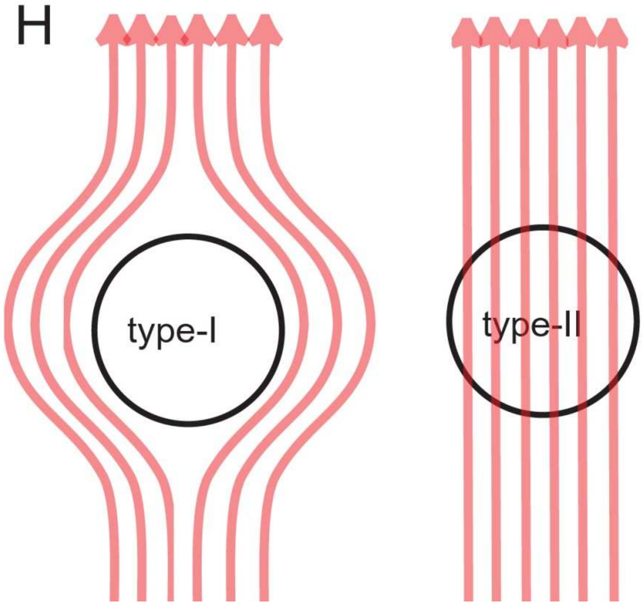

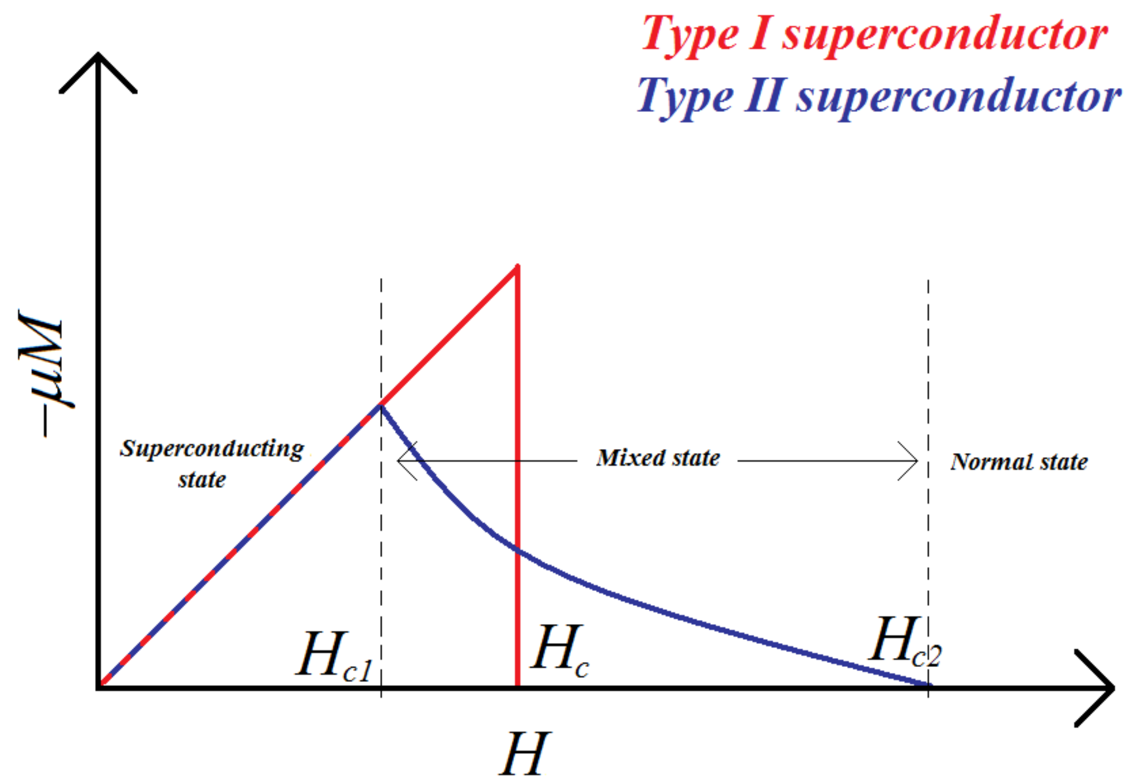

- κ<1/√2 and κ>1/√2

Flux Penetration and Flux Quanta

Magnetic flux penetrates type-II superconductor in the form of flux quanta, fluxons

$$\boxed{\Phi_0 = \frac{h}{2e}}$$

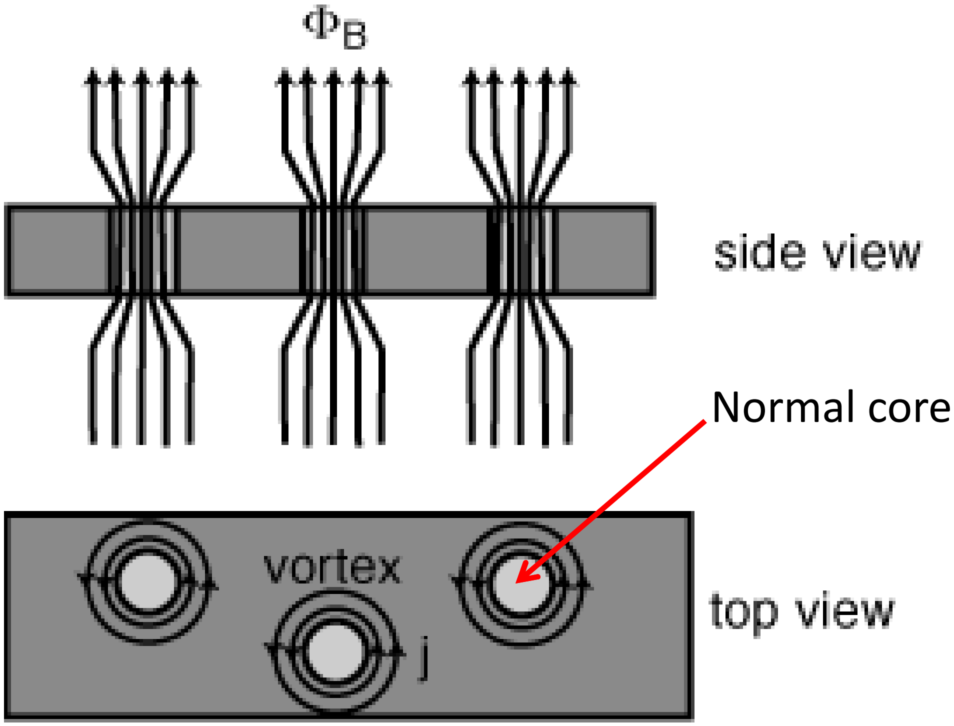

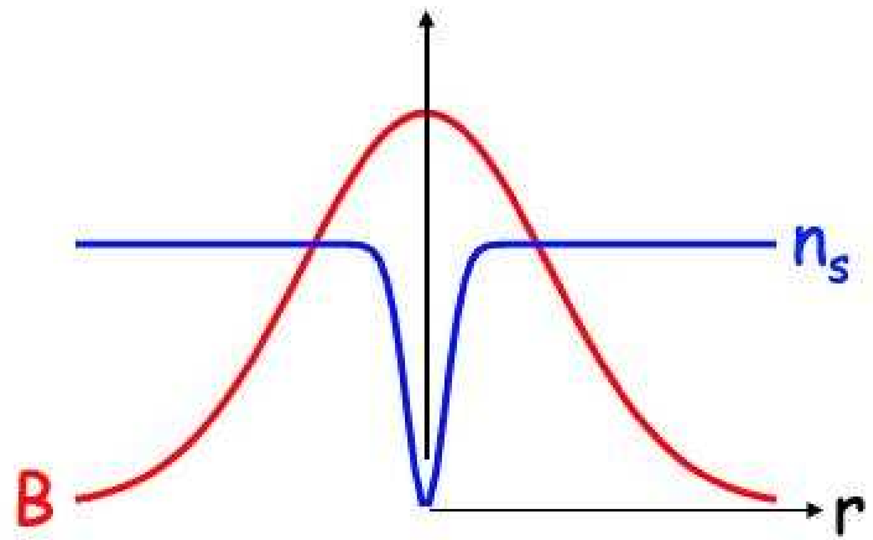

DC and RF Critical Field of Superconductor

Superheating field H_{sh}

due to surface barrier

to vertex penetration

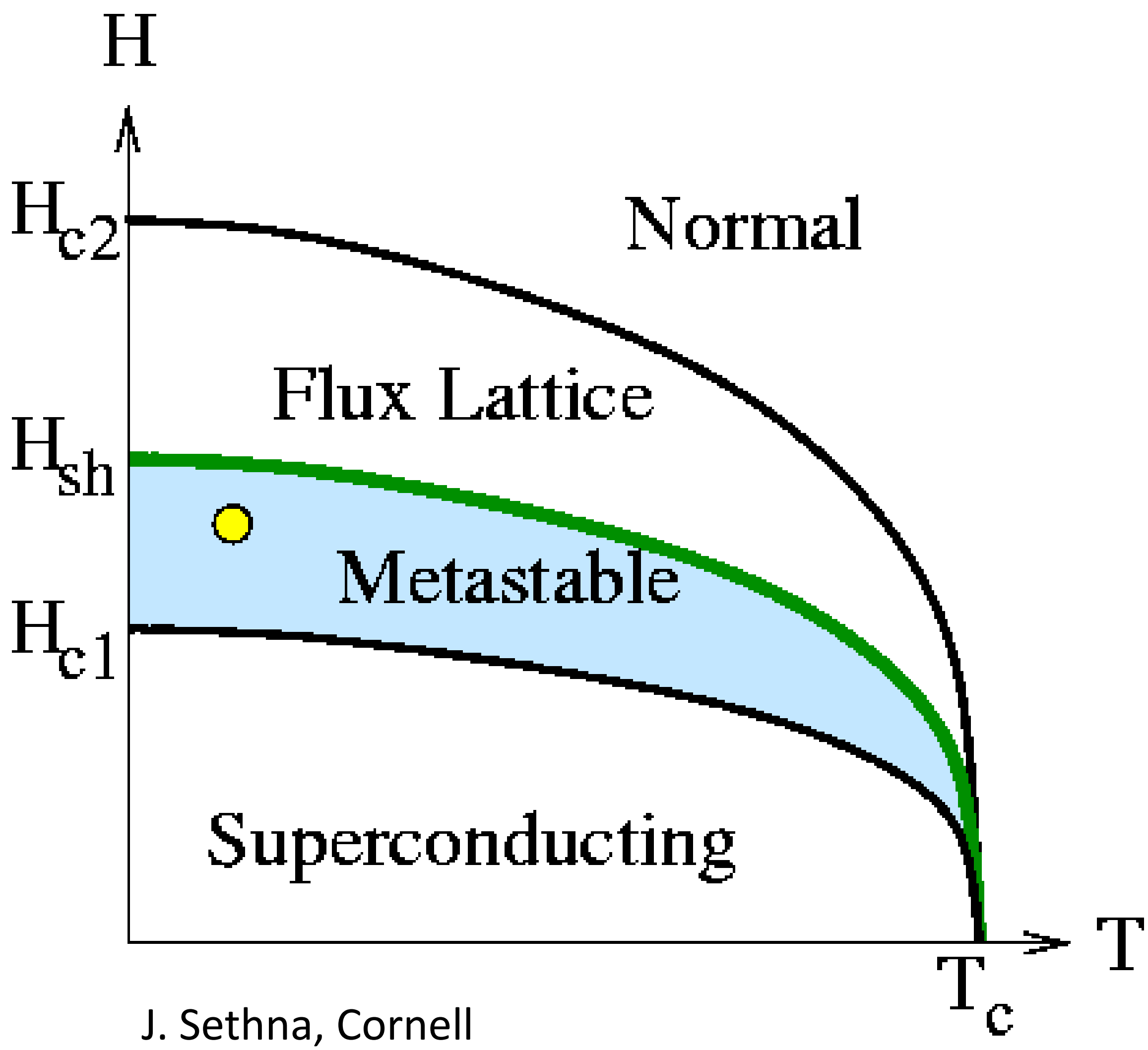

J. Sethna, Cornell

Superheating Field of niobium

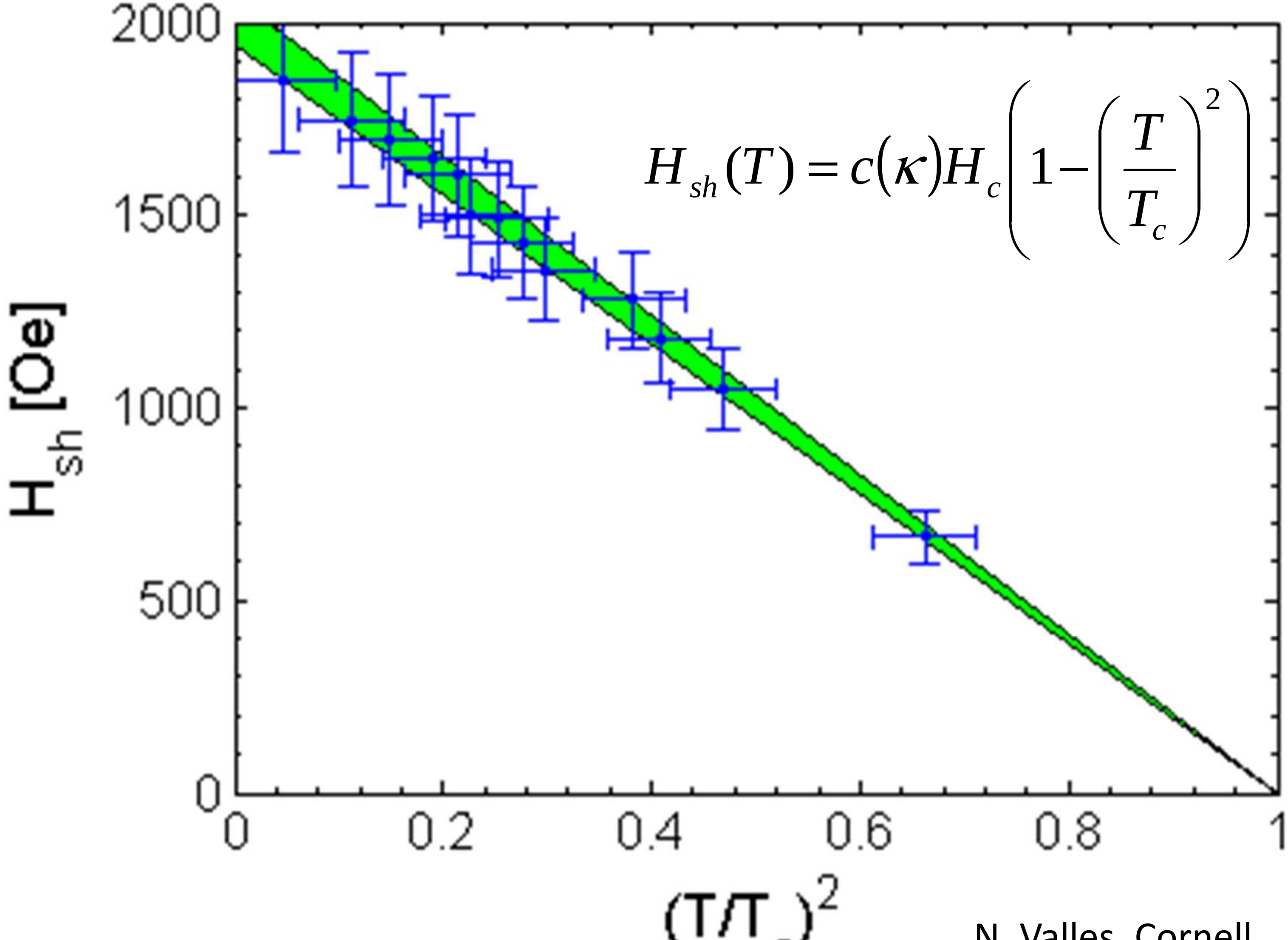

N. Valles, Cornell

Limit to SRF Cavity Performance

Ideal vs Real Performance

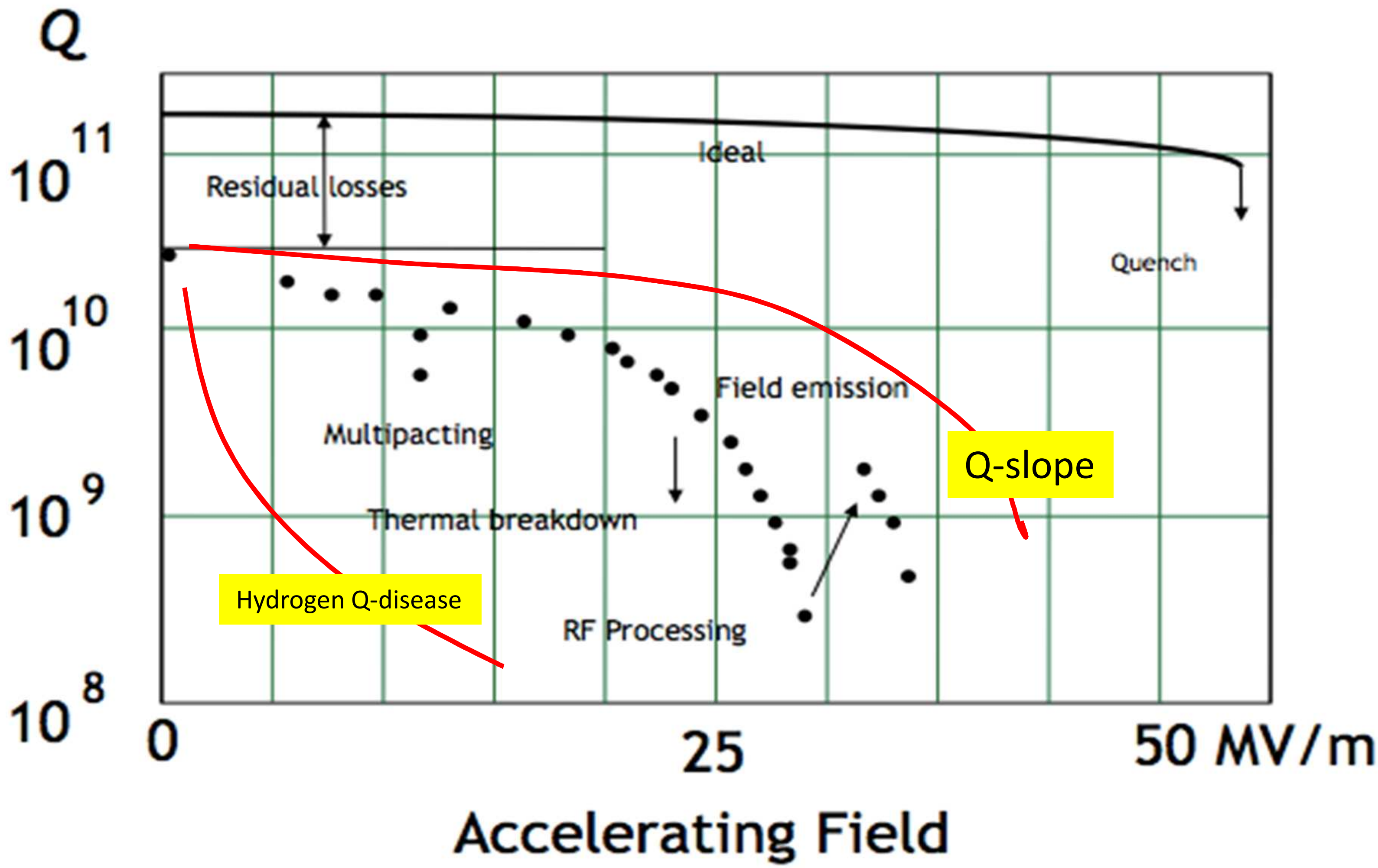

General Approach

- Symptom and Diagnostics
- Physics and Understanding
- Solutions for overcoming limits

Field Emission

Symptom of Field Emission

- Detection of ionization radiation at cavity or remote to cavity, such as above top plate of test stand
  - Mostly X-rays
  - Sometimes neutron also for high gradient cavities
- Detection of free electrons intercepted by biased probes or Faraday cup placed inside cavity
  - On order of > μA
- Excitation of pass-band modes, or 3rd harmonic

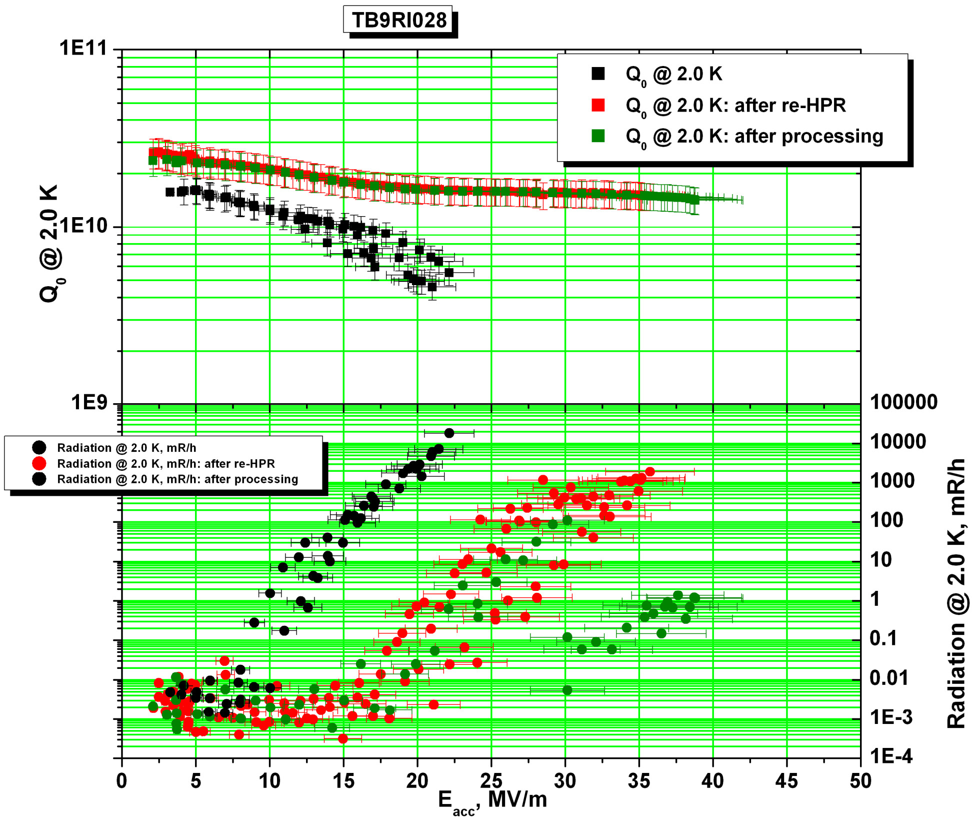

Field Emission Diagnostic

Commonly Used Radiation Detectors

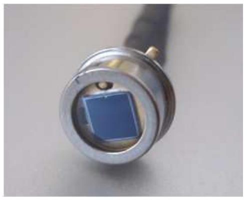

Diode for X-ray

Can be used in liquid Helium near cavity

Ion chamber probe
For X—ray

Typically used outside dewar

Neutron probe
For thermal and fast neutron

Symptom of Field Emission

- Rapid decline of Q_0 value
  - When FE is severe
  - Sometimes Q_0 decline not so obvious
- Sudden quench of RF field
  - Hence gradient limit
  - Not all quench is caused by FE (more later)

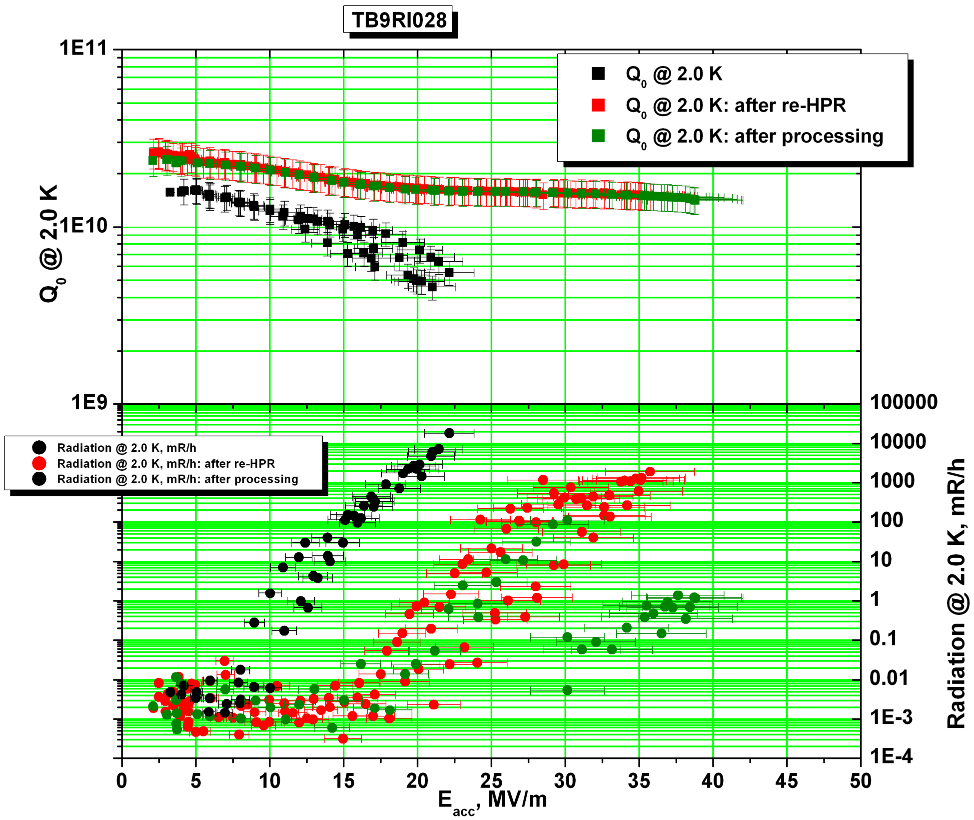

Symptom of Field Emission

- Rapid Q_0 decline followed by sudden Q_0 jumps with accompanied drop in radiation
  - This is a "processing event" (more later)

- Sudden Q_0 (and gradient) degradation with accompanied sudden increase in radiation
  - This is a "field emission turn on" event (more later)

Physics of Field Emission

- Electron emission from site of “field emitter”
- Emitted electrons captured and accelerated by RF field
- Energetic electrons strike cavity wall

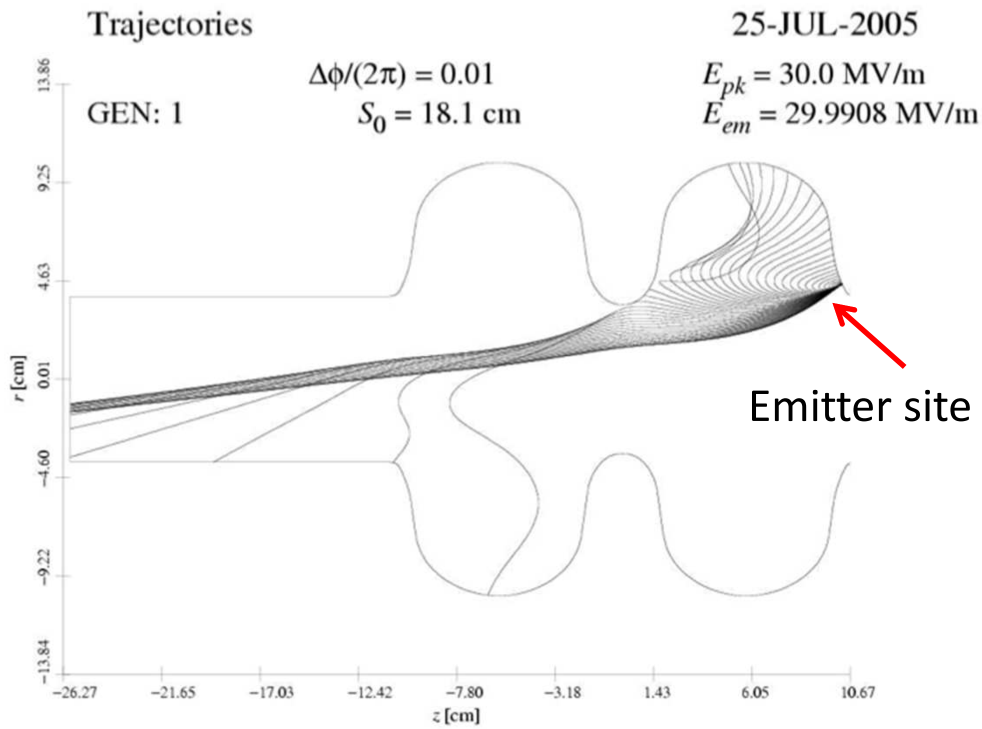

Physics of Field Emission

- Electron emission from site of “field emitter”
  - Quantum mechanical process – tunneling effect

$$I_{\mathrm{FN}} = j_{\mathrm{FN}} A_{\mathrm{FN}} = A_{\mathrm{FN}} \frac{e^3 E^2}{8\pi h \Phi t^2(y)} \exp\left(-\frac{8\pi\sqrt{2m_e\Phi^3}\,v(y)}{3heE}\right)$$

ield

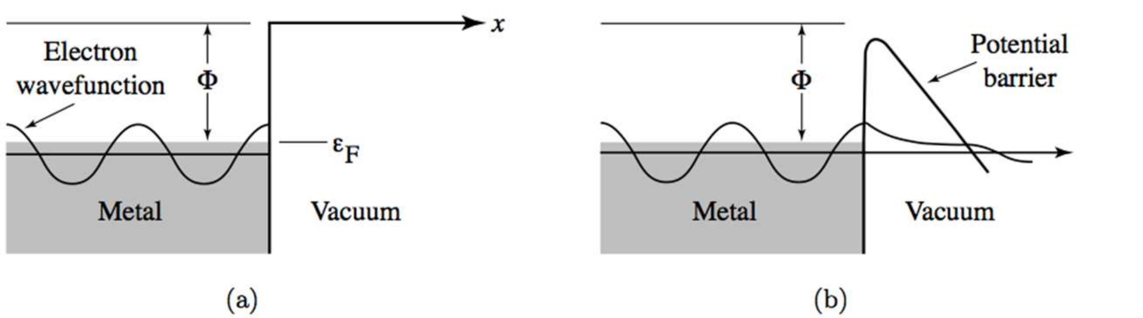

Figure 3.2: Electrostatic potential of the metal–vacuum interface. (a) No electric field applied, (b) with an electric field applied.

Physics of Field Emission

- Modified Fowler-Nordheim
  - Electric field enhancement factor β_{FN}
    - Typical value 50-500 for SRF cavity
  - Effective emitter area A_{FN}
    - Typical value $10^{-18} – 10^{-9}$ m^2

$$I_{\mathrm{FN}} \;=\; j_{\mathrm{FN}} A_{\mathrm{FN}} = A_{\mathrm{FN}} \frac{e^3 (\beta_{\mathrm{FN}} E)^2}{8\pi h \Phi t^2(y)} \exp\left(-\frac{8\pi\sqrt{2m_{\mathrm{e}}\Phi^3}v(y)}{3he\beta_{\mathrm{FN}} E}\right)$$

Note: β_{FN} and A_{FN} have no physical significance
There are different models in book

Physics of Field Emission

- Emitted electrons captured and accelerated by RF field
  - This consumes RF energy stored in cavity and hence cause rapid Q_0 decline (recall exponential increase in current as field is raised)
- Energetic electrons strike cavity wall
  - Deposit heat and cause local rise of wall temperature
    - Cause line heating at cavity wall because electrons emitted at different RF phase angle follow different trajectory in the plane defined by cavity axis and em
    - Also contribute to Q decline
  - Produce X-rays due to Bremsstrahlung Effect
  - May produce neutron through (γ,n) reaction
    - Will cause activation

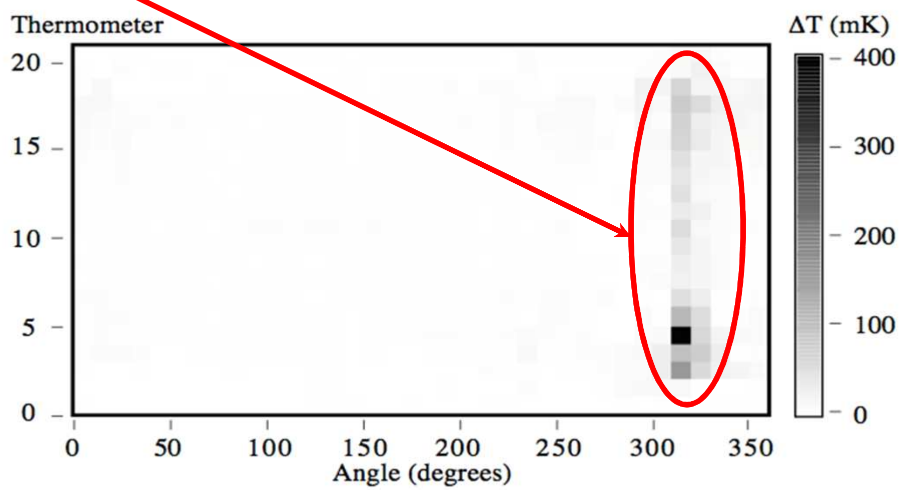

Field Emitters

- Microscopic particles
  - from external source, consist foreign material
  - Airborne
  - From cavity assembly hardware and tool

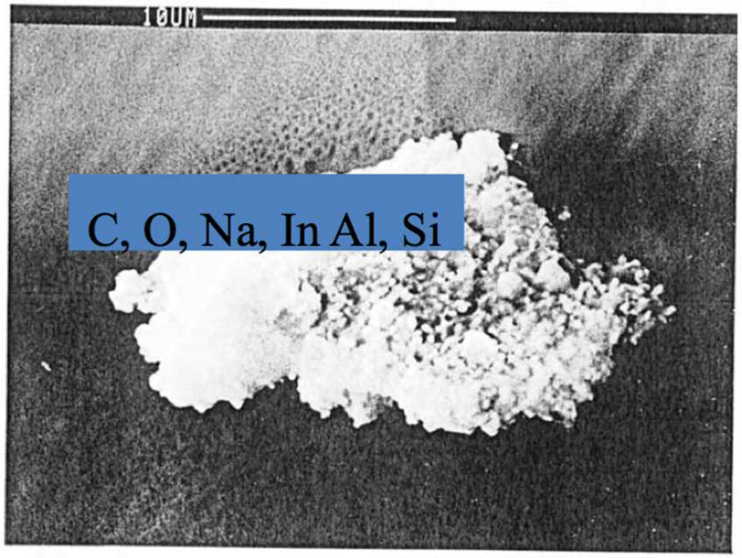

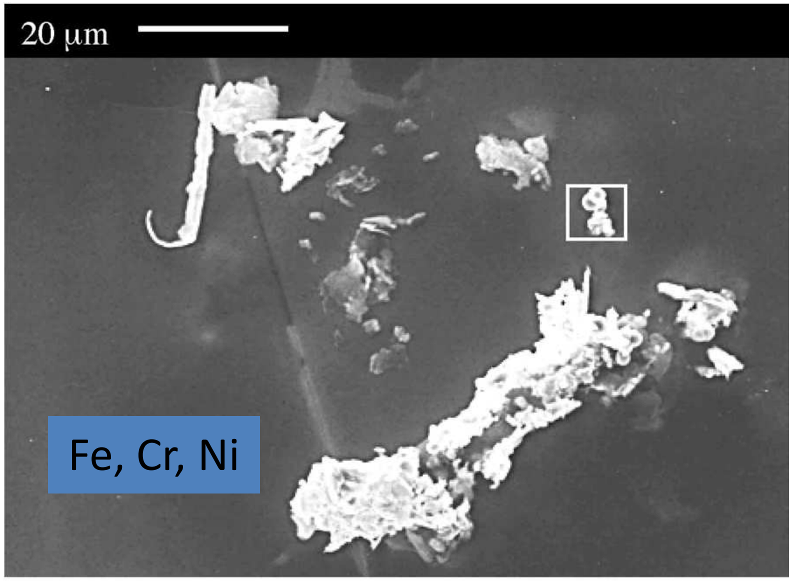

Field Emitters

- Geometrical defects
  - Is permanent feature, is part of cavity
  - Pits (from fabrication)
  - Scratches
    - HPR wand damage

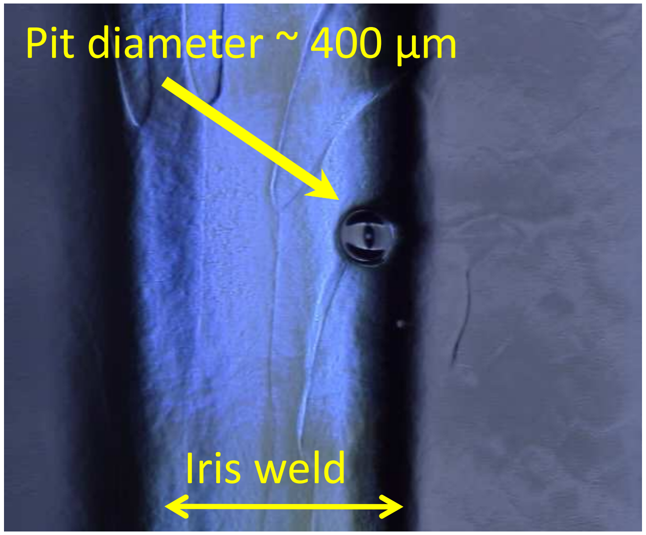

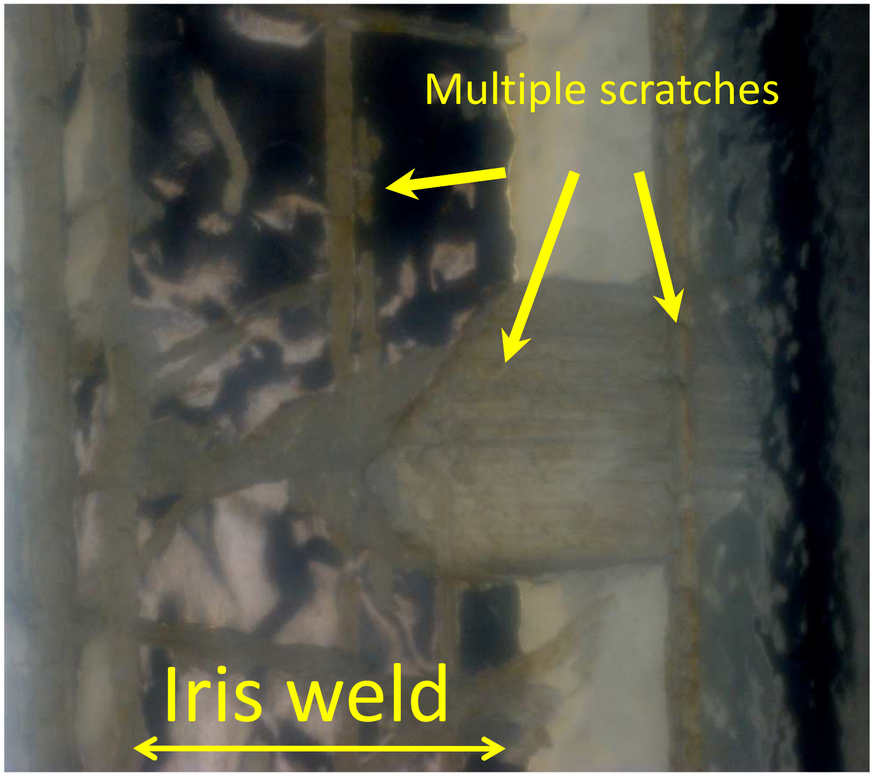

Field Emitters

- Contaminants from surface processing
  - Niobium oxide granules (electropolished surface)
  - Sulfur
    - And other element

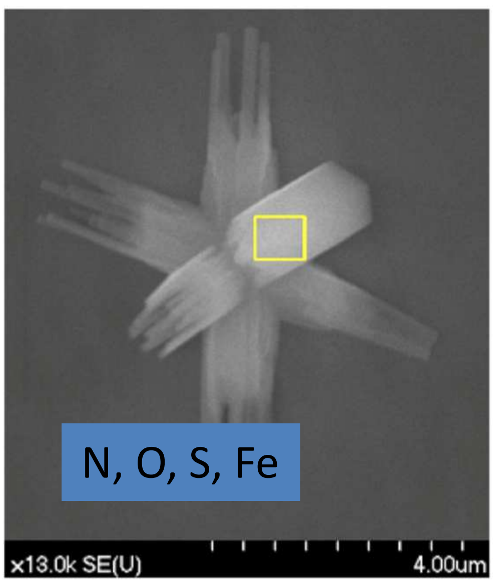

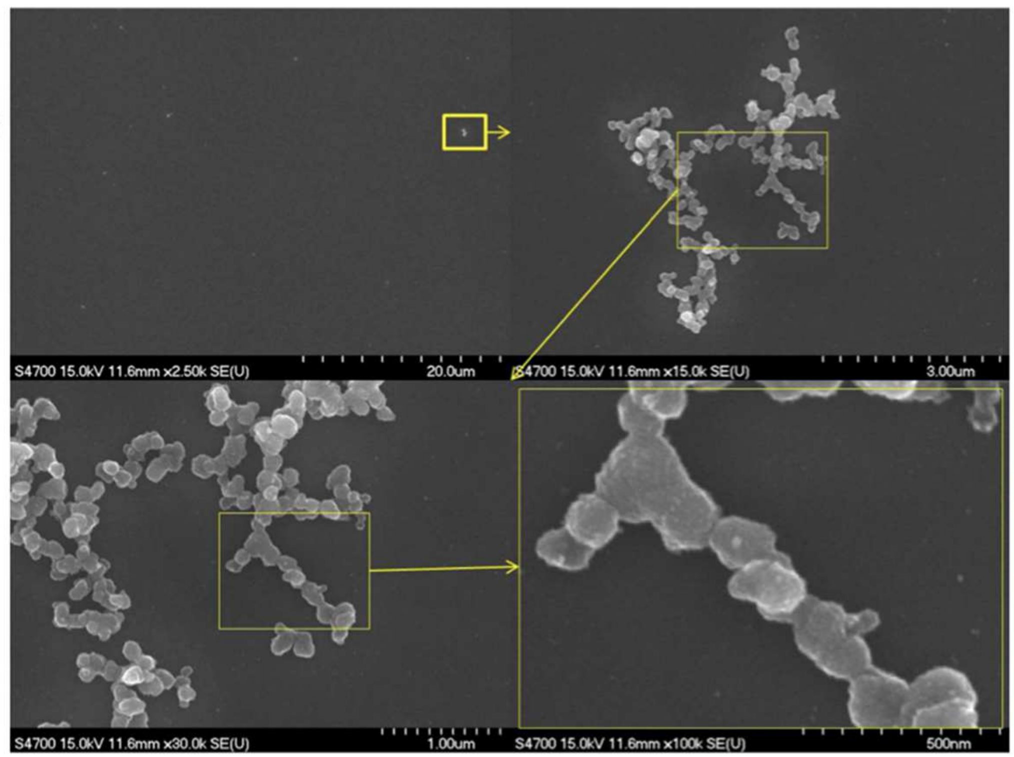

Courtesy X. Zhao

Understanding of Field Emission

- Field emission is primarily an electric field effect
  - High electric field region (arro
    critica

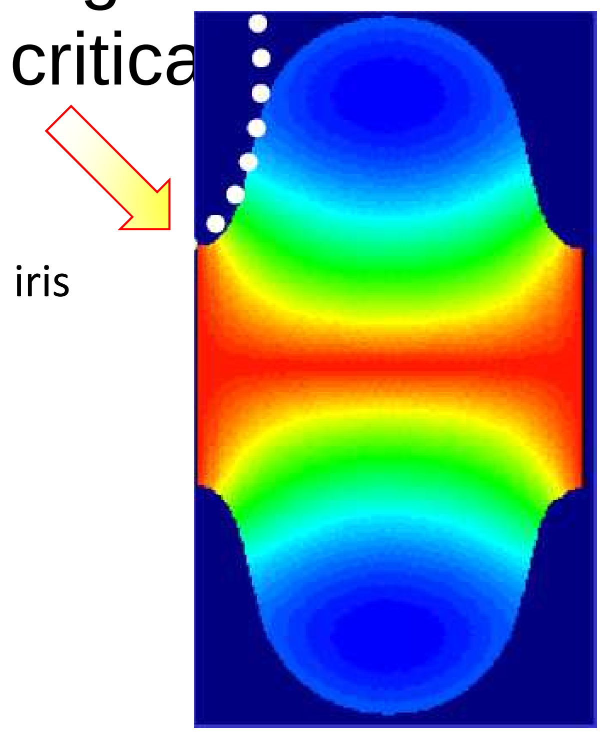

Elliptical cavity (TM-class)

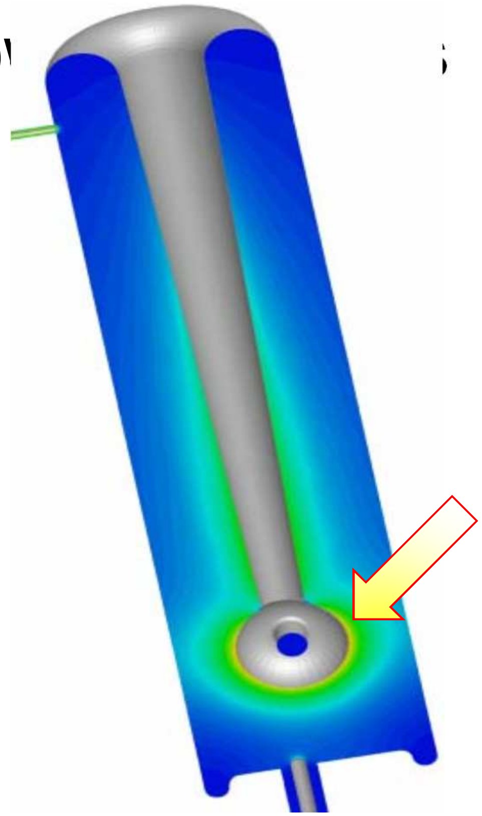

Half-wave cavity (TEM-class)

Understanding of Field Emission

- Processing events – extinction of field emitter
  - Micro-tip melting, gas release
  - Discharge/plasma
  - Breakdown/emitter destruction

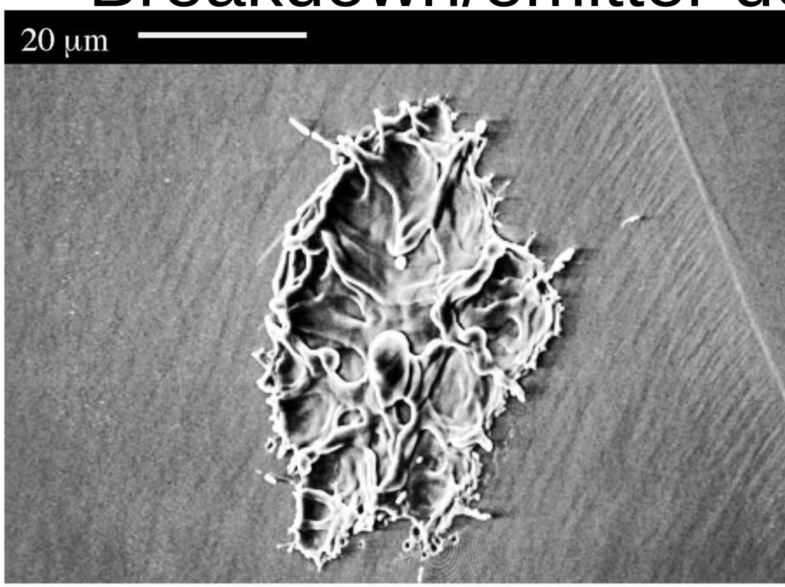

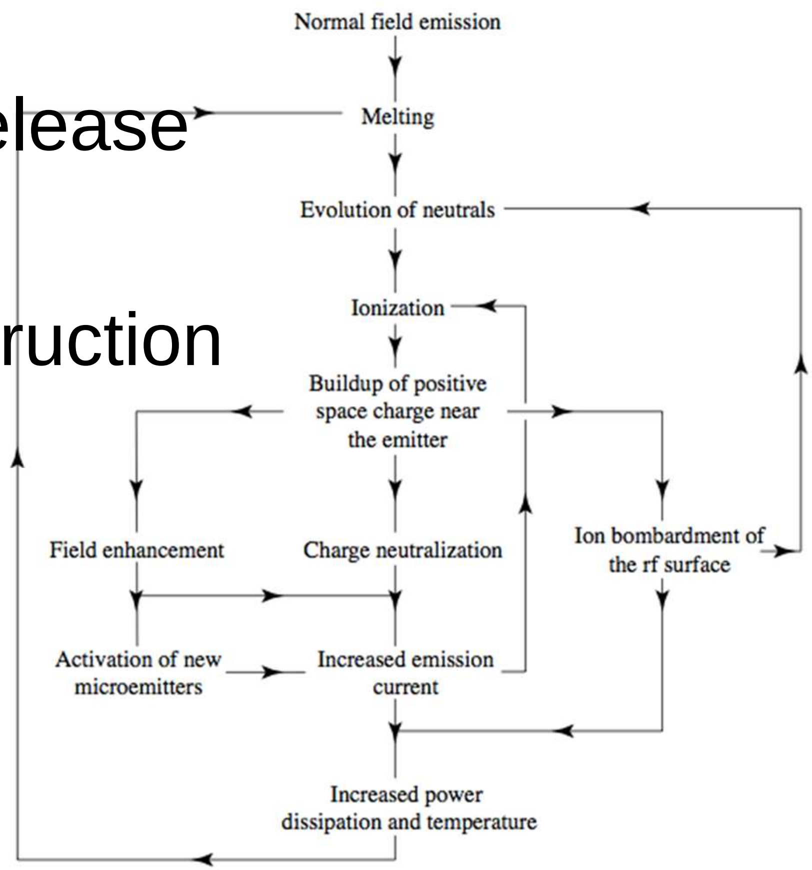

Figure 5.36: Flow chart of the feedback loop leading up to rf processing.

Understanding of Field Emission

- Field emission turn on events
  - Activation of field emitter
    - Arrival of particles
    - Condensation of gases

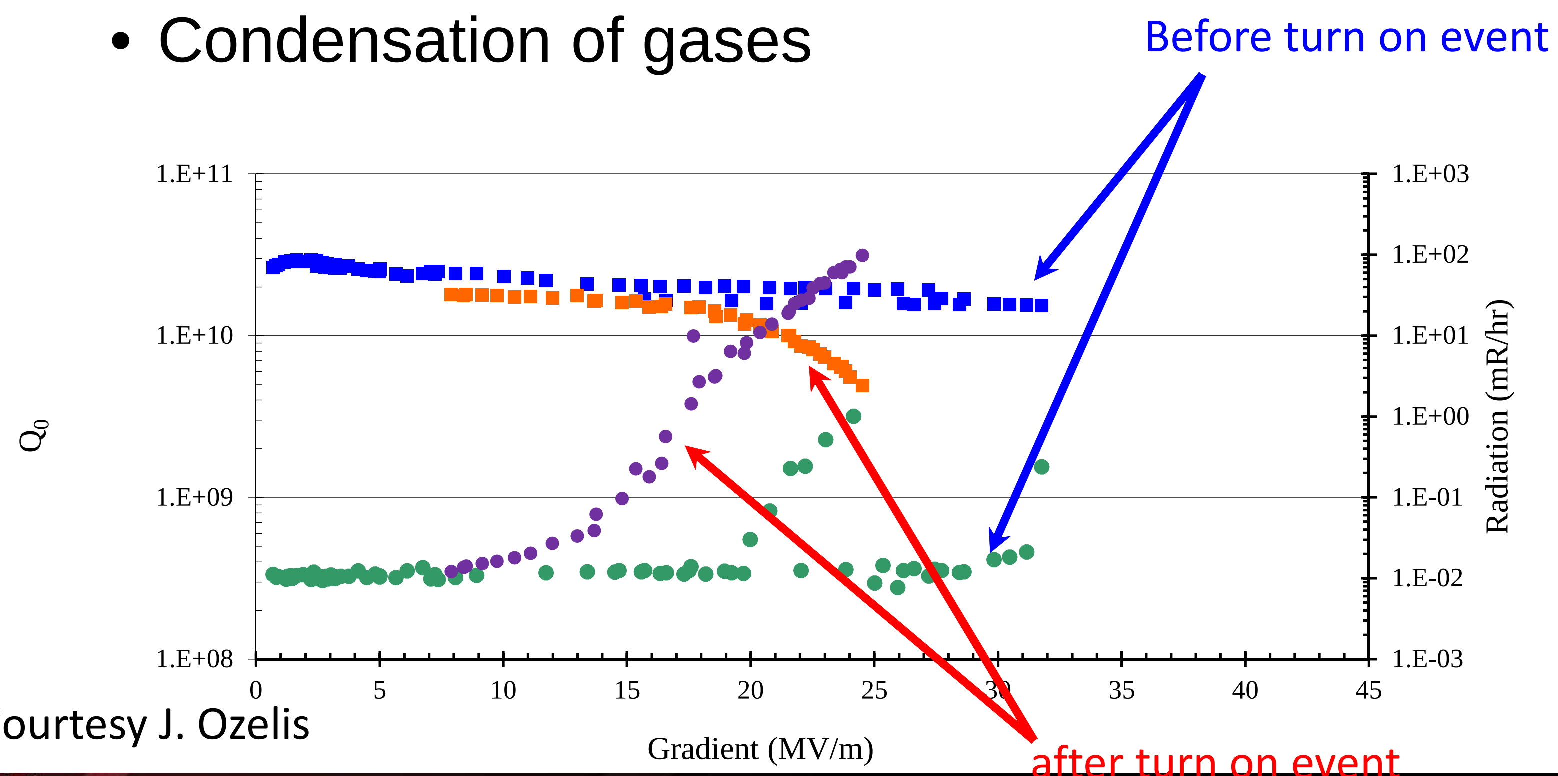

Courtesy J. Ozelis

Understanding of Field Emission

- Field emission turn on events
  - Activation of field emitter
    - Baking (120 ℃) induced (for electropolished

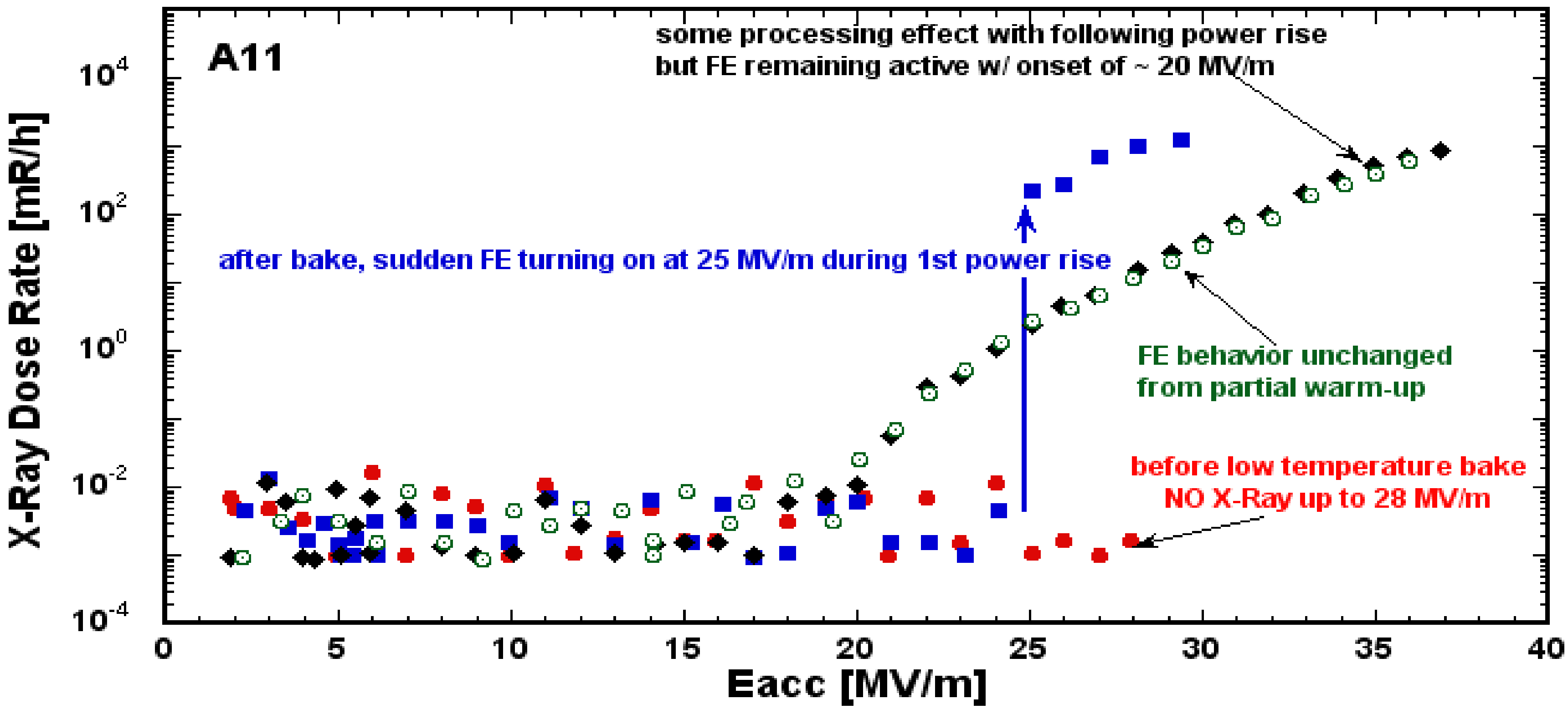

Overcoming Field Emission

- Post-Chemistry Cleaning (remove contaminants)
  - Rinsing
  - Wiping and brushing (end group components)

Overcoming Field Emission

- Post-Chemistry Cleaning
  - Ethanol rinsing
  - Ultrasonic cleaning (De-ionized water + detergent)

Overcoming Field Emission

- High Pressure Water Rinsing (HPR)
  - De-ionized water, 18 MΩ-cm resistivity
  - 1300 PSI pressure

(click photo for video)

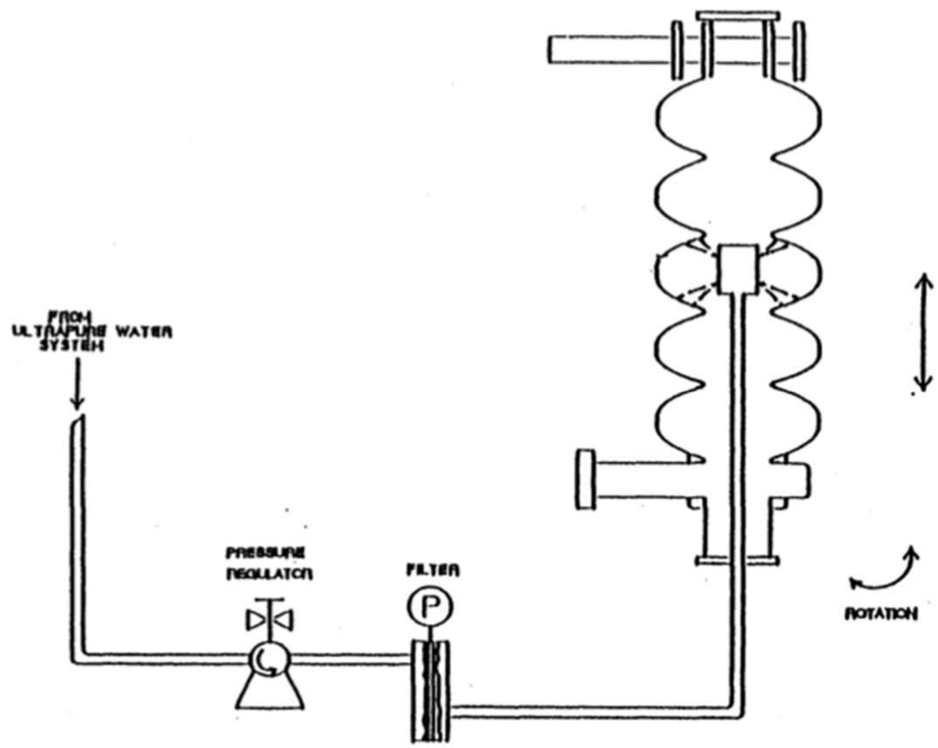

Courtesy P. Kneisel

Overcoming Field Emission

- Clean room assembly
  - Class-10
  - Or ISO 4

Overcoming Field Emission

- Slow pump down
  - Prevent re-contamination
- Oil-free pumping system

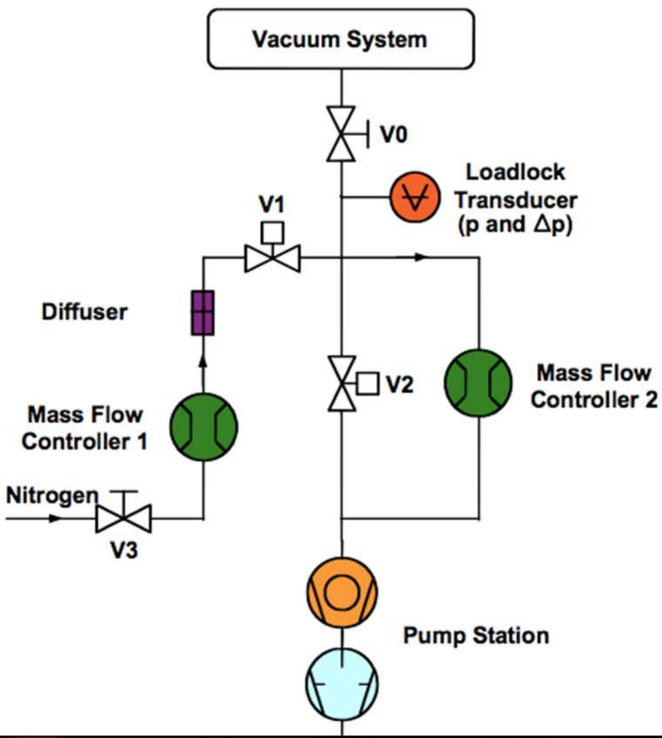

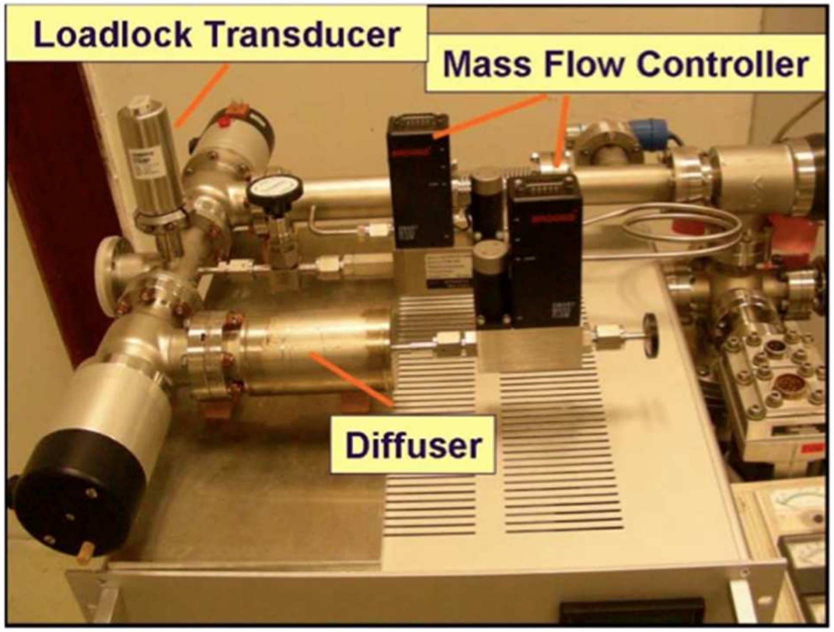

K. Zapfe and J. Wojtkiewicz, SRF2007

Overcoming Field Emission

- New techniques
  - CO2 snow cleaning
  - Horn cleaning (target end grou

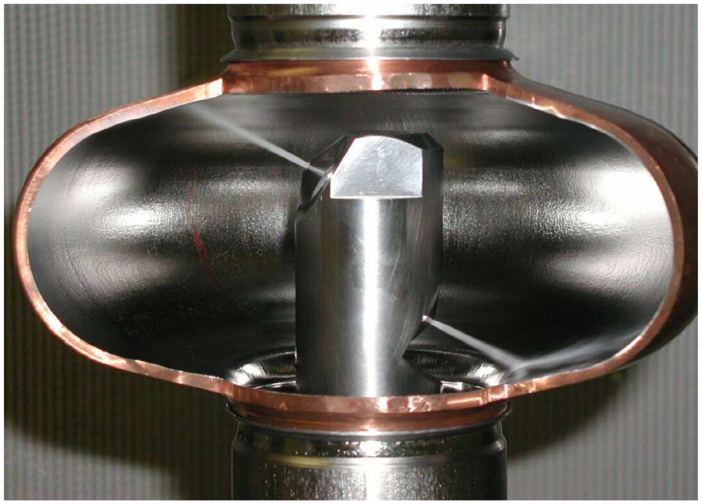

Courtesy D. Reschke

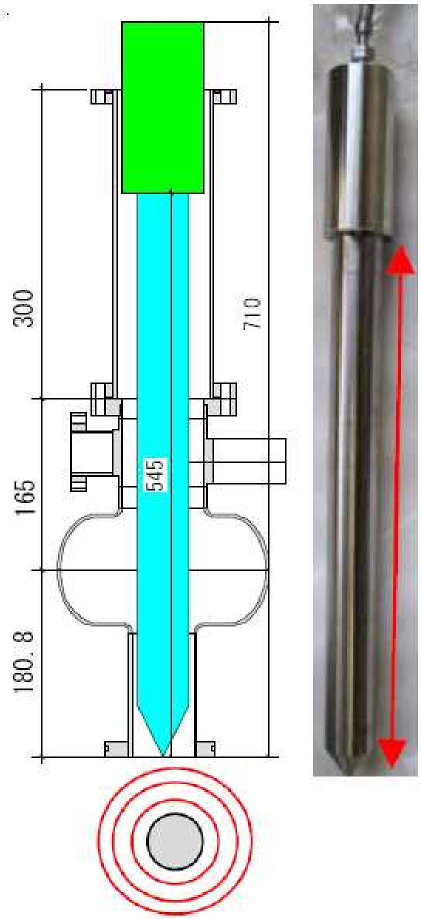

Courtesy K. Saito

Overcoming Field Emission

- Processing (to destroy emitter)
  - RF conditioning (CW or pulsed)
  - Helium processing
    - Back fill cavity with He gas to ~ 10^{-5} Torr pressure
  - High Peak Power Pulsed Processing (HPP)
    - 1 MW, 200 μs
  - Plasma cleaning

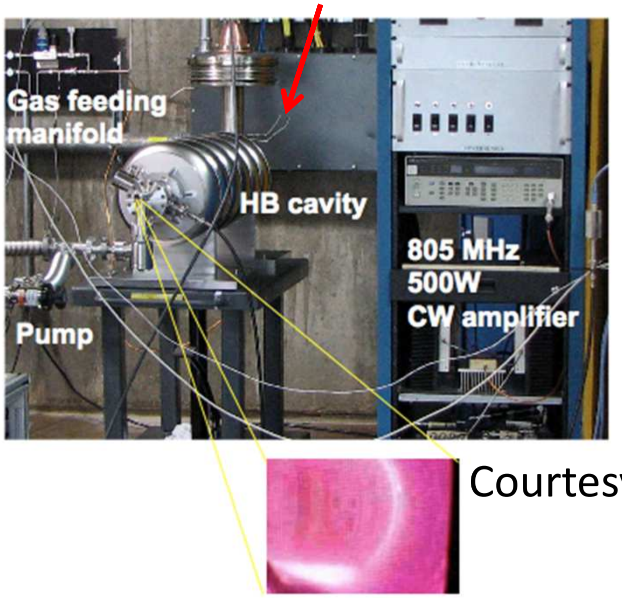

First plasma in the SNS HB cavity

300W forward
200W reflected
1e-4 torr

Courtesy J. Mommosser

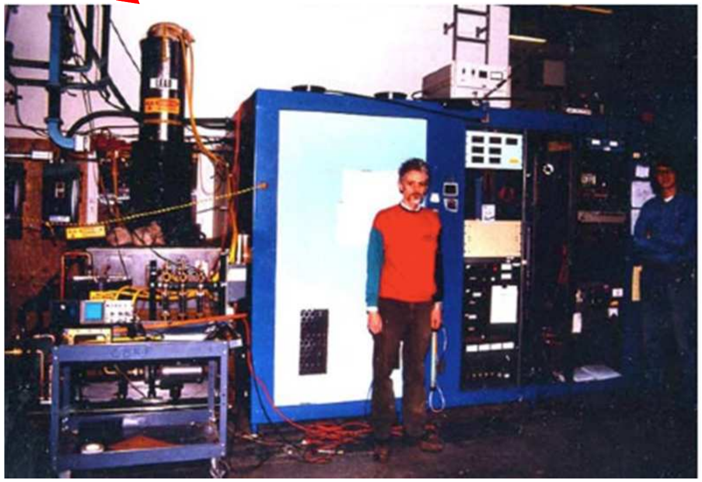

Courtesy H. Padamsee

Overcoming Field Emission

- Reducing peak surface electric field in cavity design

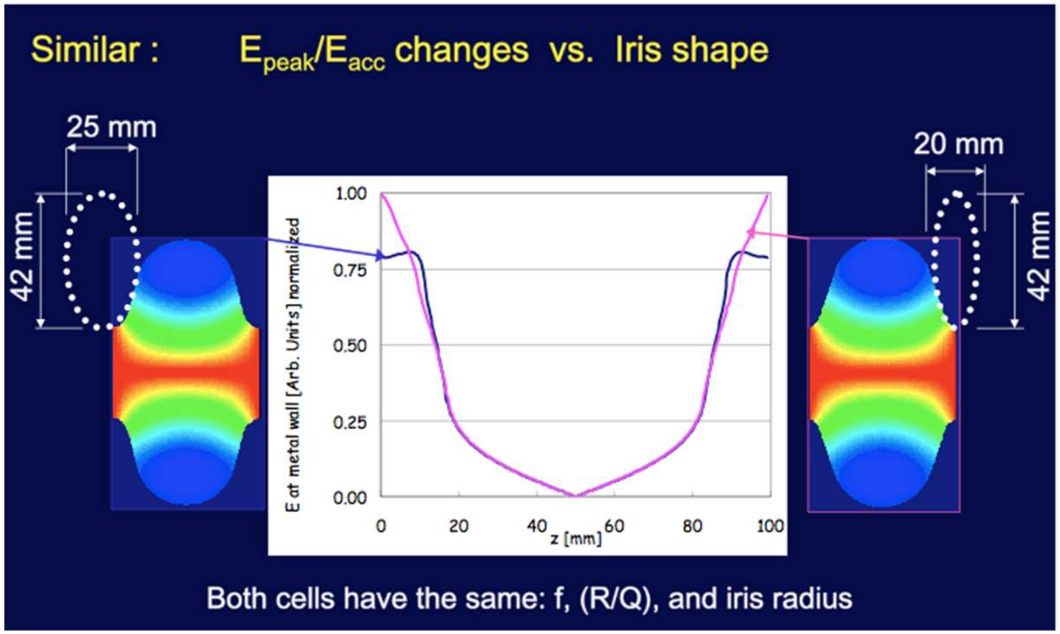

Courtesy J. Sekutowicz

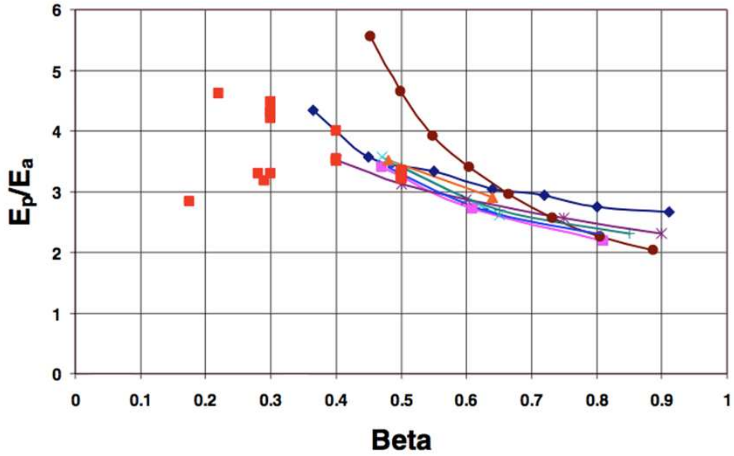

Figure 11: Ratio of peak surface to accelerating field. Data points joined by lines are for TM structures, isolated points (red squares) are for λ/2 structures.

Courtesy J. Delayen

Last Word on Field Emission

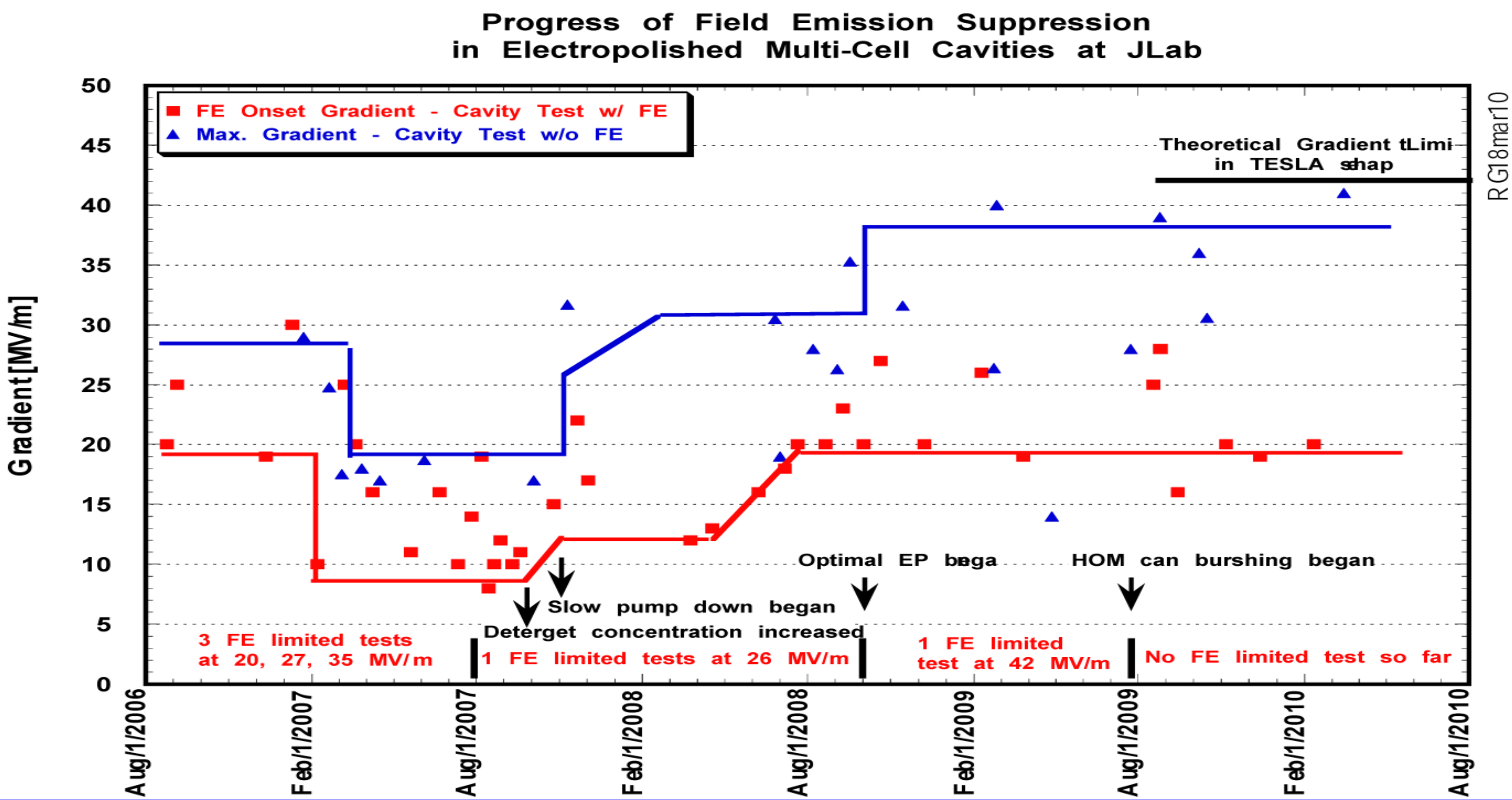

Progress has been made in recent years in reducing field emission. “Field emission free” cavity vertical testing of 1 meter long 9-cell 1300 MHz cavities has been reported at DESY, FNAL, JLab, KEK in gradient range of 35-45 MV/m. Much less cavities are limited by field emission. But challenges remain toward reliable control of field emission. Such as “sudden field emitter turn on” at high gradient, degradation from vertical test to cryomodule test. Plenty room for innovation and creativity.

Quench

Symptom of Quench

- Sudden collapse (ms time scale) of field in SRF cavity
  - Field may self recovers
  - Or may not
- Detection of temperature rise at cavity wall near quench source
  - Can be as high as a few K

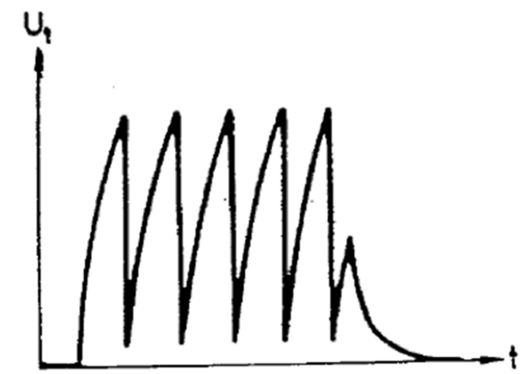

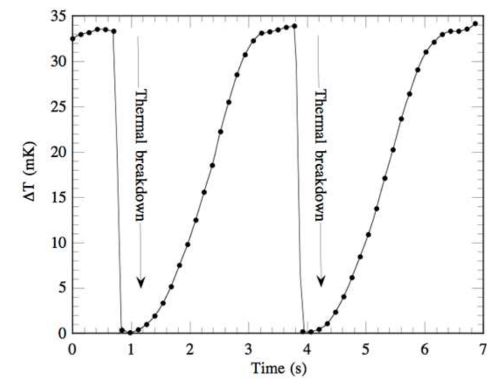

Movie courtesy G. Eremeev

(click photo for video)

Quench Diagnostic

Commonly Used Heat Pulse Detectors

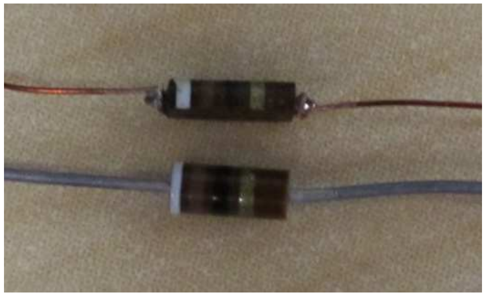

Allen-Bradley
carbon resistor
100 Ω, 1/8 W

Cernox

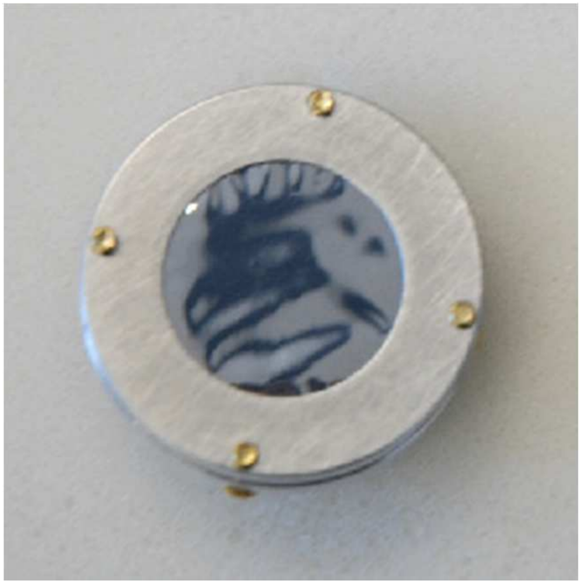

Cornell OST

Used at 1.8 K for defect localization

Physics of Quench

- Quench caused by field emission
  - Heat deposition at electron bombardment site (earlier slides)
- Quench caused by multipacting (more later)
  - Heat deposition at electron bombardment site(s)
- Quench caused by resistive heating of local normal conducting defect
  - Thermal breakdown
- Quench caused by growing normal conducting region driven by magnetic field
  - “magneto-thermal” breakdown
- Quench caused by uniform heating (Global Thermal Instability)
- Ultimate limit: quench due to RF critical field

Physics of Thermal Quench

- Power dissipation in normal conducting defect generates heat
- Poor thermal conductivity of superconducting wall limits heat conduction
- This causes temperature rise to exceed Tc (9.25 K) in surrounding superconducting region
- This causes additional resistive heating
- The normal conducting region grows rapidly, leading to quench

$$\frac{dP_c}{ds} = \frac{1}{2} R_s |\mathbf{H}|^2$$

$$\mathrm{Rs} \begin{cases} \mathrm{n}\Omega\text{, s.c.} \\ \mathrm{m}\Omega\text{, n.c.} \end{cases}$$

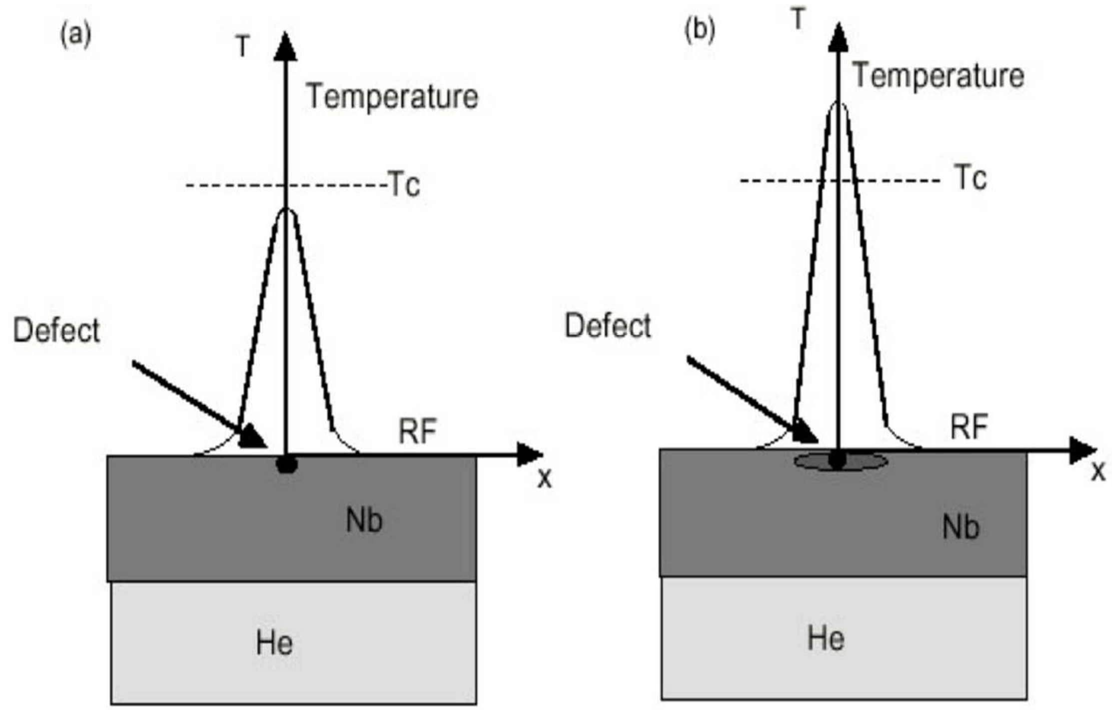

Physics of Magneto-Thermal Quench

- Initial heating at low field follows quadratic dependence of superconductor
- When a threshold field is reached, a "small domain" is driven from s.c. to n.c because local magnetic field exceed local critical field
  - Local magnetic field enhancement
  - Local critical field suppression
- Converted n.c domain is thermally stable, but causes resistive heating
- The boundary of n.c domain is not necessarily at Tc
- The normal conducting domain grows rapidly when field is further raised, leading to quench

$$\frac{dP_c}{ds} = \frac{1}{2} R_s |\mathbf{H}|^2 \qquad R_s \begin{cases} n\Omega, \text{ s.c.} \\ m\Omega, \text{ n.c.} \end{cases}$$

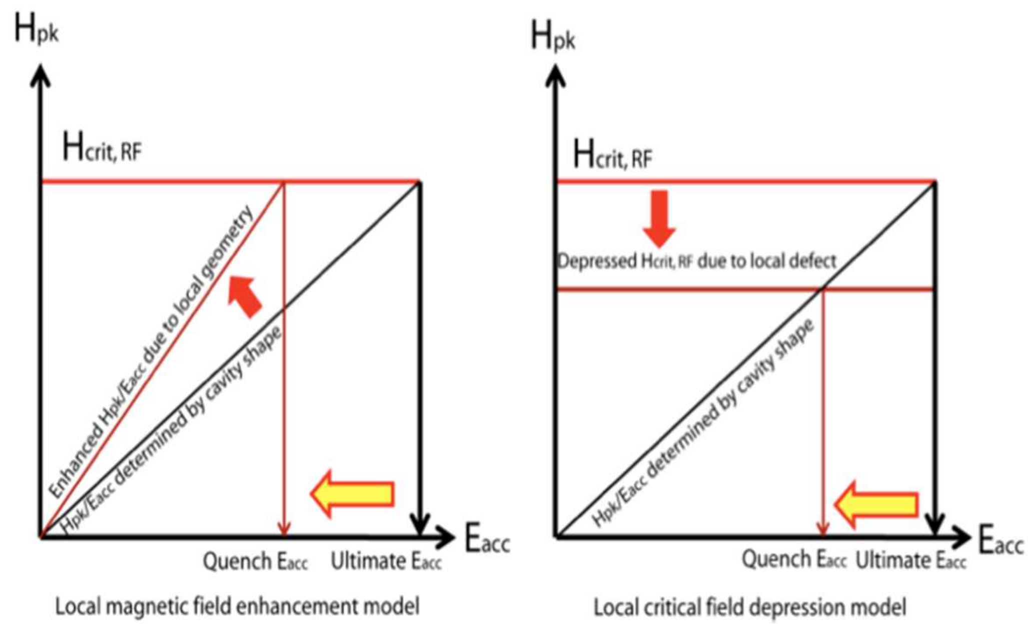

Note: no n.c. defect is involved

Defects

- N.C. defect with foreign material
  - inclusion
  - Stain
  - Copper particle

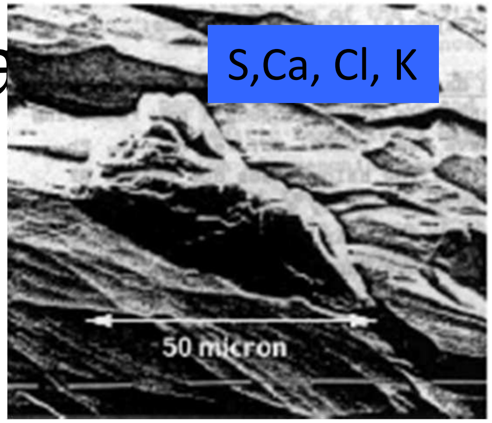

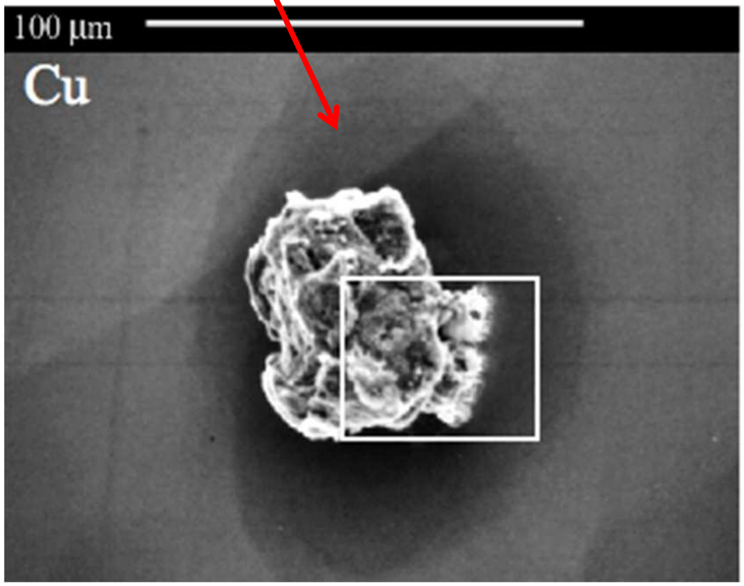

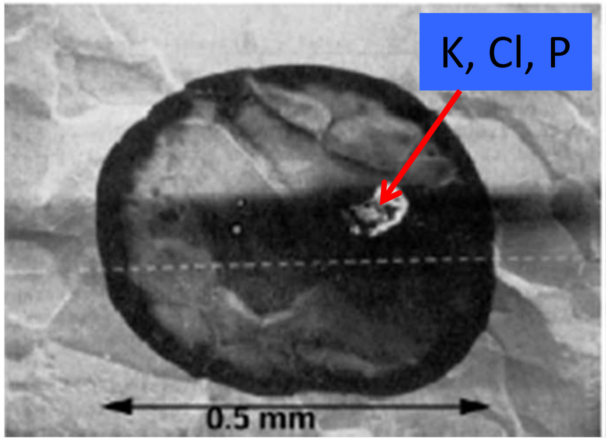

50-500 µm

Defects

- Geometrical defect (no foreign material)
  - pit
  - Bump
  - hole

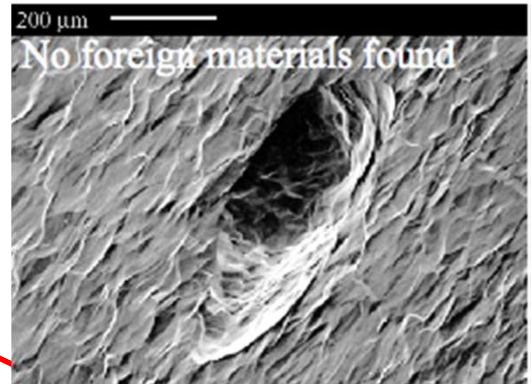

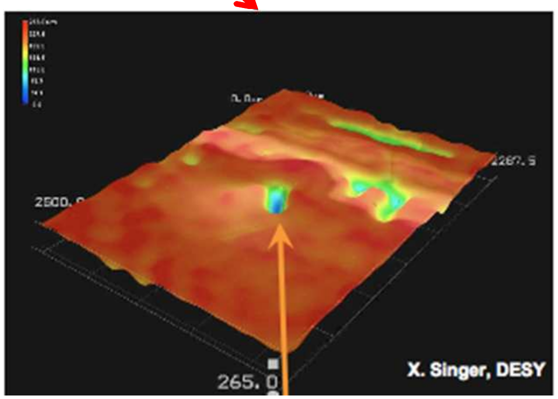

200-800 µm

Courtesy W. Singer

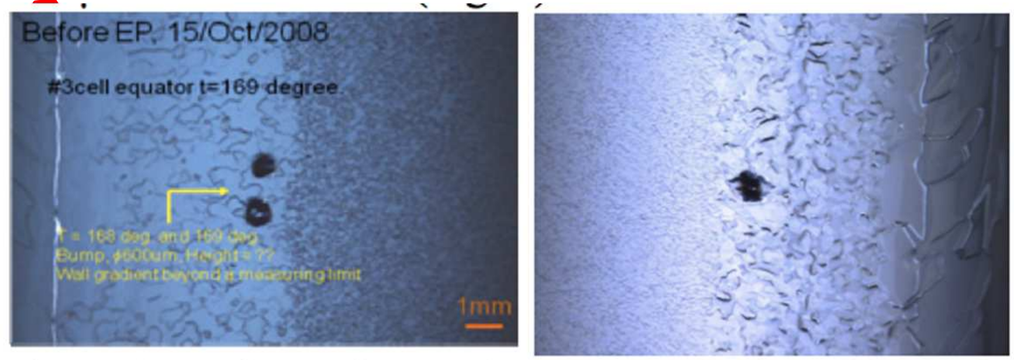

Figure 2: Defects observed near quench site of AES1(L) & AES3(R), limited at 16 & 21 MV/m, respectively. These circular defects have a diameter of ~ 600 µm and are outside the equator EBW (5-10 mm from weld seam).

Understanding of Thermal Quench

- Thermal breakdown field is determined by
  - Defect size (r_d)
  - Defect surface resistance (R_d)
  - Thermal conductivity of wall material (~ Tc)
  - Heat transfer across Nb/LHe interface (Kapitza)

$$H_{\mathrm{tb}} = \sqrt{\frac{4\kappa_T(T_{\mathrm{c}} - T_{\mathrm{b}})}{r_{\mathrm{d}} R_{\mathrm{d}}}}.$$

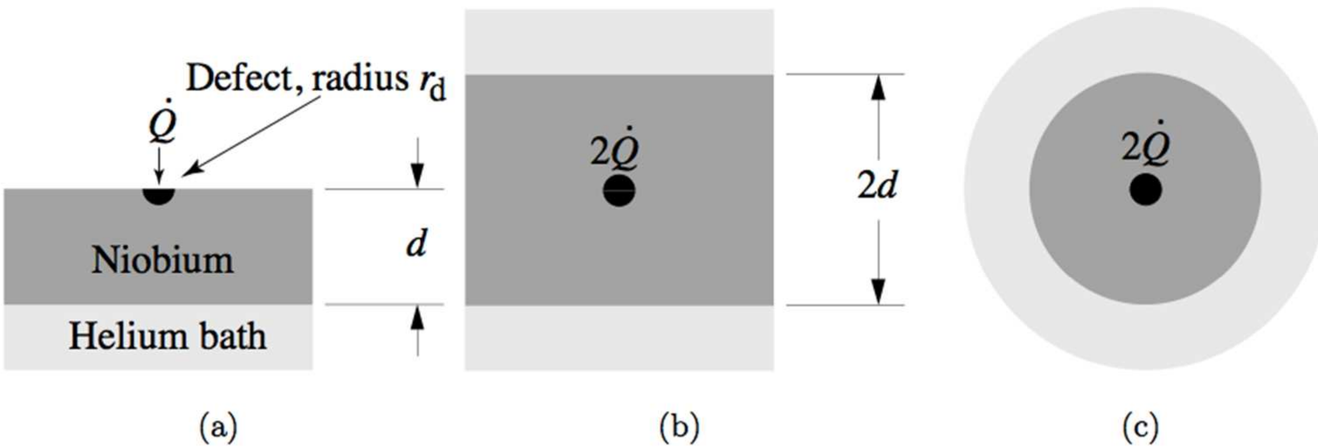

Figure 3.10: Geometry used to determine the thermal breakdown field due to a defect.

Understanding of Magneto-Thermal Quench

- Magneto-thermal breakdown is determined by $h \propto (r/R)^n$
  - Local magnetic field enhancement factor
  - Thermal conductivity of wall material (< Tc)

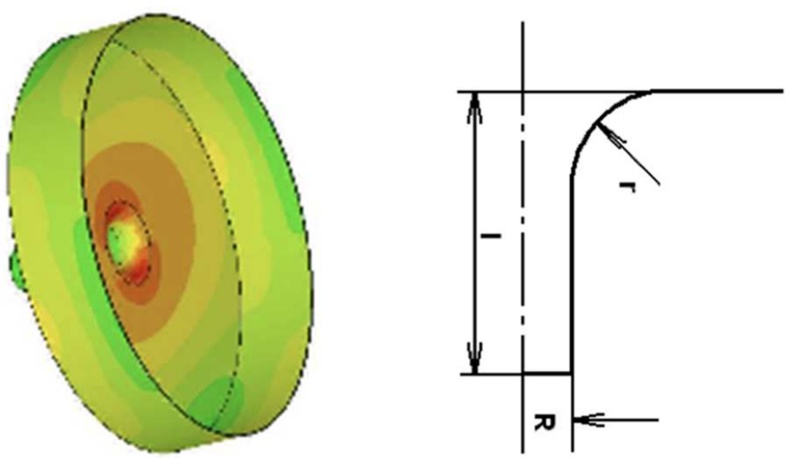

Courtesy V. Shemelin

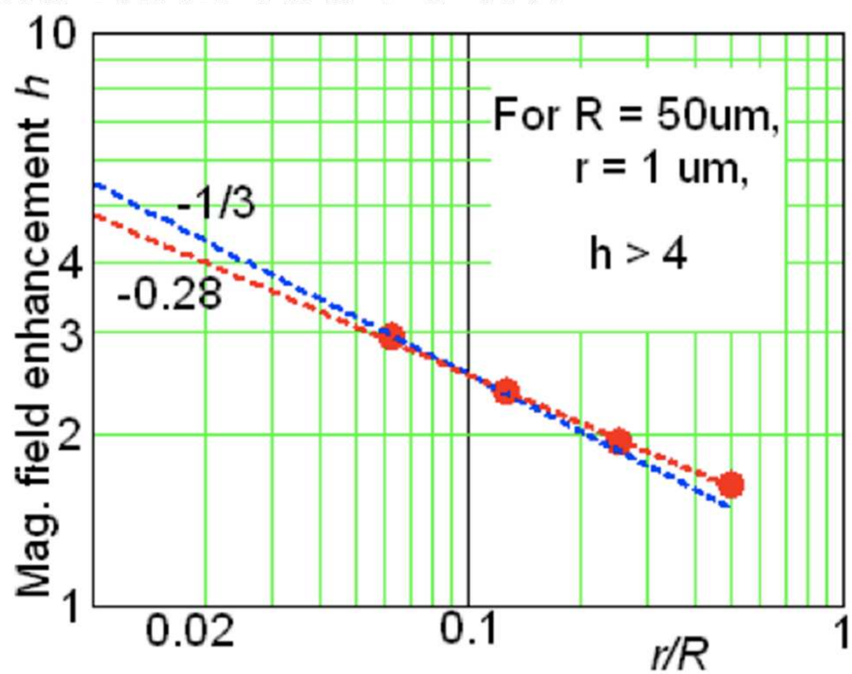

Understanding of Thermal and Magneto-Thermal Quench

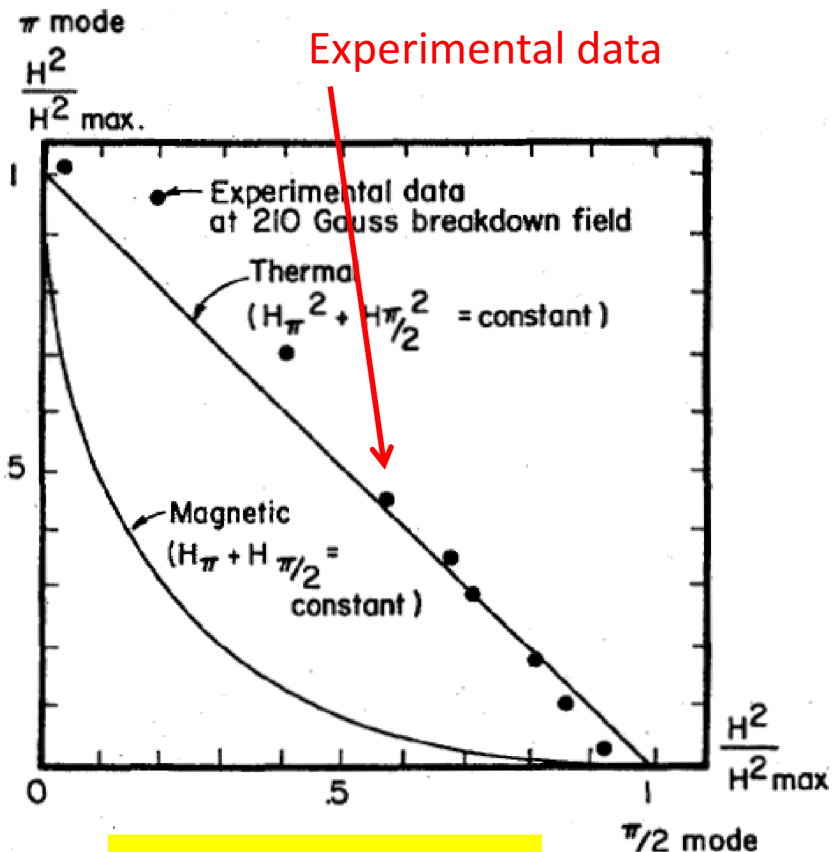

Thermal breakdown

Courtesy H. Padamsee

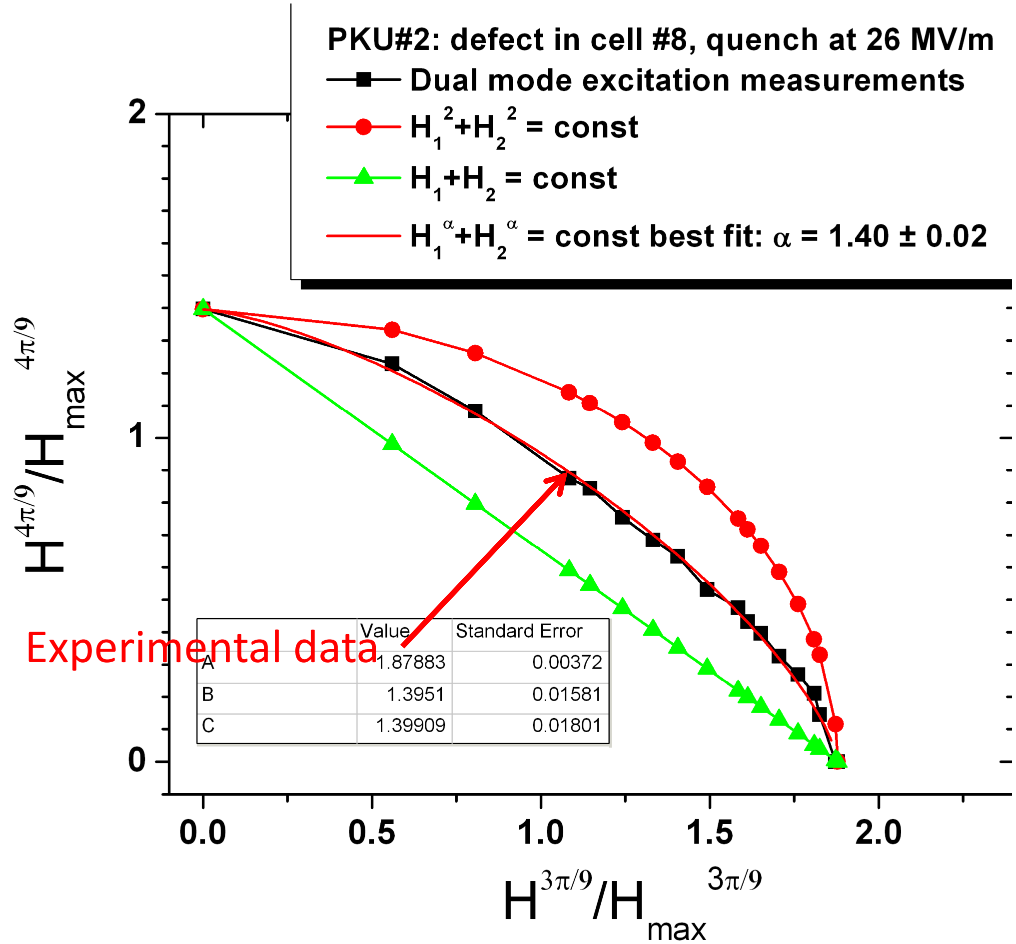

Magneto-Thermal breakdown

Understanding of Magneto-Thermal Quench

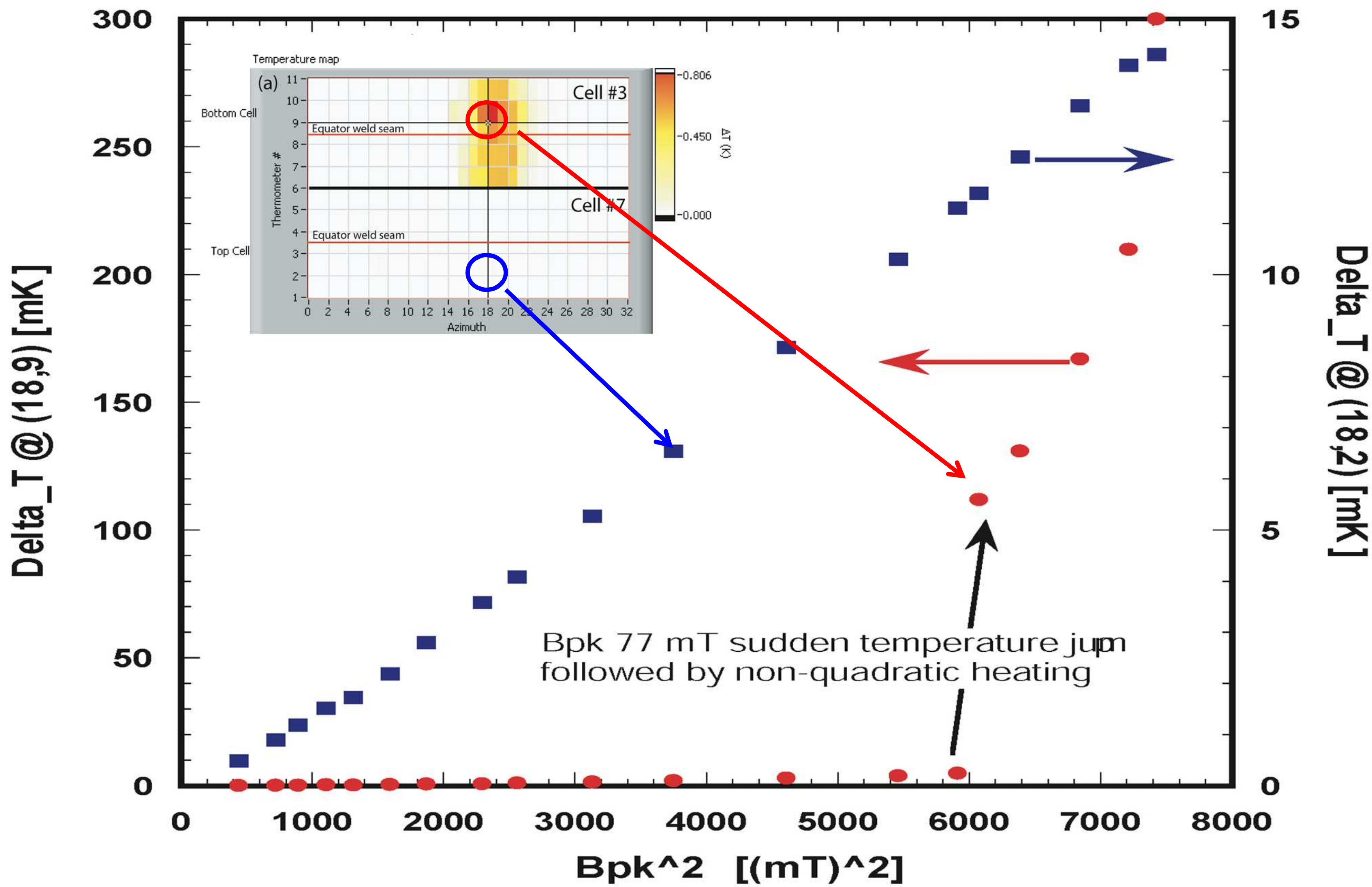

Understanding of Quench

- Quench is primarily a magnetic field effect
  - High magnetic field region (arrow) in cavity is critical

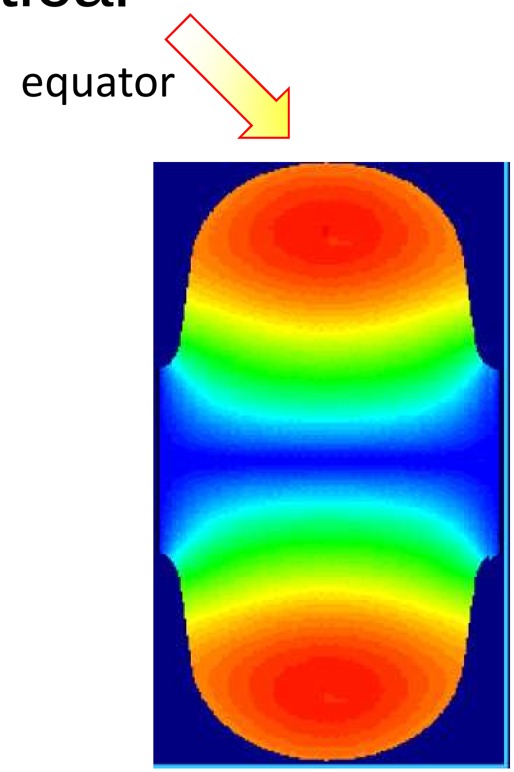

Elliptical cavity (TM-class)

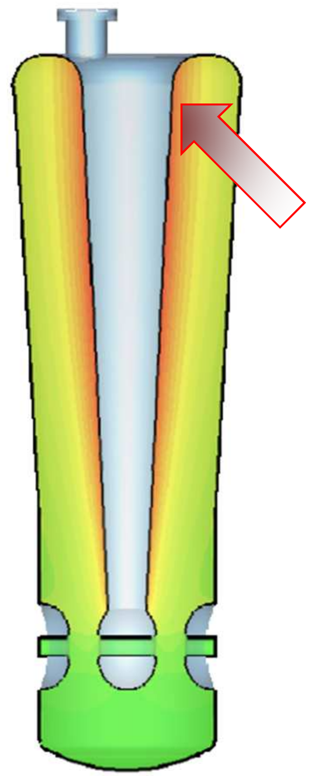

Half-wave cavity (TEM-class)

Overcoming Thermal Breakdown

- Raise bulk thermal conductivity near Tc
  - High purity niobium (RRR >300)
  - Multiple re-melting

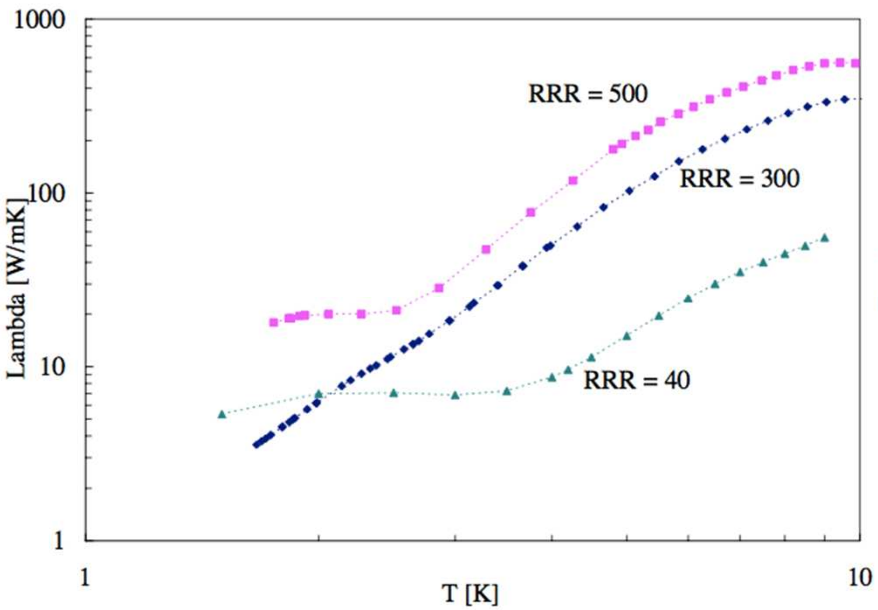

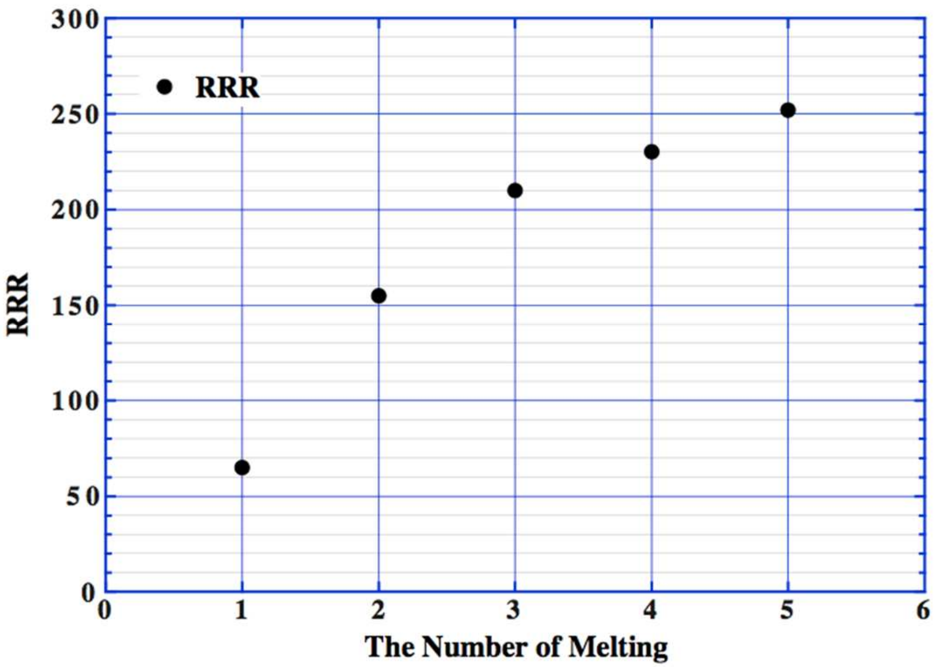

T. Shishido et al., SRF1999

Overcoming Thermal Breakdown

- Raise bulk thermal conductivity
  - Post-fabrication purification

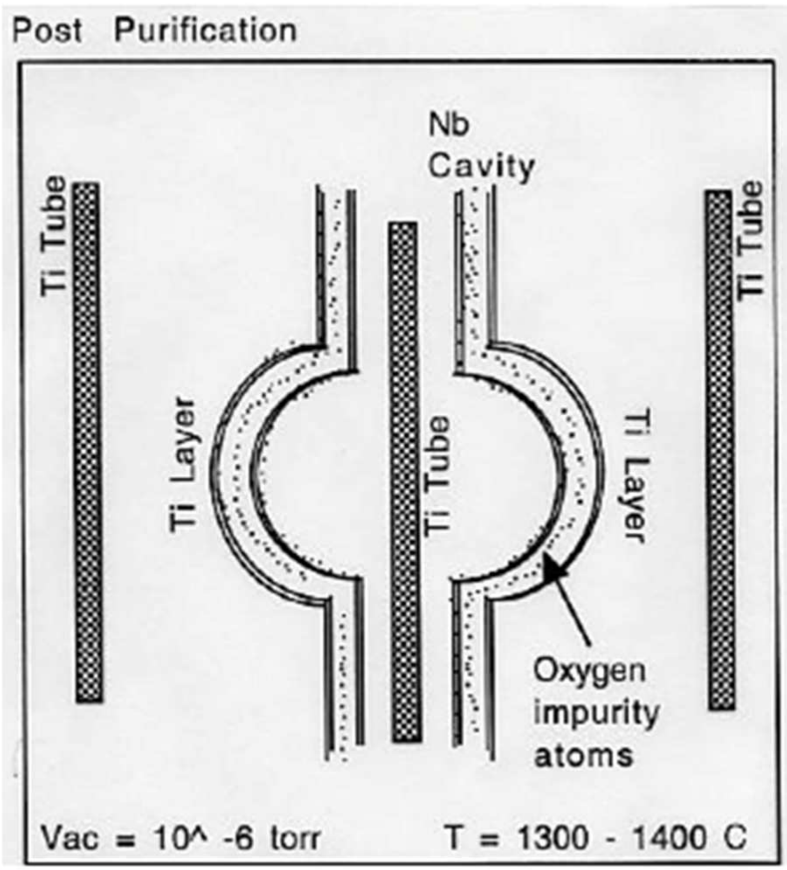

- Heat in vacuum furnace to ~ 1400 C
- Evaporate Ti on cavity surface
- Use titanium as getter to capture impurities
- Later etch away the titanium
- Doubles the purity (RRR ~ 600 if originally RRR = 300)

Courtesy H. Padamsee

Overcoming Thermal Breakdown

- Avoid normal conducting defects
  - Eddy current scanning of starting sheets

Detlef Reschke

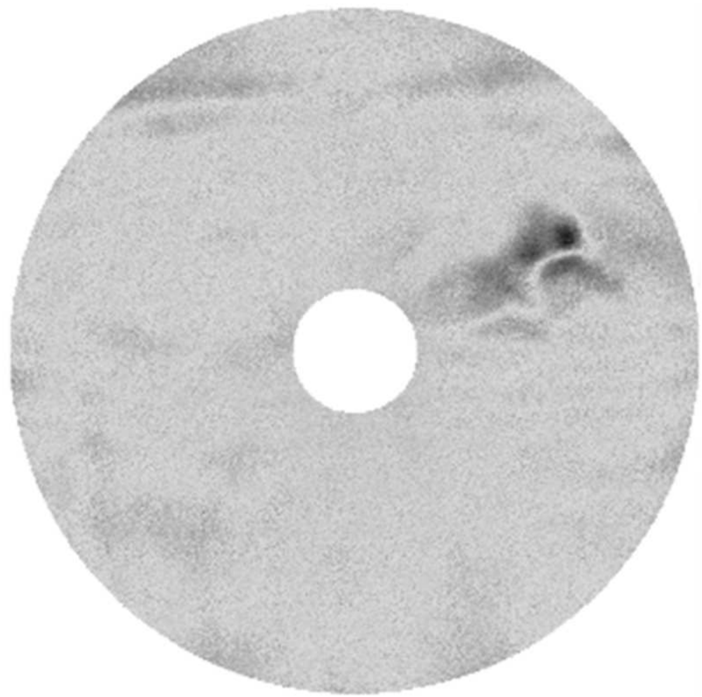

Courtesy D. Reschke

Overcoming Magneto-Thermal Breakdown

- Produce smooth surface
  - Global mechanical polish

Courtesy C. Cooper

Overcoming Magneto-Thermal Breakdown

- Raise bulk thermal conductivity at T < Tc
  - Heat treatment cold worked niobium
  - Use large-grain niobium material

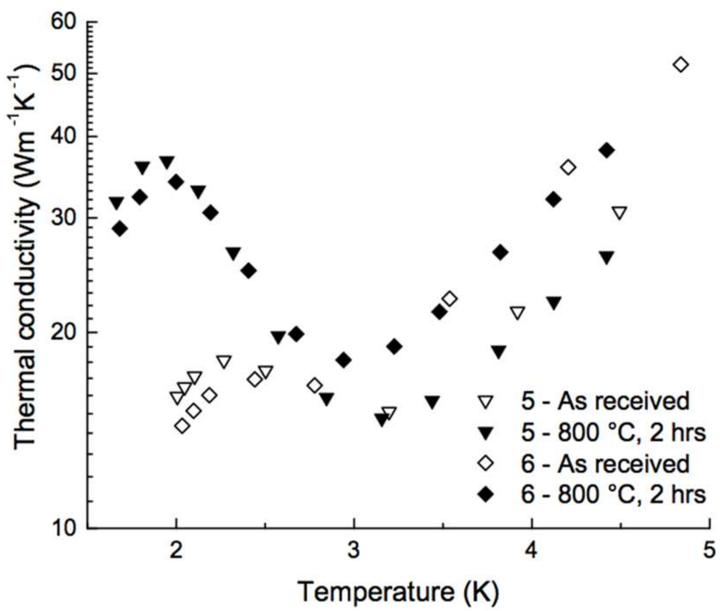

S.K. Chandrasekaran et al., SSTIN 2010

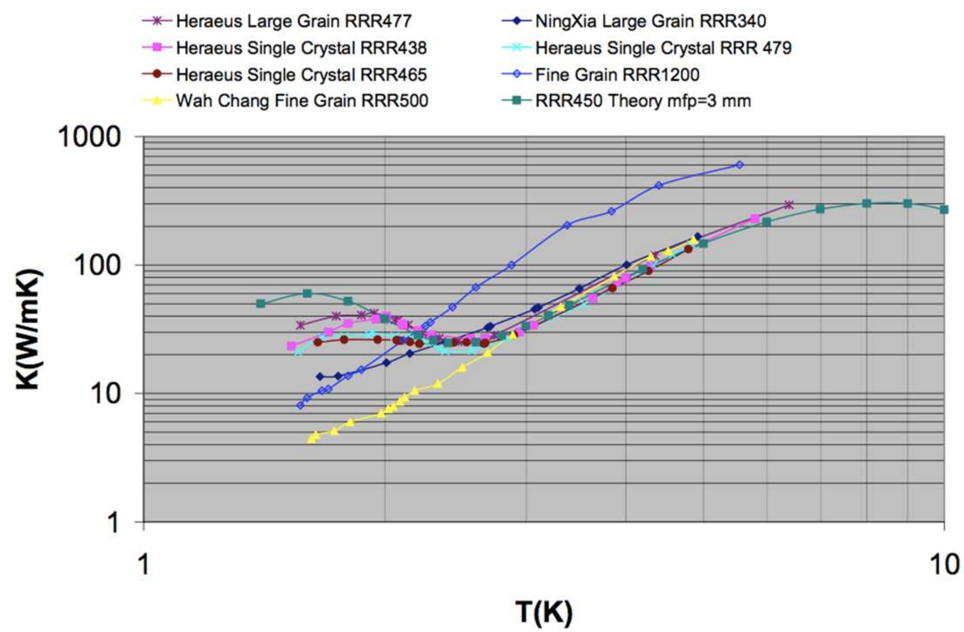

A. Ermakov et al., EUCAS 2007

Overcoming Magneto-Thermal Breakdown

- Removal quench-causing geometric defects
  - First localize defect
    - OST for rapid quench location
  - Then assess quench region
    - high-resolution optical inspection

Courtesy H. Hayano

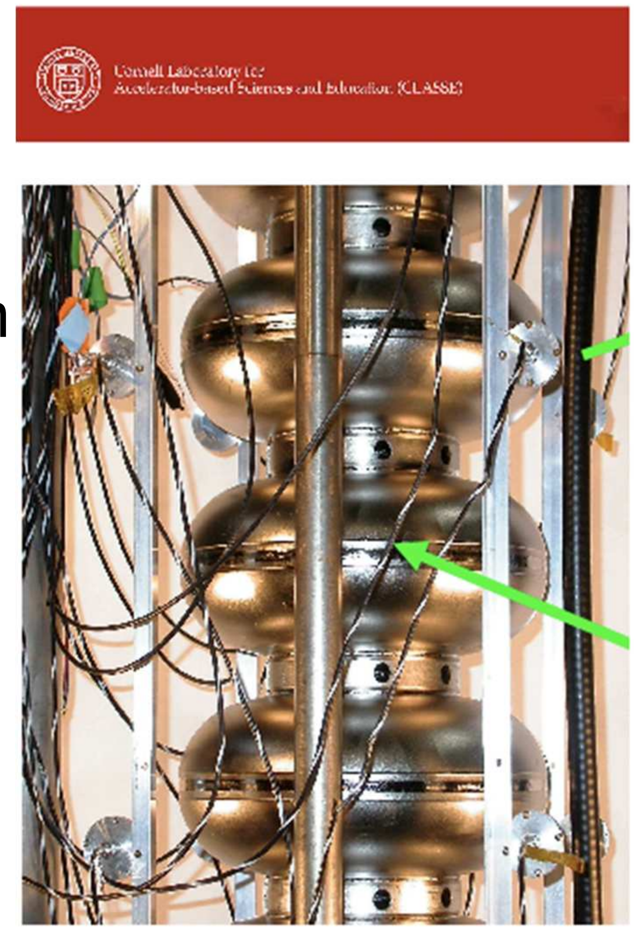

Overcoming Magneto-Thermal Breakdown

- Removal quench-causing geometric defects
  - Then remove identified defects
    - Local grinding by using robotic tc
    - Tumbling individual cell w/ defect
      - Leave other cell undisturbed
    - Local electron-beam re-melting
    - Local laser re-melting

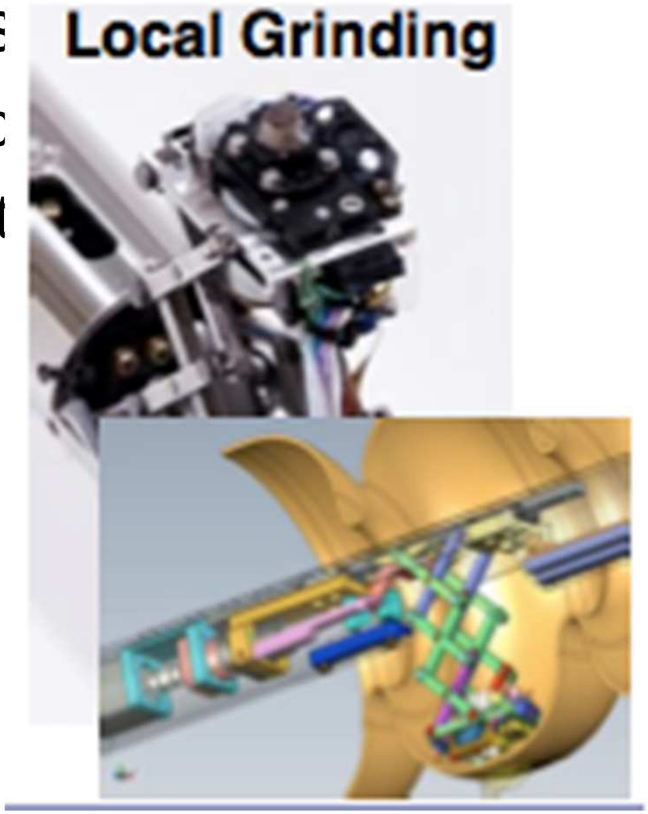

Courtesy H. Hayano

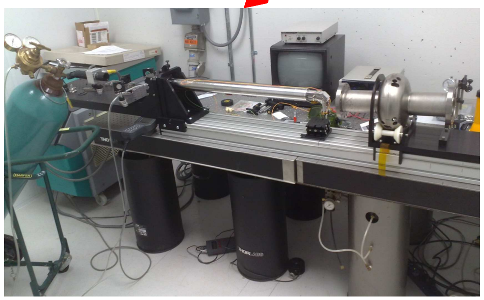

Courtesy M. Ge, G. Wu

Overcoming Quench

- Reducing peak surface magnetic field in cavity design

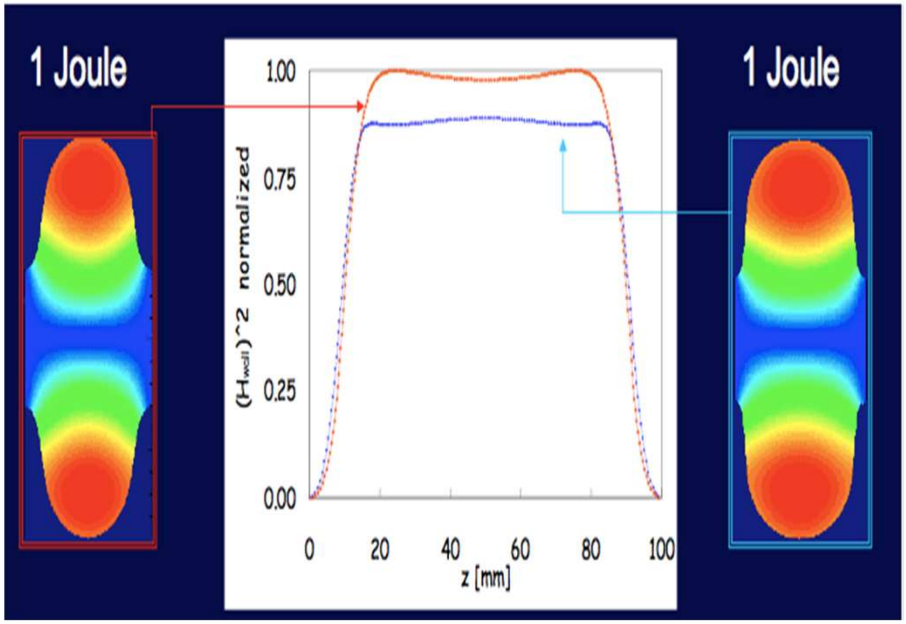

Courtesy J. Sekutowicz

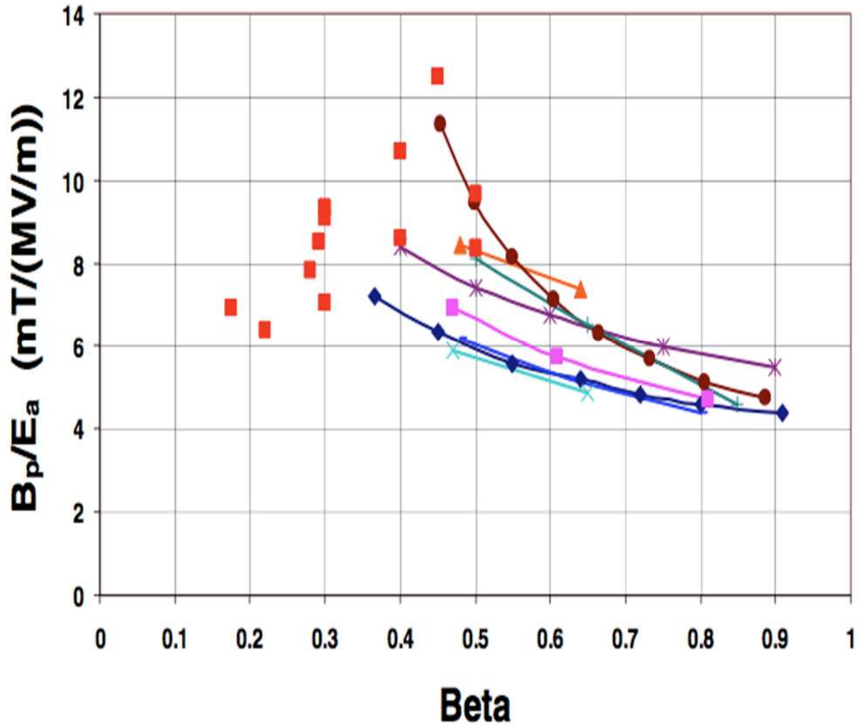

Overcoming Quench

- Use high thermal conductivity material for cavity wall
  - Nb/Cu clad material
  - Thin film coated copper or aluminum cavit

Some prototypes of Nb/Cu laminate cavities fabricated at DESY. Singer SRF-05

Courtesy W. Singer

1.3 GHz Nb coated Cu cavity by INFN in evaluation at JLab

Overcoming Quench

"Knobs" for improved reproducibility in overcoming local quench at very high gradient of 40-50 MV/m

Material
Nb: > 2000 Oe (exp.)
2400 Oe (the.)
Nb_3Sn: > 4000 Oe (the.)

Achievable gradient

Cavity surface chemistry

$$E_{acc}^{max} = d \cdot \frac{r \cdot H_{crit,RF}}{\beta_{MAG} \cdot (H_{pk}/E_{acc})}$$

Cavity wall thermal conductance

Cavity surface smoothness

Cavity shape

(1) Alternate cavity shape for reduced Hpk/Eacc ratio. In hand (LL, RE, LSF).
(2) Uniform cavity processing for reduced local "bad" spots. In hand (EP).
(3) Smooth surface for reduced local magnetic field enhancement. In hand(CBP & derivative + EP).
(4) Improved wall thermal conductance for increased local heating tolerance.
   - Cavity heat treatment optimization for "phonon peak engineering"
   - Use Nb/Cu composite material (such as explosion bonded material)
(5) The game-changing knob is a Nb replacement material (such as Nb_3Sn or Mg_2B w/ multi-layer).

Last Word on Quench

- RF critical field sets ultimate limit in achievable gradient
  - Still not settled theoretically
  - Experimentally observed quench seems to be always caused by local defect
    - There is one claim of 1-cell cavity reaching RF critical field experimentally
    - More measurements needed for independent confirmation
  - Experimental record peak surface magnetic field
    - Cornell 1-cell 1300 MHz re-entrant shape cavity: 2065 Oe
    - DESY 9-cell 1300 MHz large-grain TESLA-shape cavity: 1950 Oe
- Niobium is still the dominant material for known SRF based projects
  - Plenty intricate issues remain further understanding
  - Still room for improvement
- Niobium replacement materials are being actively explored

Multipacting (MP)

Symptom of Multipacting

- Gradient stops rising despite more RF power is provided to cavity
  - Barrier
- Detection of X-rays
- Detection of electrons by biased probes at right place
- “wavy” transmitted and reflected power signal
- Detection of temperature rise
  - “hot spot” may move

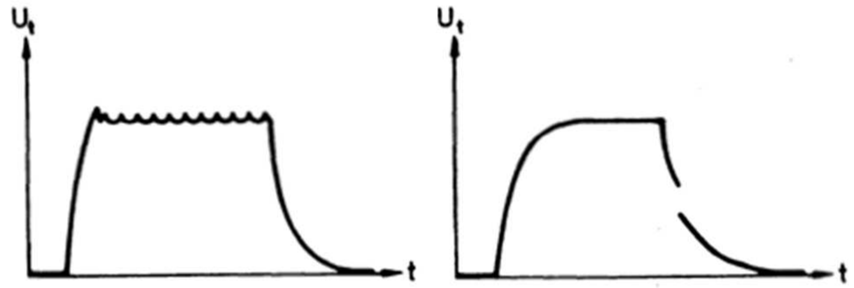

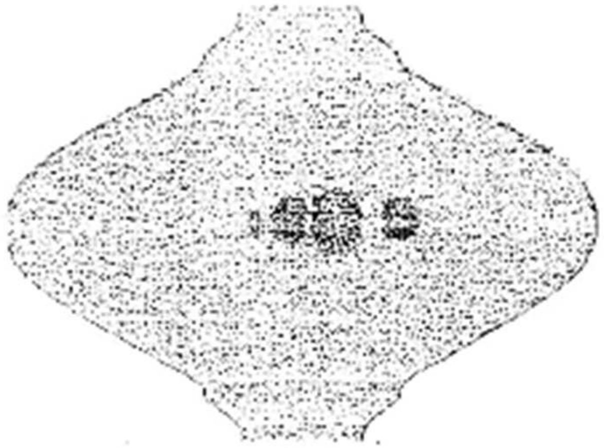

Symptom of Multipacting

- Barrier can be overcome if RF field is sustained (RF conditioning)
  - "Soft barrier" can be processed through in a few minutes
  - "Hard barrier" may take much longer time
- "Memory effect"
  - Some processed barrier may re-appear – "lost memory"
  - Some will not re-appear once processed – "memorized"
- Barrier usually has specific field range
  - Multipacting band width
- One cavity may have multiple barriers

Multipacting Diagnostics

- RF signal by crystal detector
- X-ray detector
- Thermometer
- Electron pick up probe

See previous slides on X-ray, thermal and electron diagnostic sensors

Physics of Multipacting

- Rapid growth of number of electrons from noise due to existence of conditions for resonant electron movement in cavity space
- Electron trajectories occupy only a small volume near cavity surface due to "confinement effect" by RF magnetic field
- Confined electrons return to cavity surface
- Electrons gain energy due to acceleration by RF electric field
- Energetic electrons bombard surface, causing secondary electron emission
- Process becomes self sustained when secondary electron emission coefficient of surface is larger than 1

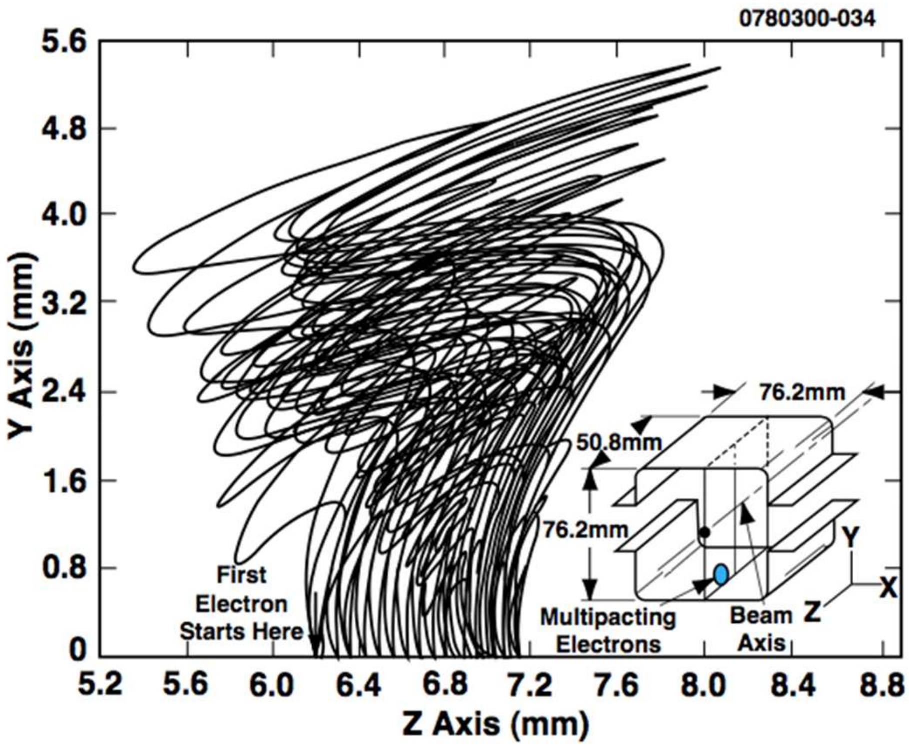

Understanding of Multipacting

- Electrons gain kinetic energy by consuming energy stored in cavity RF field
  - This causes Q_0 drop
- Energetic electrons bombard cavity surface
  - This deposit heat, causing local temperature rise
    - When Tc is exceeded, local surface area becomes normal conducting
      - Normal region grows due to resistive heating, leading to quench
  - This produce X-rays due to Bremsstrahlung effect

Understanding of Multipacting

- Secondary electron emission
  - Secondary electrons are low energy 2-5 eV
  - Secondary electron yield (SEY) depends on impact energy of primary electrons
    - First cross-over energy E_1
    - Second cross-over energy E_2
  - SEY is a material property and sensitive to surface condition
    - Electron bombardment reduces SEY
      - Conditioning effect

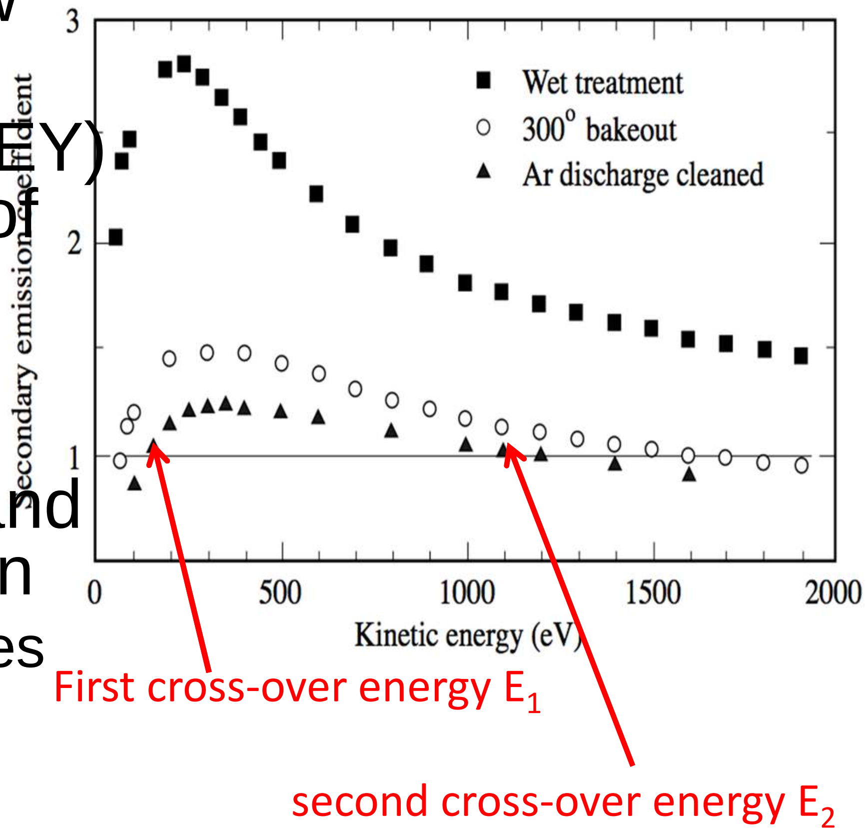

Understanding of Multipacting

- Resonant conditions are met for limited field ranges
  - MP bands are separated with finite bandwidth
- MP electrons travel time from emission to bombardment is integer multiple of RF period or integer multiple of half period
  - This explains linear frequency scaling of MP barrier
    - Emitted secondary electron experiences more acceleration within 1- or ½-period at lower frequency
      - Electron reach the first cross-over energy (E_1) at a lower gradient
  - This explains higher order MP barrier at lower gradient

Elliptical cavity
2-point MP
Frequency scaling

$$B[mT] = 5 + 55f[GHz]$$

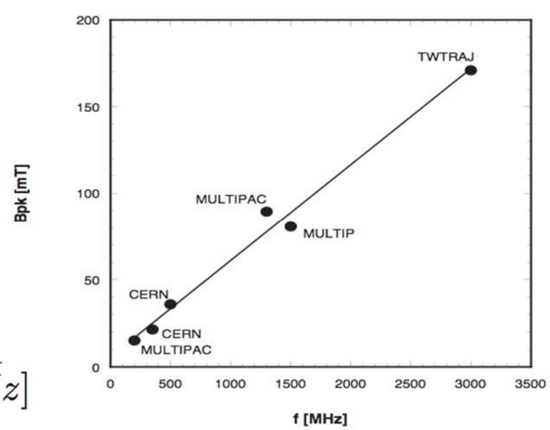

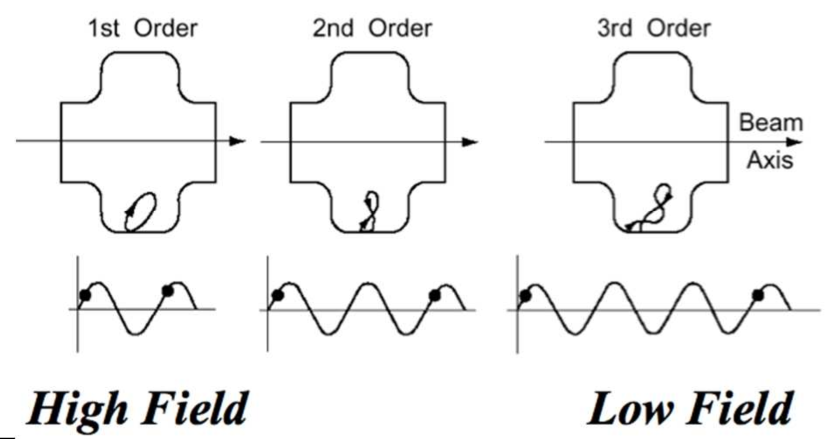

Understanding of Multipacting

- One or more local areas might be involved in MP
  - 1-point MP (1-side MP)
  - 2-point MP (2-side MP)

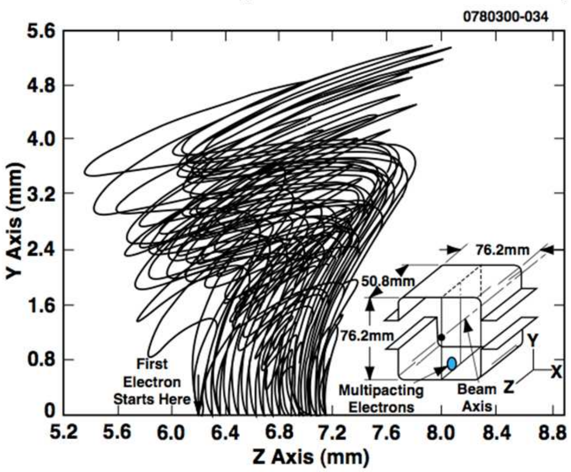

1-point MP
Muffin-tin cavity

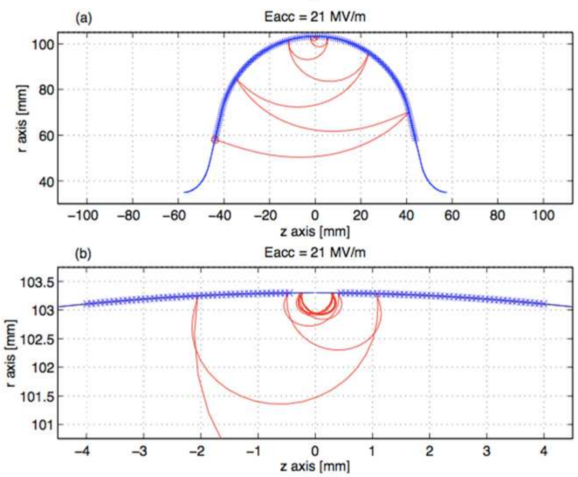

2-point MP
Elliptical β=1 cavity

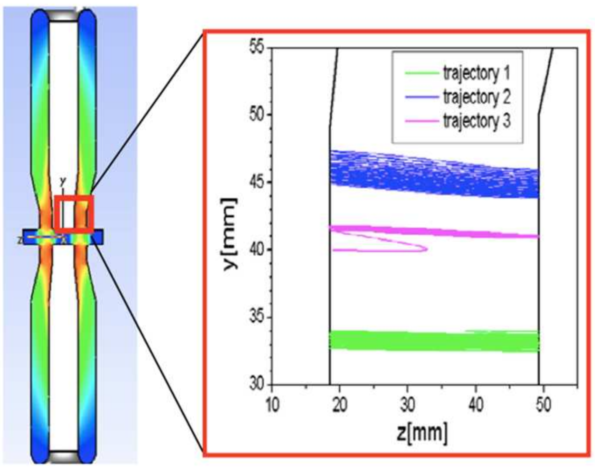

2-point MP
Half-wave β<1 cavity

Understanding of Multipacting

- Multipacting in beam pipe transition

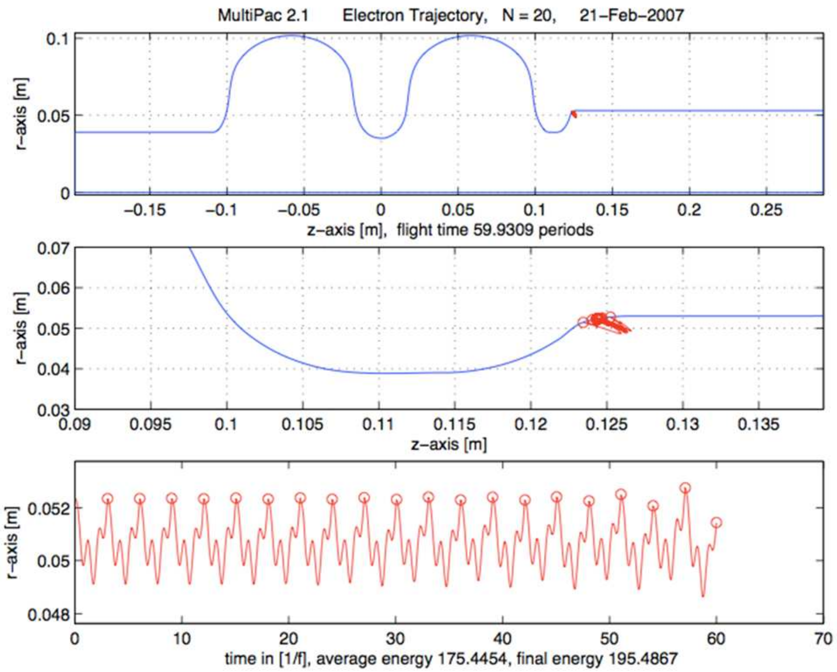

2-cell Cornell Injector prototype

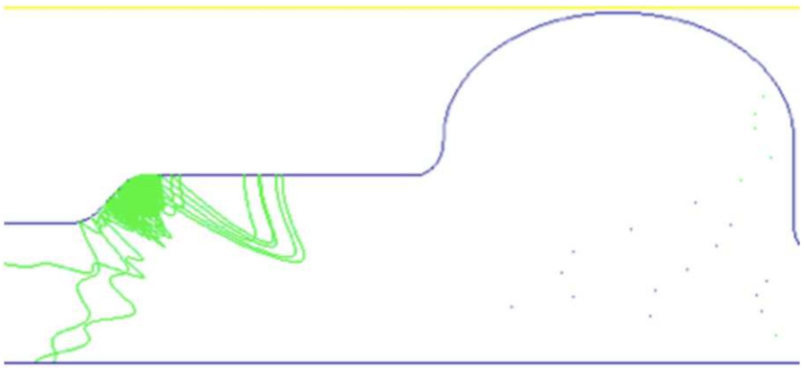

ICHIRO cavity early design

Courtesy Y. Morozumi

Understanding of Multipacting

- Multipacting is an issue of interest in higher order mode coupler and fundamental power coupler for cavity

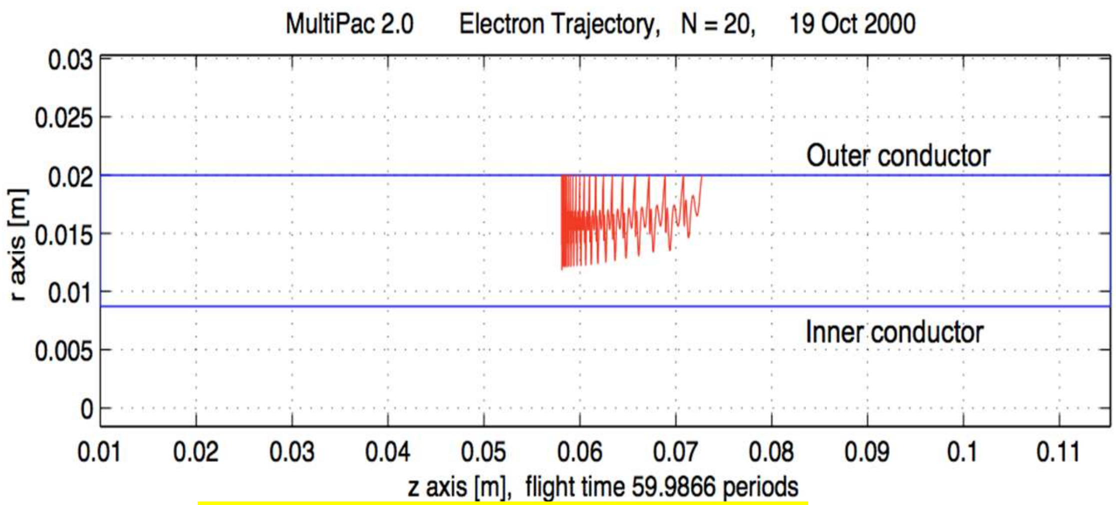

1-side 3rd order MP in coaxial coupler

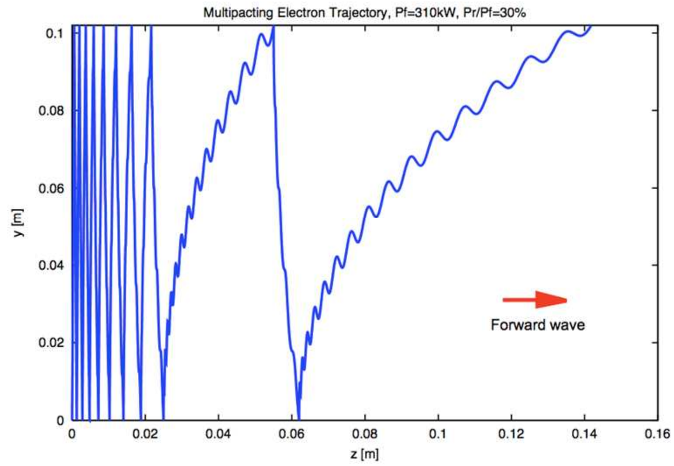

2-side 5th order MP in waveguide coupler

P. Ylä-Oijala, TESLA Report, TESLA 97-21, (1997).

Overcoming Multipacting

- Avoid high SEY surface
  - Clean surface
  - Oil free pumping system
- Mitigate by RF conditioning
  - Use fundamental mode
  - Use other modes
    - Pass-band modes
    - Lower order modes

Overcoming Multipacting

- Design cavity RF structure that is free from MP
  - Not easy to do for 3D structures, good new is that modern simulation tools are improving (see example below)

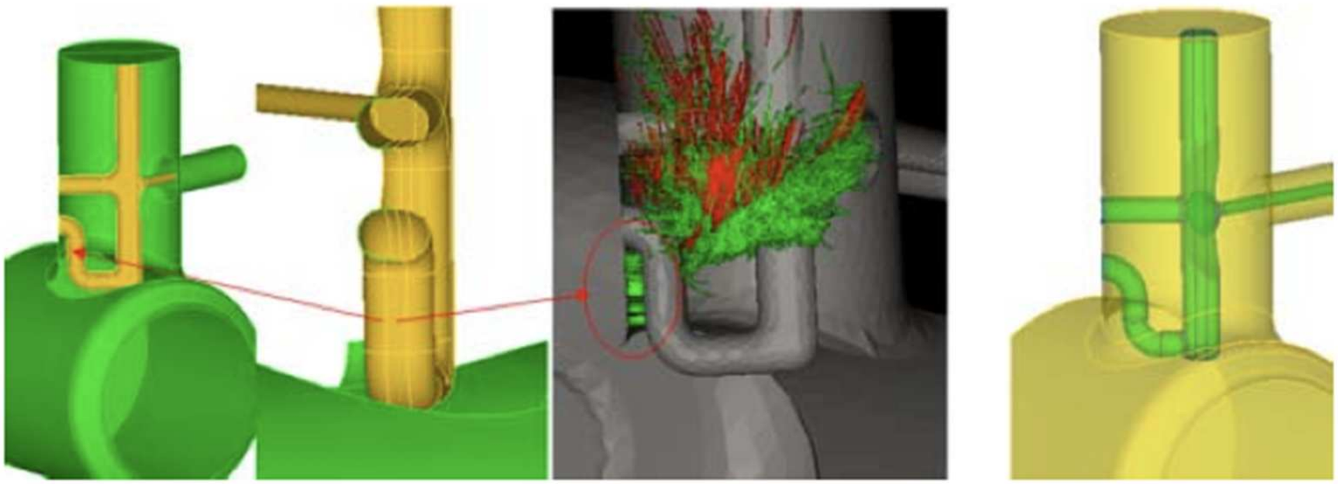

Figure 8: Multipacting in the HOM coupler (left). The multipacting was eliminated by changing the loop geometry from a racetrack cross section to a circular cross section (right).

Z. Li et al., SLAC-PUB-13088

Last Word on Multipacting

- Elliptical β=1 cavities are reaching very high gradients at 1300 MHz with no known limit due to hard MP
  - Soft MP barriers appear to ubiquitous
- MP issue needs further attention in following cavities
  - Elliptical β<1 cavities at 500-900 MHz
  - All TEM class cavities
- Experimental measurements are still essential in assessing MP characteristics of new cavity designs

Residual Losses

Symptom of Residual Losses

- Q_0 lower than what is expected from theory
  - BCS theory predicts exponentia $R_s \propto_n \omega^2 \lambda_L^3 \ell \exp\left(-1.86T_c/T\right)$ dependence of surface resistance
    - Recall $Q_0 = \frac{G}{R_s}$
  - Temperature independent term is called residual resistance
  - Residual resistance limits achievable Q_0

Symptom of Residual Losses

- Q-disease
  - Q_0 at low field degrades when cavity parked at a temperature 70-150 K for extended period of time
  - Similar effect when cavity cool down rate is slower than 1K/min in passing 70-150 K

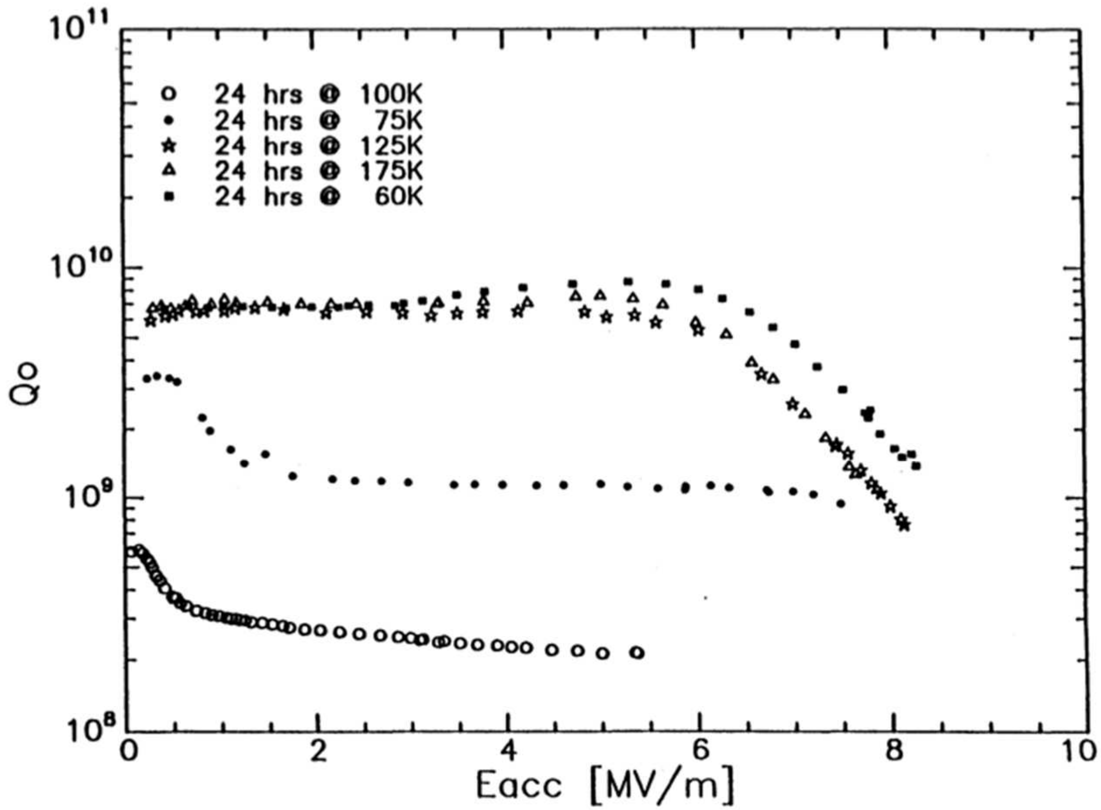

Figure 1 : Eacc – Dependence of Q – Degradation on "Holding"Temperature

J. Halbritter, P. Kneisel, K, Saito, SRF1993

Understanding of Residual Losses

- There are multiple sources for residual losses
- Known sources
  - Surface contamination
    - Dielectric losses
  - Electric interface
  - Grain boundaries
  - Frozen flux effect
  - Hydride phase (Q-disease)

J. Halbritter, "On RF residual losses in superconducting cavities," in *Proc. 2nd Workshop on RF Supercond., Geneva, Switzerland, 1984, pp. 427-446.*

Understanding of Residual Losses

- Frozen flux effect
  - DC magnetic field is “trapped”
    - Fluxon
    - Normal conducting core
  - Sources of DC magnetic field
    - Earth magnetic field
    - Thermal-electric current due to temperature gradient during cavity cool down or local quench during test
  - Mechanisms of losses
    - RF dissipation at n.c. core
    - Fluxon dynamical flow

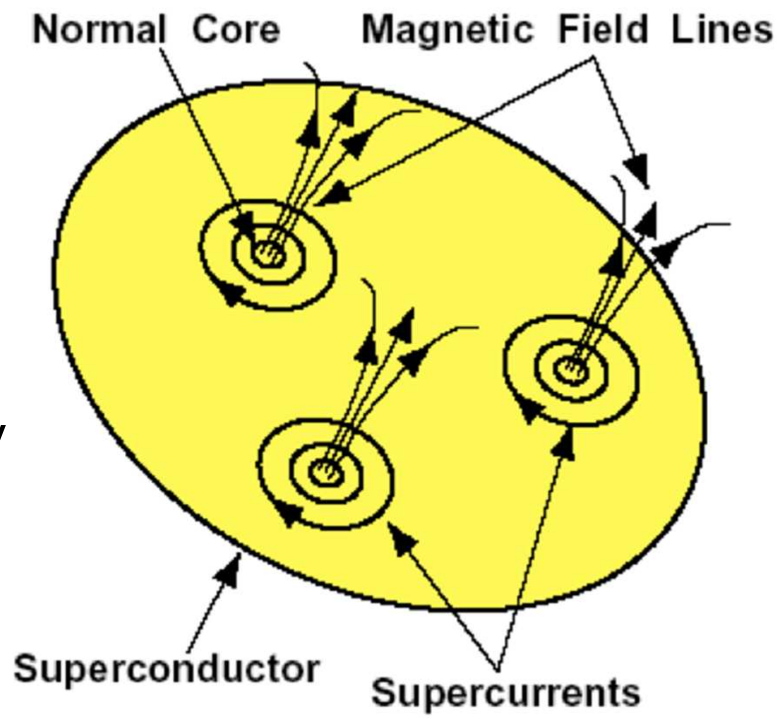

Understanding of Residual Losses

- Scaling of residual resistance due to frozen flux effect
  - Linear dependence on external field H_{ext}
  - Inverse linear dependence on second critical field H_{c2}
  - Linear dependence on superconductor's normal state surface resistance R_n
- Frequency scaling: $\sqrt{f}$
  - Recall $R_n \sim \sqrt{f}$

$$R_{\Phi} \approx \frac{H_{\mathrm{ext}}}{2H_{\mathrm{c2}}} R_{\mathrm{n}}$$

For Nb, residual resistance contribution due to frozen flux:

$$R_{res} = \alpha H_{dc} \sqrt{f / GHz}$$

α = 0.2-0.3 nΩ/mG

Understanding of Residual Losses

- Hydride phase
  - Nb-H system undergoes phase transition at low temperatures
  - H mobility still high at 100 K
    - H in bulk Nb precipitates
    - Forms islands of weak superconductor
  - Danger arises when bulk H concentration in Nb > 2 wt ppm
  - Higher danger for high purity Nb
    - H is bound by impurities

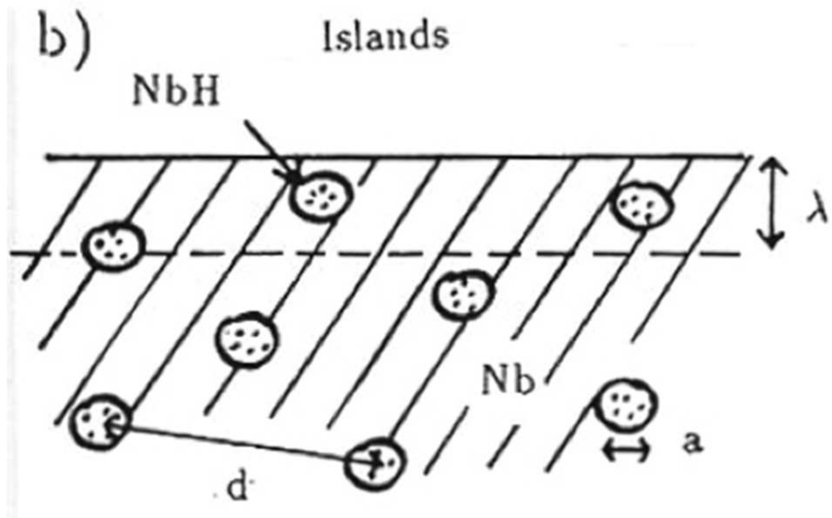

Overcoming Residual Losses

- Shield ambient magnetic field
  - < 15 mG or better
- Use non-magnetic material and low-permeability material within shield
- Nb-Cu thin film cavity
  - Much less sensitive to frozen flux effect due to high Hc_2
- Go to low frequency
  - Take advantage of $\sqrt{f}$

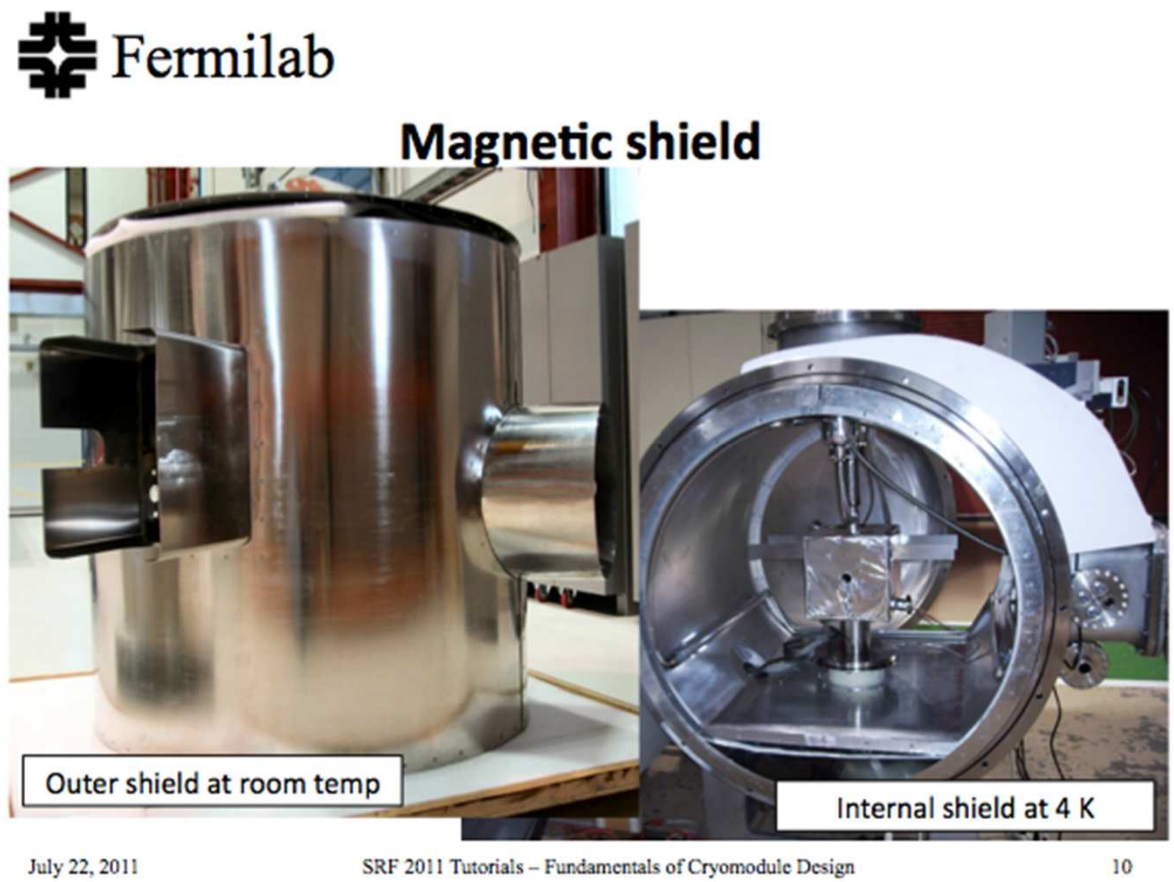

Friday tutorial by T. Nicol, FNAL

Overcoming Residual Losses

- Minimize H uptake from processing
  - BCP etching at < 15 ℃
  - “H free” EP
- Hydrogen out-gassing in vacuum furnace
  - 800 ℃ x 2hr
  - Or at lower temperature for longer time
- Minimum or no chemistry after out-gassing

Overcoming Residual Losses

- Use large-grain Nb

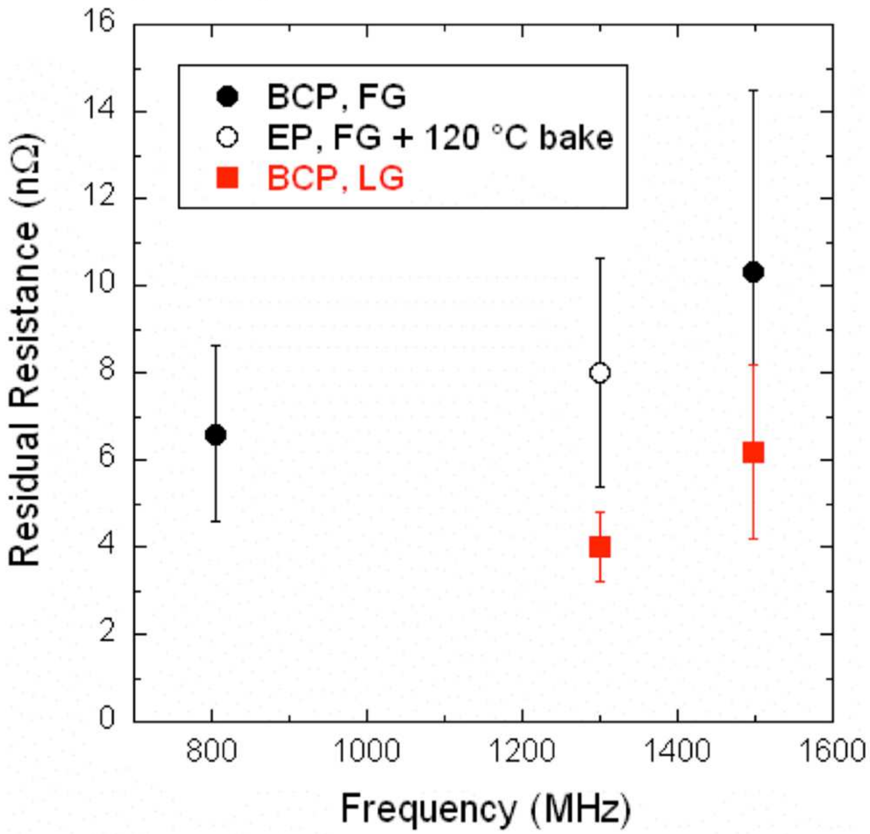

BCP etched large grain cavity
$\langle R_{res} \rangle = 4$ nΩ

G. Ciovati et al., STTIN2010

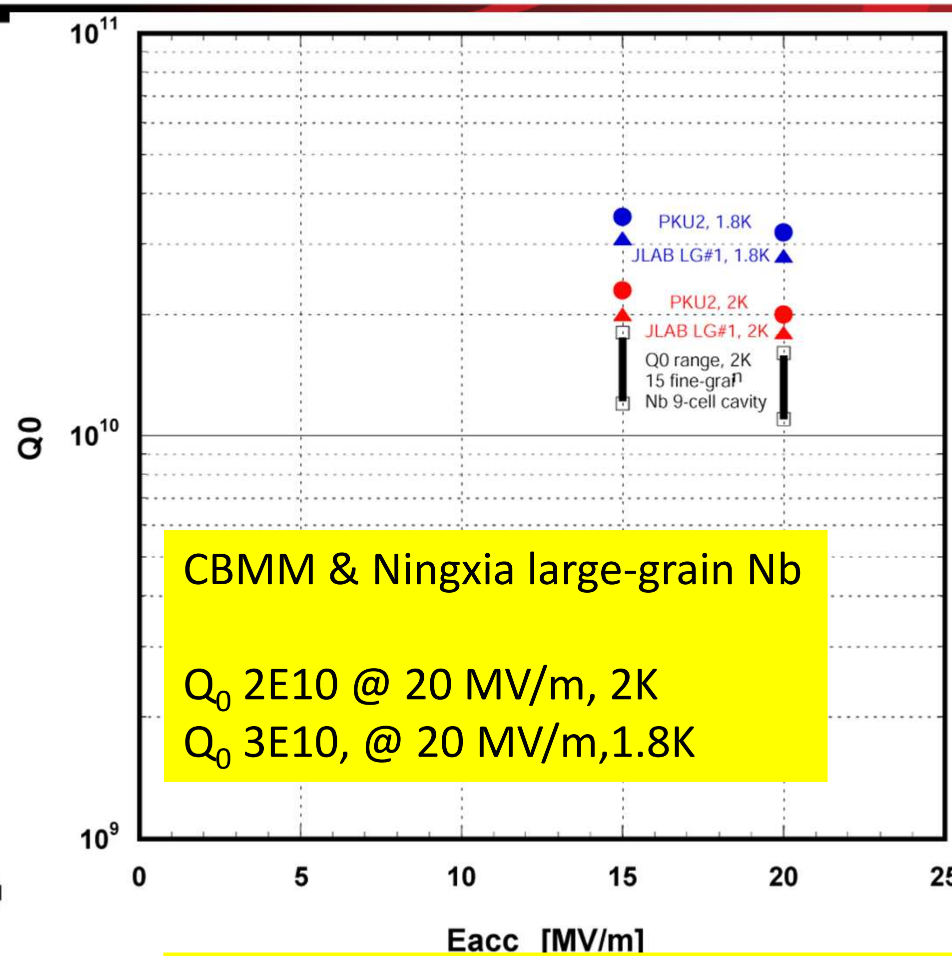

CBMM & Ningxia large-grain Nb

Q_0 2E10 @ 20 MV/m, 2K
Q_0 3E10, @ 20 MV/m,1.8K

Latest 9-cell 1300 MHz cavity data with final EP tested in the same dewar
$\langle R_{res} \rangle = 8$ nΩ, finge grain Nb cavity
$R_{res} = 3\text{-}4$ nΩ, large-grain Nb cavity

Overcoming Residual Losses

- Use large-grain Niobium material

BCP etched large grain cavity
9-cell 1300 MHz
Consistent lower surface resistance with more than 10 cavities

Heraeus large-grain Nb

$<Q_0> = 2E10$ @ 20 MV/m, 2K
Q_0 3-4E10 @ 20 MV/m, 1.8K

W. Singer et al., STTIN2010

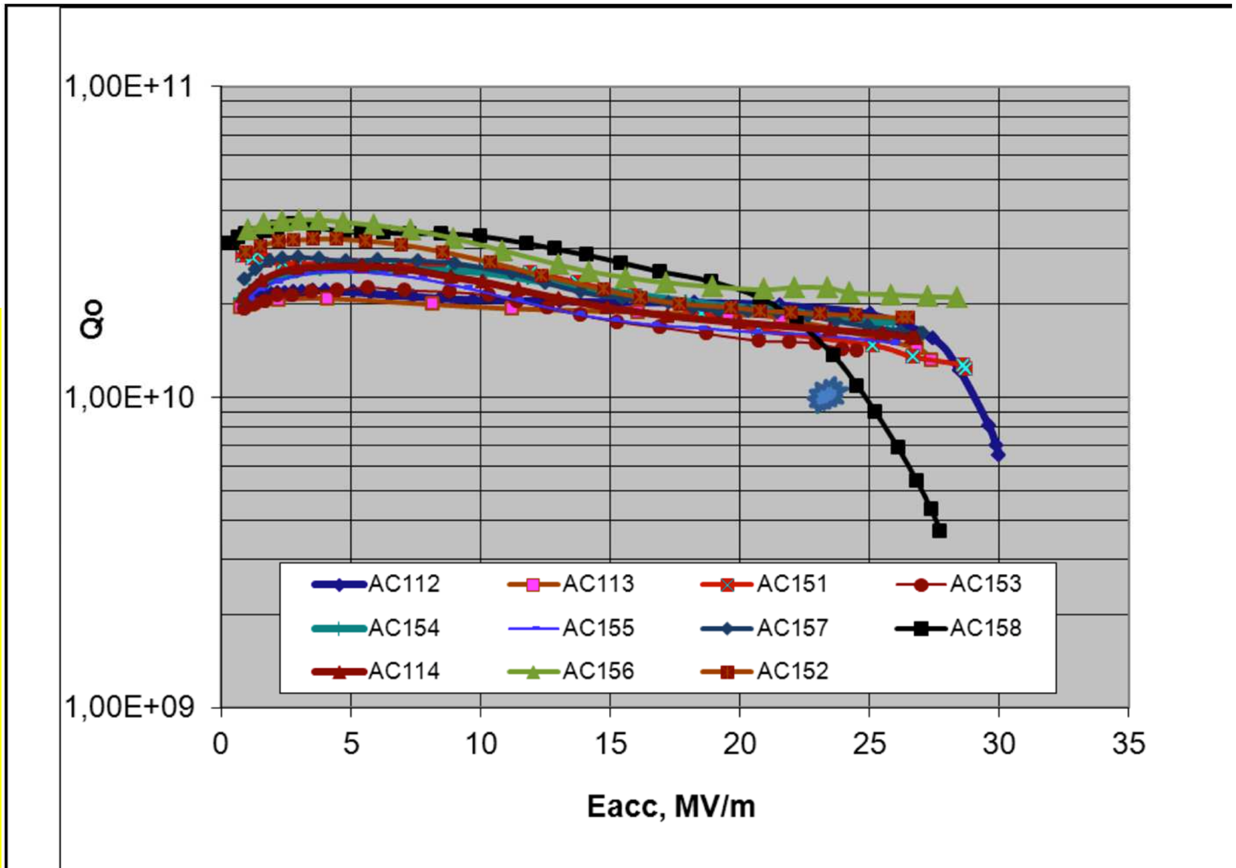

Figure 7: Q(Eacc) of the cavities AC112- AC114 and AC151-AC158 at 2K. Test after 100 µm rough BCP, annealing at 800°C for 2h followed by a fine BCP 20 µm and baking at 120°C for 48h (AC112 was not baked). Star shows the XFE requirements

Q-Drop/Q-Slope

Symptom of Q-drop/Q-slope

- Q_0 declines as field is raised
  - Without any X-ray present
  - Decline starts at gradient 3-4 MV/m
    - "Medium field Q-slope"
  - Rapid decline above 20 MV/m
    - "High field Q-slope"
  - Observable in bulk Nb cavities, Nb thin film coated Cu cavities and Nb_3Sn coated cavities

Understanding of Q-drop/Q-slope

- This is an active area of research presently in SRF community
  - Theoretical
    - Non-linear BCS
    - Vertex
    - …
  - Experimental
    - Oxygen
    - Dislocation
    - Magnetic impurities
    - …

Overcoming Q-drop/Q-slope

- Fine-grain Nb cavities
  - Electropolishing + 120 ℃ bake (48 hours)
- Large-grain Nb cavities
  - Buffered Chemical Polishing + 120 ℃ bake (12-24 h ours) also

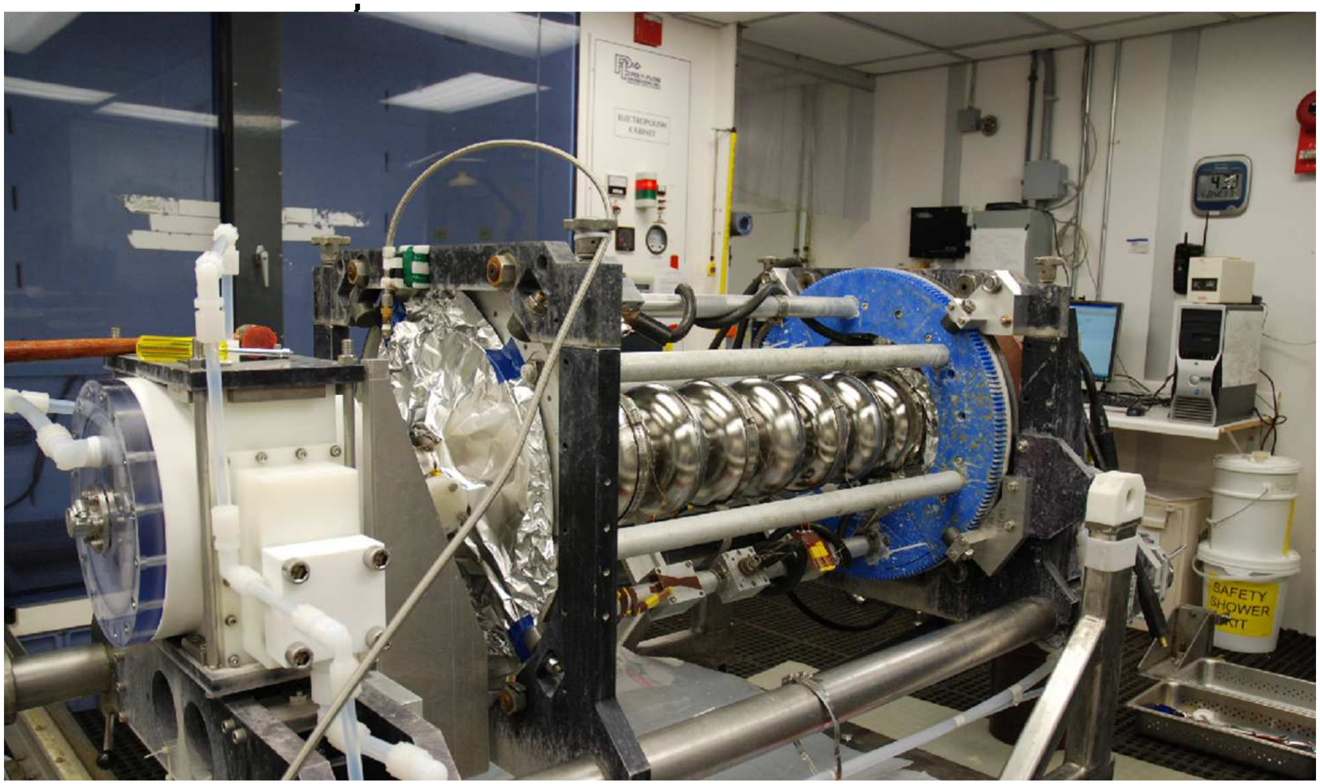

• Mixture of HF and sulfuric acid half-filled, flows slowly in closed-loop
• Aluminum cathode runs across cavity length
• 14.5 V voltage
across cathode and cavity, draws a current of 100-200 A
• cavity slowly rotates, cell temperature controlled

Overcoming Q-drop/Q-slope

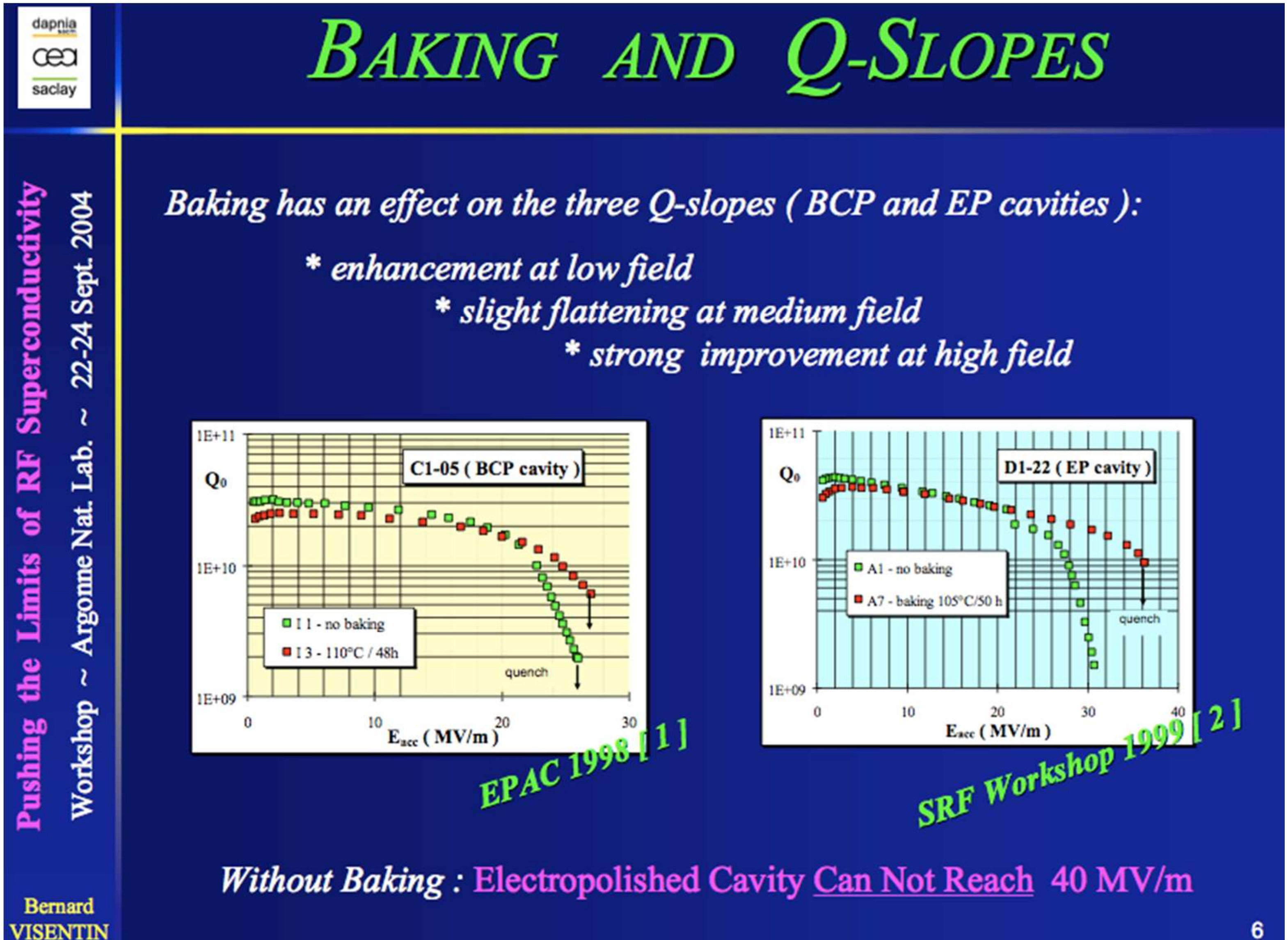

Cavity Performance Limits
and
SRF Based Accelerators

Performance Pushing Directions

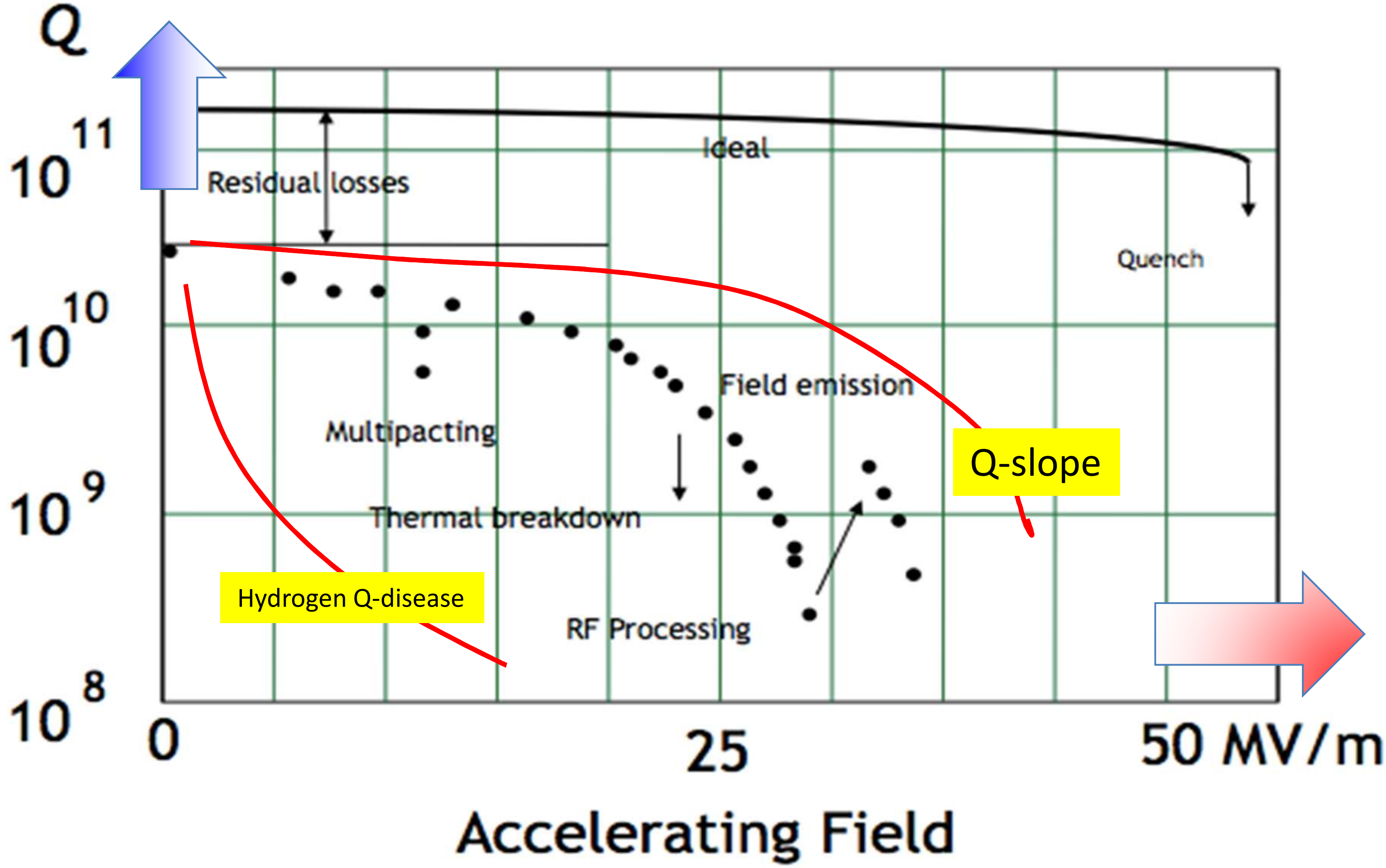

Achieved Peak Surface Electric Field in L-band SRF Niobium Cavities
(Circle: Single-Cell Cavity; Triangle: Multi-Cell Cavity)

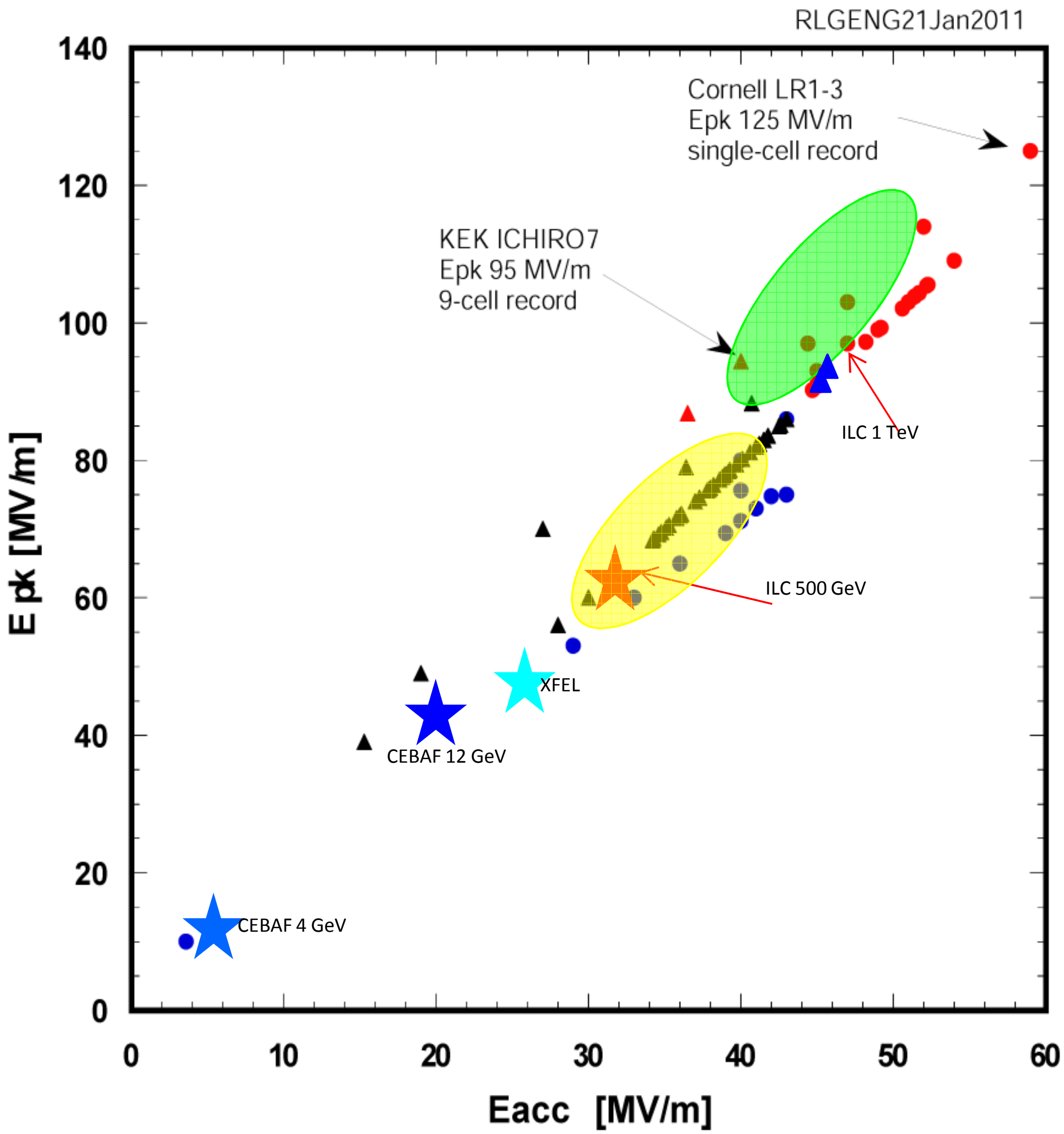

Achieved Peak Surface Magnetic Field in L-band SRF Niobium Cavities
(Circle: Single-Cell Cavity; Triangle: Multi-Cell Cavity

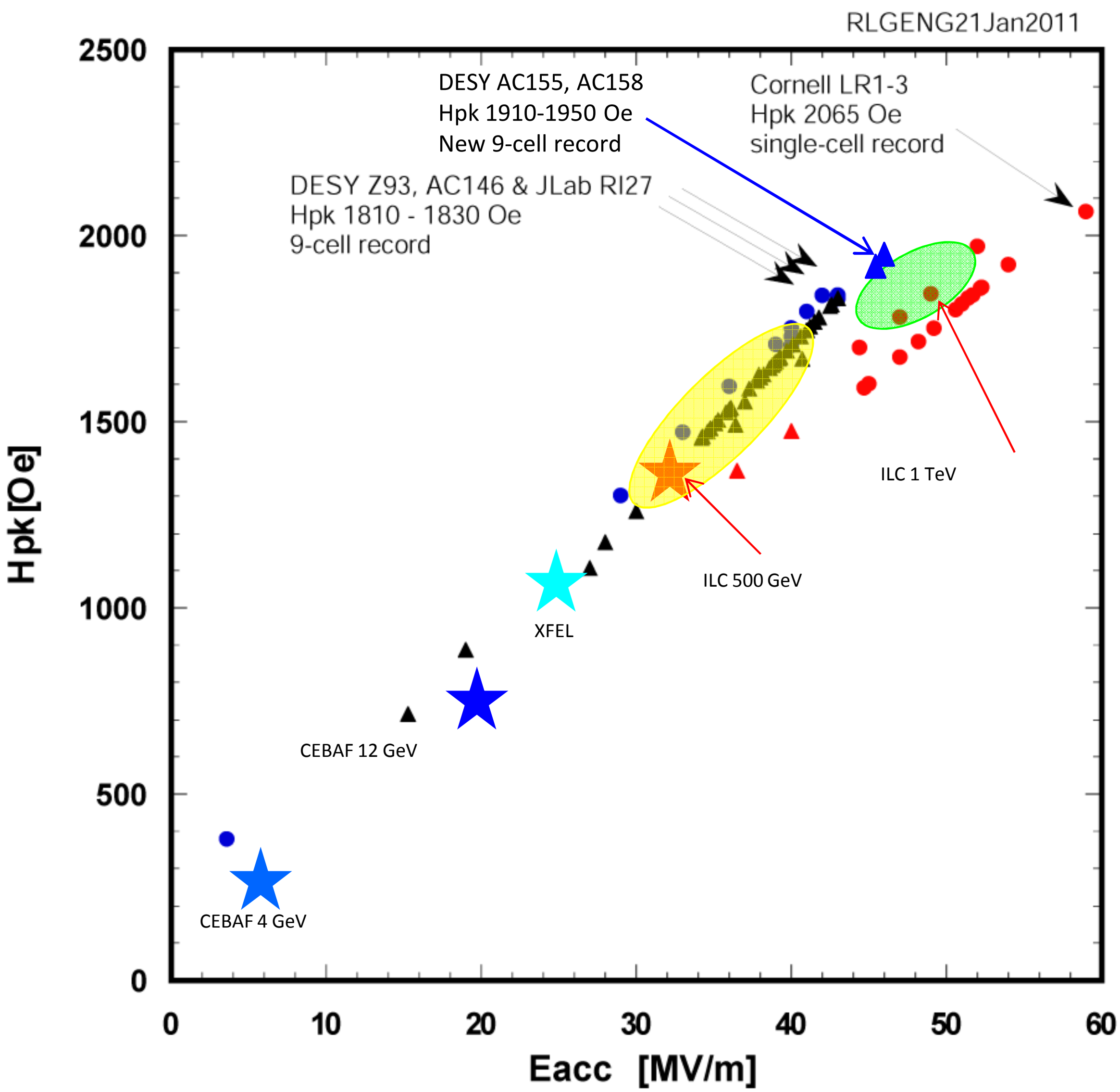

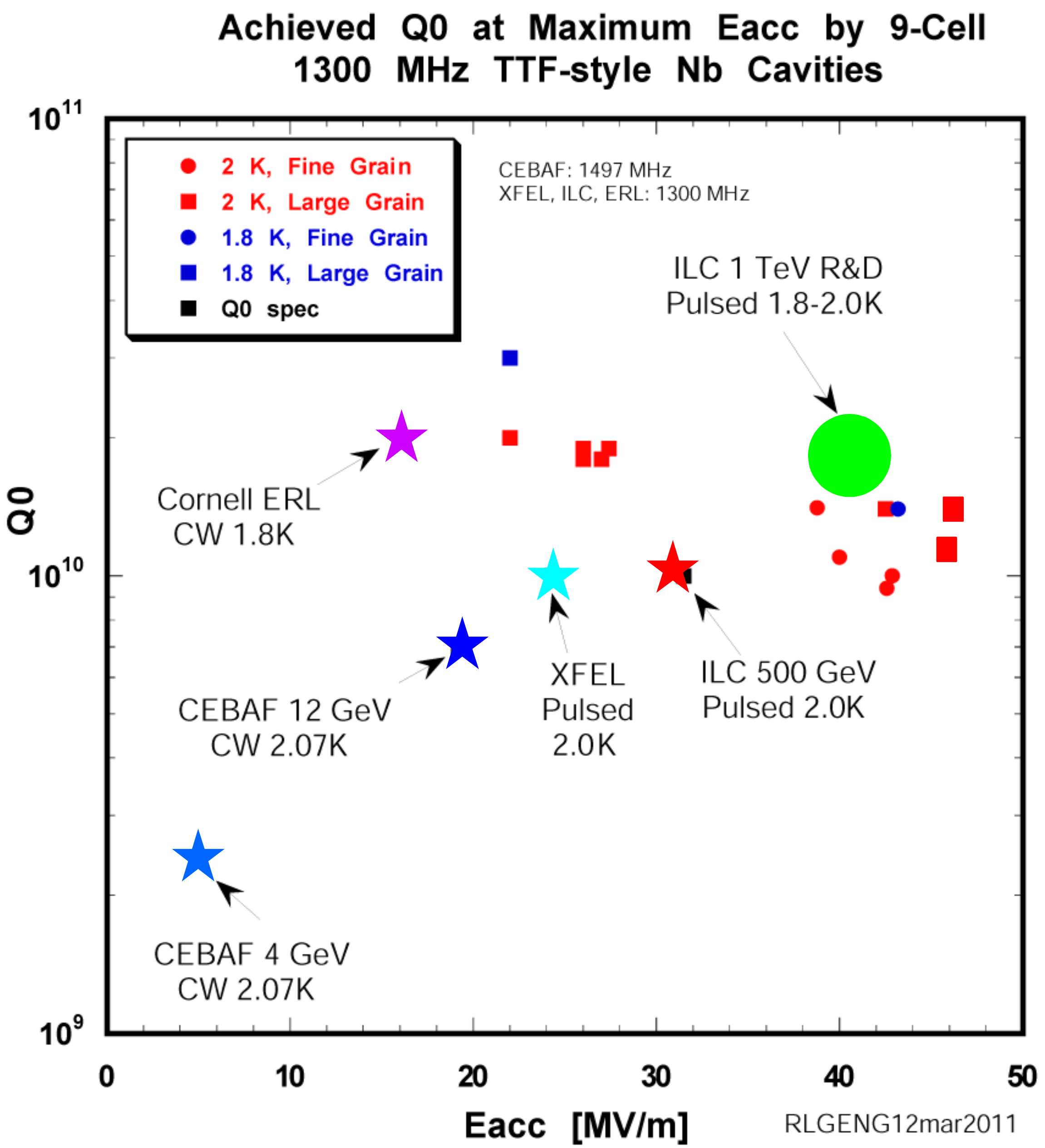

Achieved Q0 at Maximum Eacc by 9-Cell
1300 MHz TTF-style Nb Cavities
2 K, Fine Grain
2 K, Large Grain
1.8 K, Fine Grain
1.8 K, Large Grain
Q0 spec
CEBAF: 1497 MHz
XFEL, ILC, ERL: 1300 MHz
ILC 1 TeV R&D
Pulsed 1.8-2.0K
Cornell ERL
CW 1.8K
XFEL
Pulsed
2.0K
ILC 500 GeV
Pulsed 2.0K
CEBAF 12 GeV
CW 2.07K
CEBAF 4 GeV
CW 2.07K
Q0
10^{11}
10^{10}
10^{9}
0
10
20
30
40
50
Eacc [MV/m]
RLGENG12mar2011

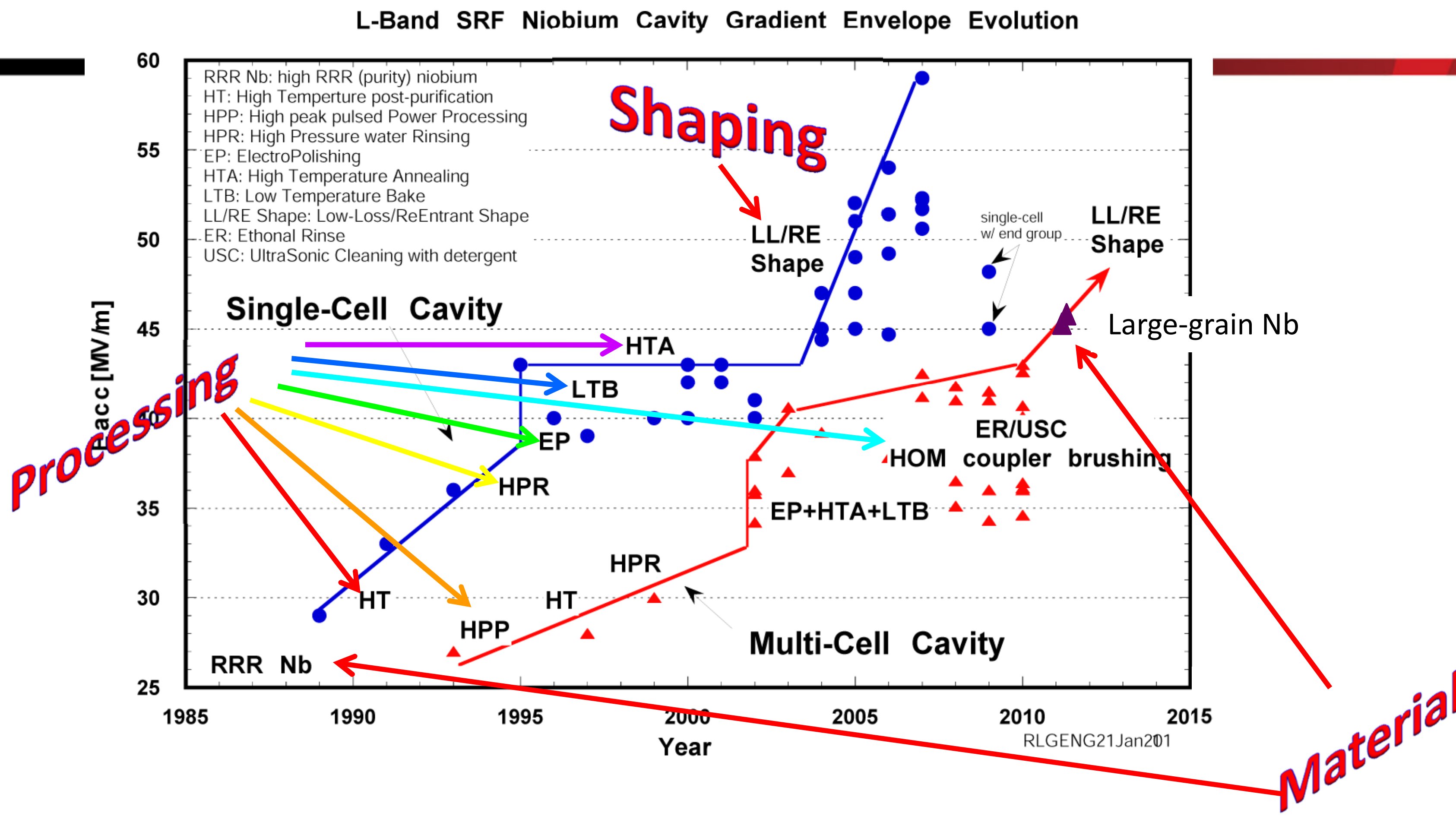

Understanding in gradient limits and inventing breakthrough solutions are responsible for gradient progresses. This has been a tradition in SRF community and rapid gradient progress continues. Up to 60 MV/m gradient has been demonstrated in 1-cell 1300 MHz Nb cavity. 45-50 MV/m gradient demonstration in 9-cell cavity is foreseen in next 5 years.

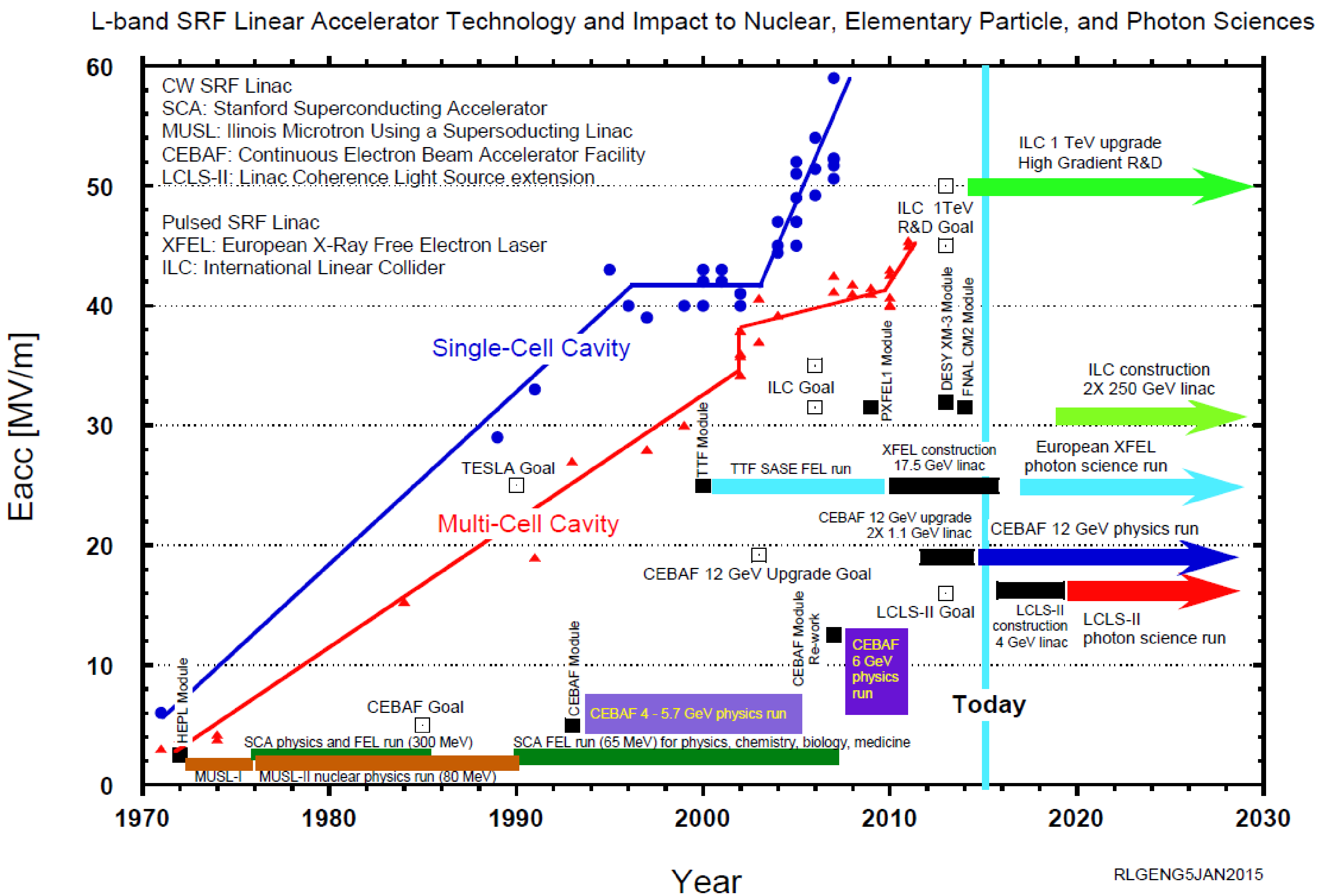
L-band SRF Linear Accelerator Technology and Impact to Nuclear, Elementary Particle, and Photon Sciences
CW SRF Linac
SCA: Stanford Superconducting Accelerator
MUSL: Ilinois Microtron Using a Supersoducting Linac
CEBAF: Continuous Electron Beam Accelerator Facility
LCLS-II: Linac Coherence Light Source extension
Pulsed SRF Linac
XFEL: European X-Ray Free Electron Laser
ILC: International Linear Collider
Eacc [MV/m]
Year
Single-Cell Cavity
Multi-Cell Cavity
ILC 1 TeV upgrade High Gradient R&D
ILC 1TeV R&D Goal
ILC construction 2X 250 GeV linac
ILC Goal
TESLA Goal
TTF Module
TTF SASE FEL run
XFEL construction 17.5 GeV linac
European XFEL photon science run
PXFEL1 Module
DESY XM-3 Module
FNAL CM2 Module
CEBAF 12 GeV upgrade 2X 1.1 GeV linac
CEBAF 12 GeV physics run
CEBAF 12 GeV Upgrade Goal
LCLS-II Goal
LCLS-II construction 4 GeV linac
LCLS-II photon science run
CEBAF Module Re-work
CEBAF 6 GeV physics run
CEBAF Module
CEBAF 4 - 5.7 GeV physics run
CEBAF Goal
HEPL Module
SCA physics and FEL run (300 MeV)
SCA FEL run (65 MeV) for physics, chemistry, biology, medicine
MUSL-I
MUSL-II nuclear physics run (80 MeV)
Today
RLGENG5JAN2015

Cavity Fabrication and Processing

Niobium Material

- Niobium is the elemental superconductor with the highest critical temperature and the highest critical field
- Formability like OFHC copper
- Commercially available in different grades of purity (RRR> 250)
- Can be further purified by UHV heat treatment or solid state gettering

- High affinity to interstitial impurities such as C,H,O,N (in air at temperature < 150 ℃)
- Require electron beam welding for joining
- Metallurgy not so easy
- Hydrogen can be easily absorbed, leading to Q-disease

Niobium and Other SC Materials

Material	Tc [K]	Hc, Hc1 [Oe]	Type	Fabrication
Pb	7.2	803	I	electroplating
Nb	9.25	1900, 1700	II	Forming+EBW or film coating
Nb_3Sn	18.2	5350,300	II	Film coating
MgB_2	39	4290,300	II	Film coating

Niobium Production

- Niobium Ore in Araxa mine (open air pit) is Bariopyrochlor with 2.5% Nb_2O_5
- The ore is crushed and magnetite is magnetically separated from the pyrochlor.
- By chemical processes the ore is concentrated in Nb contents (50 –60 % of Nb_2O_5
- A mixture of Nb_2O_5 and aluminum powder is being reacted to reduce the oxide to Nb
- This Nb is the feedstock for the EBM processes

H.R.Salles Moura,"Melting and Purification of Nb", Proc.Intern.Sumposium Niobium 2001,Dec 2-5, 2001, Orlando Fl, p.147

CBMM deposit in Araxa, Brazil

EBM Ingots at CBMM

Electron Beam Melting

- High purity niobium is made by multiple electron beam melting steps under vacuum
  - This eliminates volatile impurities
- Several companies produce RRR niobium in large quantities
  - Cabot (USA), CBMM(Brazil), Tokyo Denkai (Japan), W.C. Heraeus (Germany), OTIC(China), Wah Chang (USA)
- RRR: Residual Resistivity Ratio
  - resistivity at room temperature divided by the resistivity at 4.2K in the normal conducting state
  - RRR scales roughly linearly with thermal conductivity at 4.2K
    - *K*(4.2K)~RRR/4

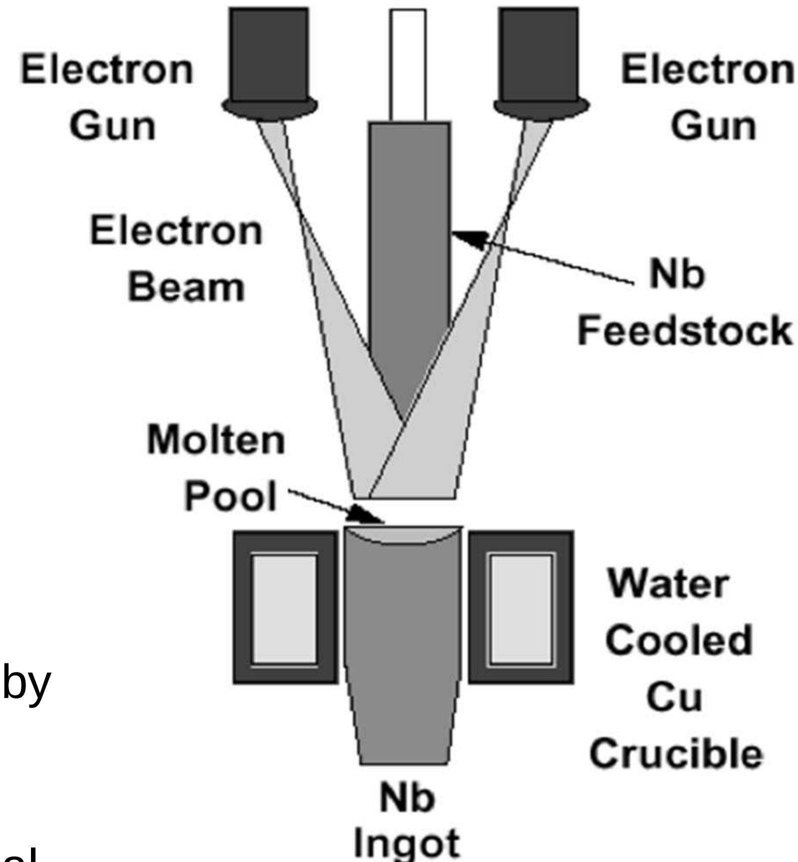

Process flow of the industrial Nb production

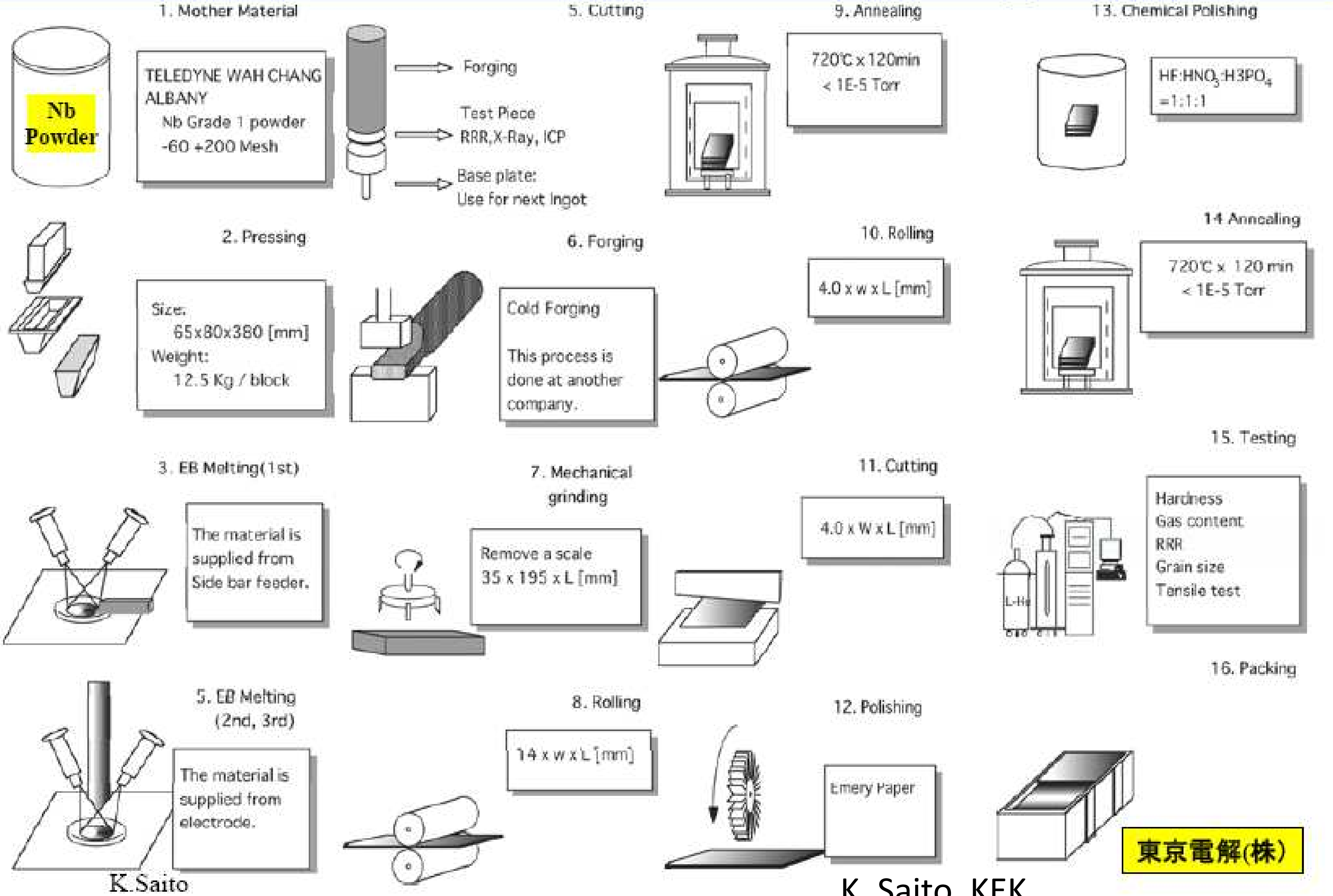

K. Saito, KEK

Large-Grain Material Multi-Wire Slicing

Successfully Developed Wire Sawing Method for Nb Ingot

KEK/Tokyodenkai/Izumi-tech

インゴットのスライス法に関する
特許申請中！

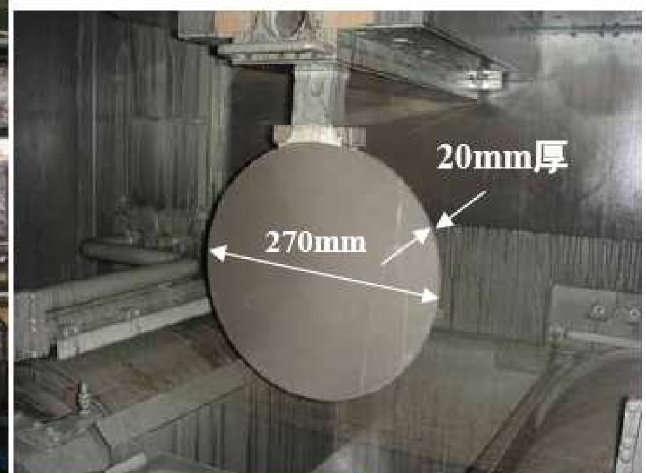

所時間:39時間

中講義2008

K. Saito, KEK

Overview of Cavity Fabrication

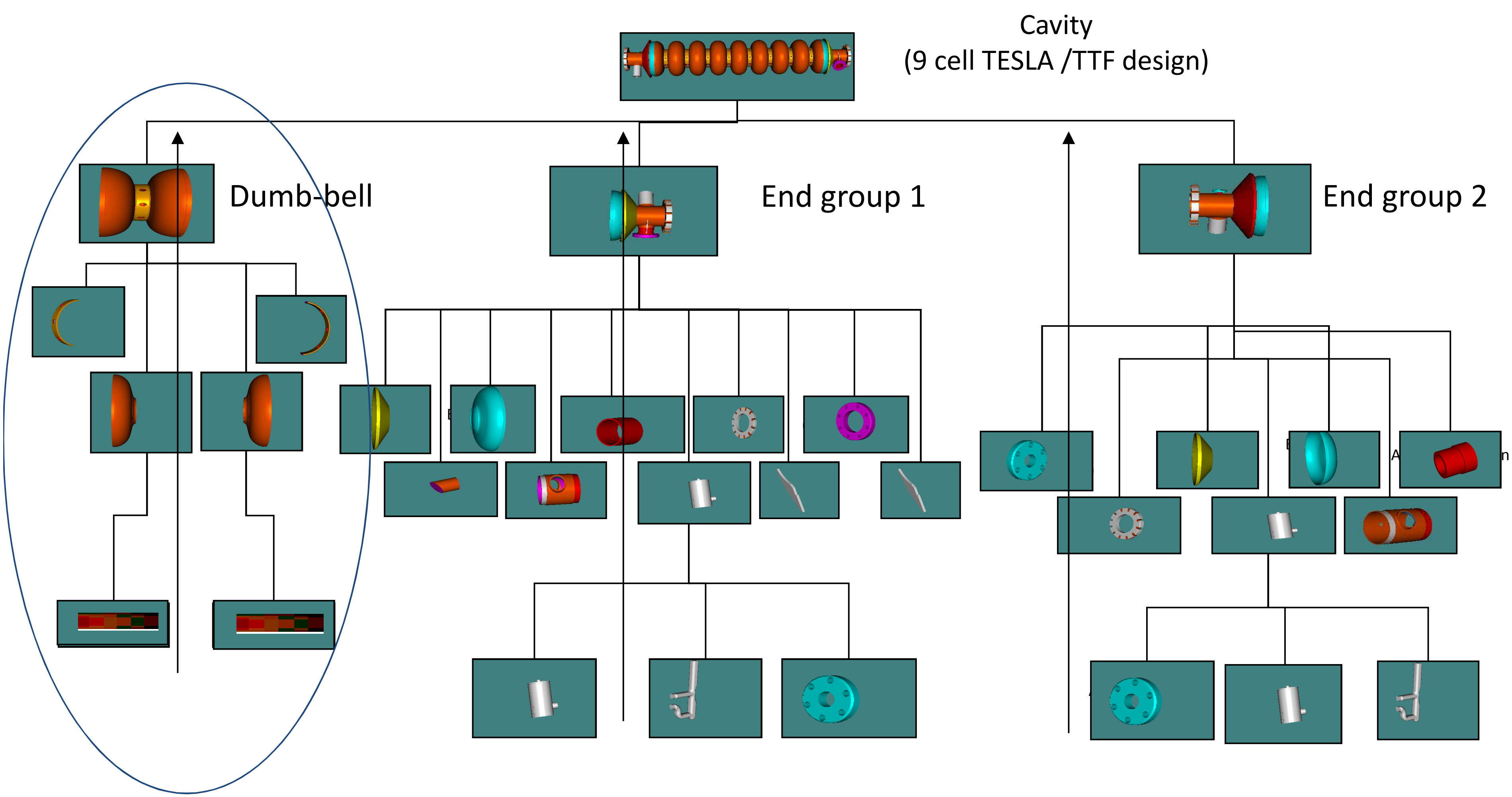

A. Matheisen, DESY

Example: Dumbbell Fabrication

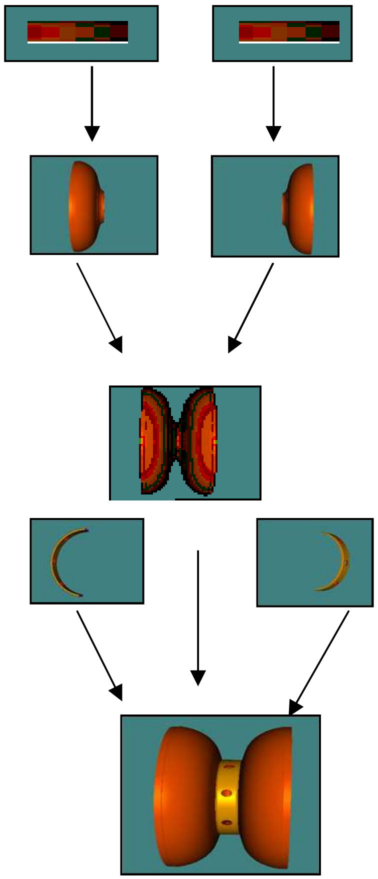

Dumb- bell

1. Mechanical measurement
2. Cleaning (by ultra sonic [us] cleaning +rinsing)
3. Trimming of iris region and reshaping of cups if needed
4. Cleaning
5. Rf measurement of cups
6. Buffered chemical polishing + Rinsing (for welding of Iris)
7. Welding of Iris
8. Welding of stiffening rings
9. Mechanical measurement of dumb-bells
10. Reshaping of dumb bell if needed
11. Cleaning
12. Rf measurement of dumb-bell
13. Trimming of dumb-bells (Equator regions)
14. Cleaning
15. Intermediate chemical etching (BCP /20- 40 µm)+ Rinsing
16. Visual Inspection of the inner surface of the dumb-bell local grinding if needed + (second chemical treatment + inspection)

Fabrication SNS/JLab

Fabrication SNS/JLab

SNS/JLab

Fabrication (JLab)

Endgroups



Cavity


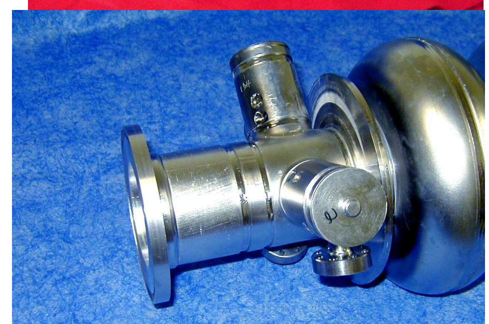
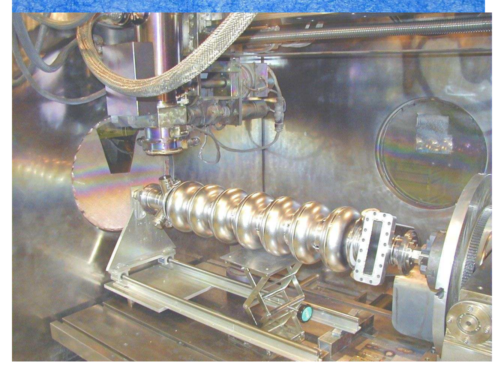

Electron Beam Welding (JLab)

Dumbbells

Tack- Welding:	4 tacks, focused beam
Voltage :	50 kV
Current:	15 mA
Rotational Speed :	20 inches/min
Distance of gun to work : 6 "	
Final weld Current:	33 mA
Rotational speed:	18"/min
Focussing:	elliptical pattern

Stiffening Rings

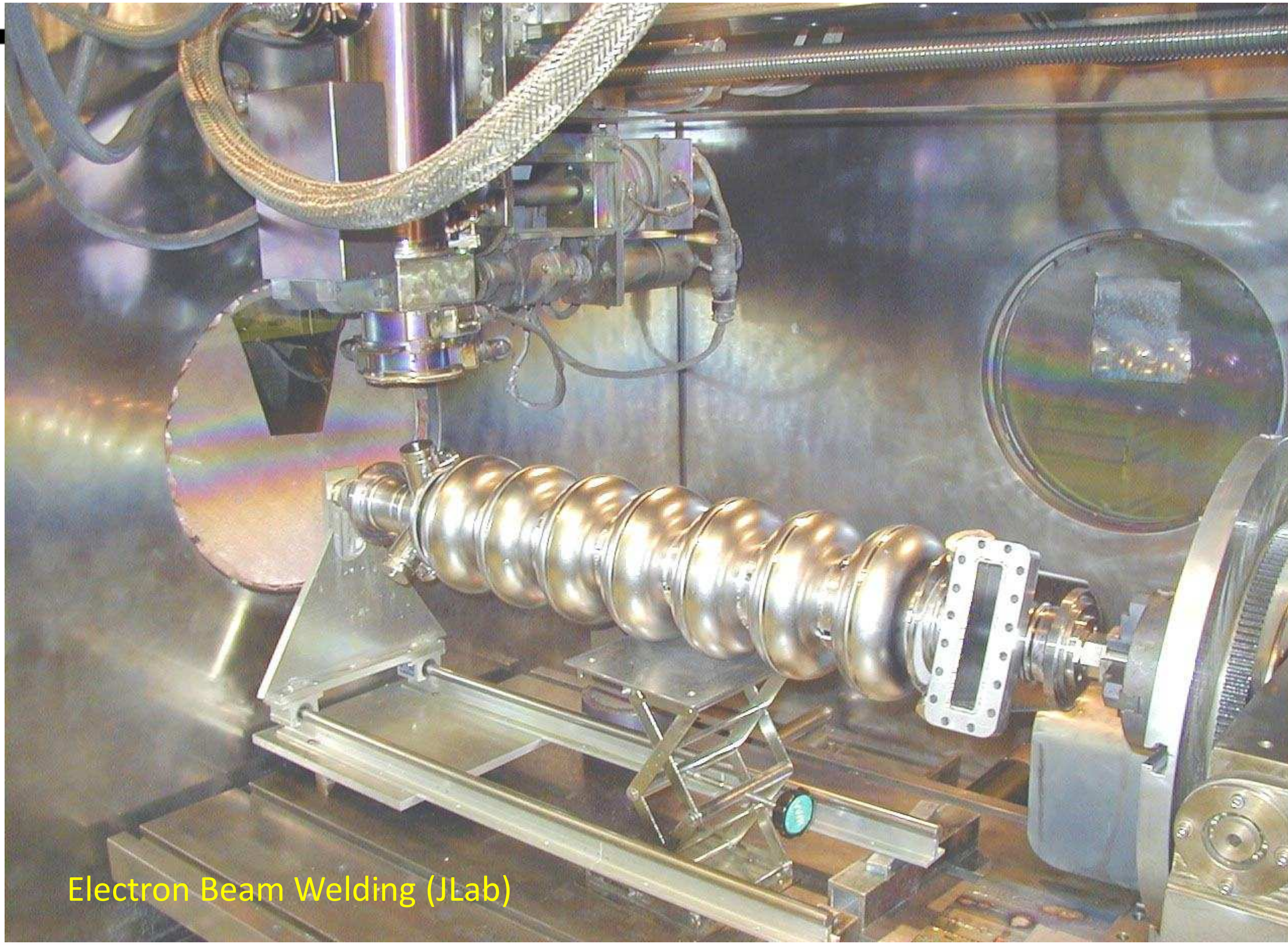
Electron Beam Welding (JLab)

Tuning

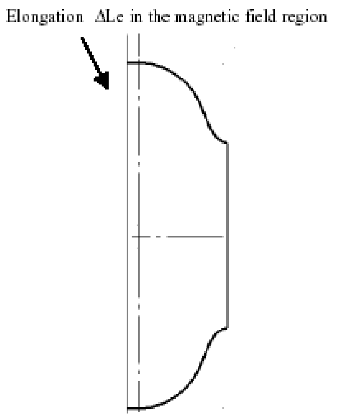

Figure 3: Trimming of the equator to adjust the elongation at the equator

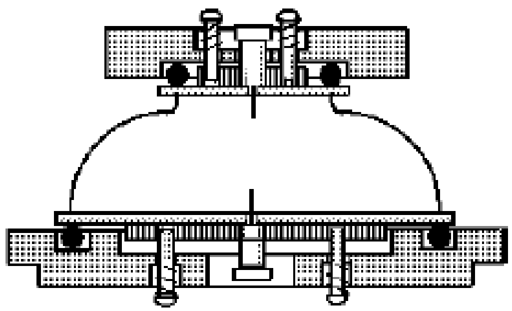

Computerized tuning machine at DESY

- Equalizing stored energy in each cell by squeezing or pulling
- Straightening of cavity

Field flatness after pre-tuning

- •mode frequency 1298.774 MHz

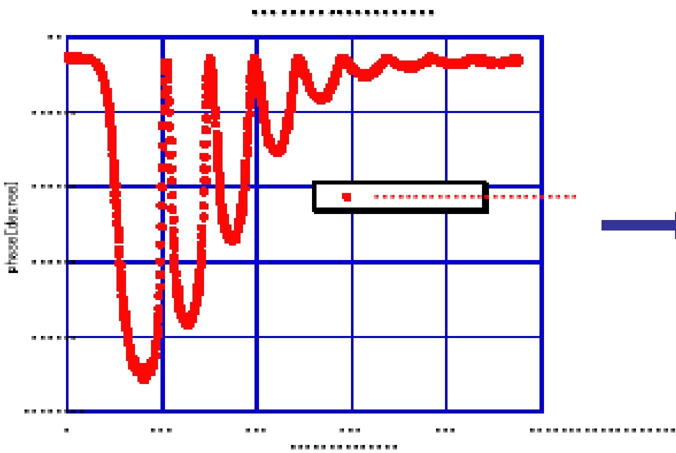

Field flatness = 0.1 %
(as delivered to KEK)

- •mode frequency 1298.547 MHz

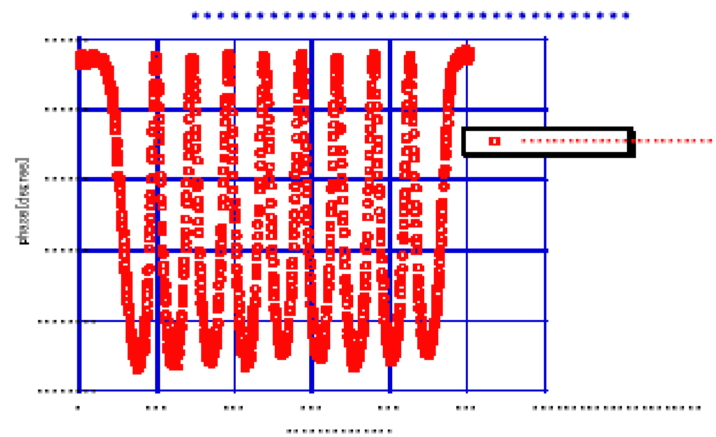

Field flatness = 98 %
(after pre-tuning)

Cavity	Field flatness (min/max) as delivered / after pre-tuning	Freq. target 1298.141 (MHz) @R.T. as delivered / after pre-tuning
1st	0.1% / 98%	1298.774 / 1298.547
2nd	57.6% / Not yet	1301.447 / Not yet
3rd	31.5% / Not yet	1301.577 / Not yet
4th	51.5% / Not yet	1301.696 / Not yet

Cell-to-cell coupling is as small as 1.6%, but no problem in pre-tuning.

Alternative Fabrication
Seamless Cavity

- Hydro forming (W.Singer,DESY) Spinning (V.Palmieri,INFN Legnaro)

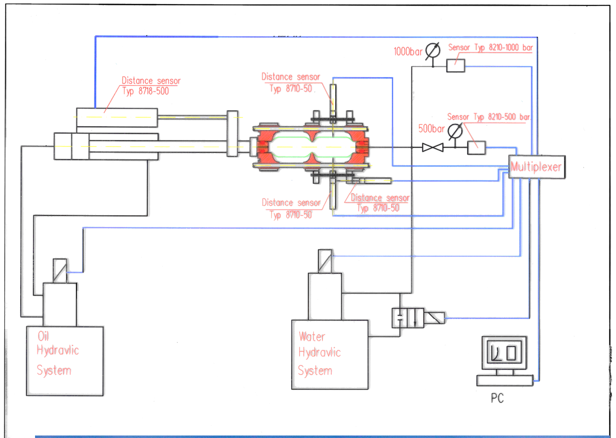

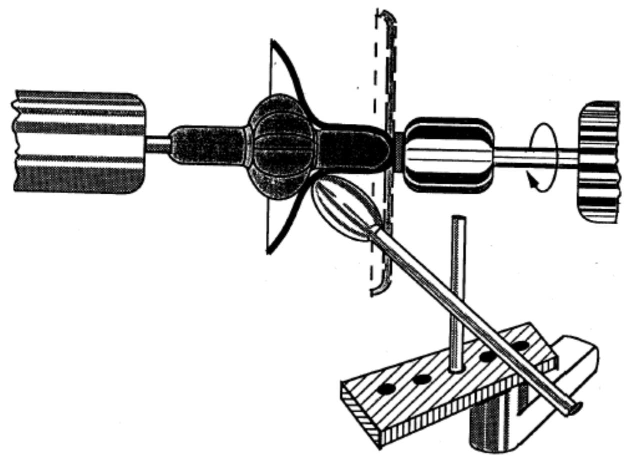

Alternative Fabrication

Nb Thin Film Coated Copper Cavity

US-CERN-JAPAN-RUSSIA Accelerator School, Nov. 6-14, 2002, Long Beach, California, USA

Niobium Film Coated Cavities

Developed in CERN for LEP II Superconducting RF cavities

f=350 MHz ⟶ big cavity (diameter :780mm) ⟶ Reduce Nb material for cost down

Copper half cell for LEP-II SC cavity

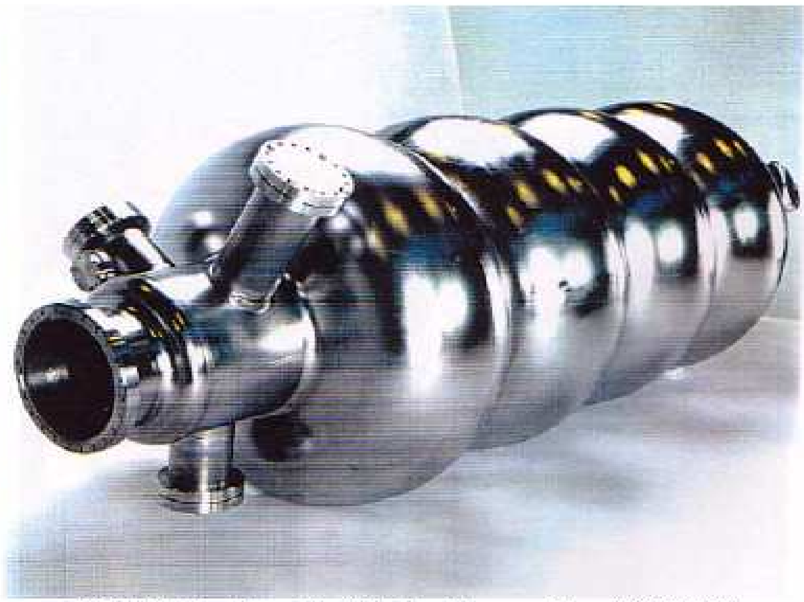

350MHz 4-cell Nb bulk cavity (CERN)

Fabrication of Low Beta Cavities

- Bulk Nb (by far the most used)
  - highest performance, many manufacturers, any shape and *f*
    - *performance* **** *cost* **

- Sputtered Nb on Cu (only on QWRs)
  - high performance, lower cost than bulk Nb in large production, simple shapes
    - *performance* *** *cost* ***

- Plated Pb on Cu (being abandoned)
  - lower performance, lowest cost, affordable also in a small laboratory
    - *performance* ** *cost* ****

Large-Grain Ingot Niobium

Large grain Ingot “D” from CBMM

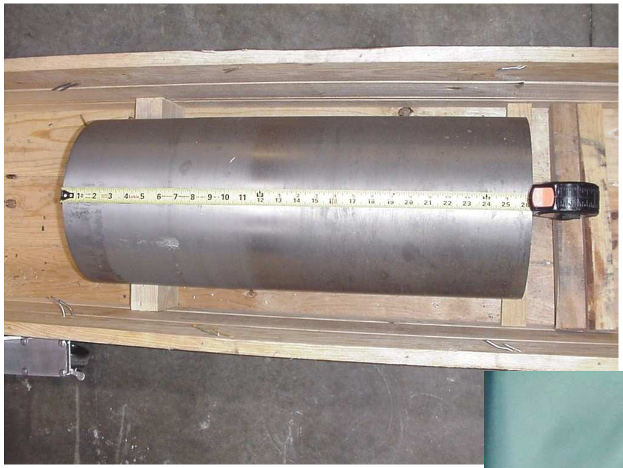

Impurity Doping of Bulk Nb Cavity

- Surface diffusion of some foreign atomic species (N, Ti etc) into Nb at high temperature results in large increase of Q0.
- 800°C vacuum for 3 hours is used to degas dissolved H from the niobium bulk.
- ~20 mTorr nitrogen gas @ 800°C for a few minutes.
- Lossy nitrides on the surface are removed by light > 2 μm electropolish.
- Resulting rf surface resistance decreases with field to unprecedented low levels (< 10 nOhm @ 2.0K, 1.3 – 1.5 GHz)= **high Q_0**

Nitrogen doping

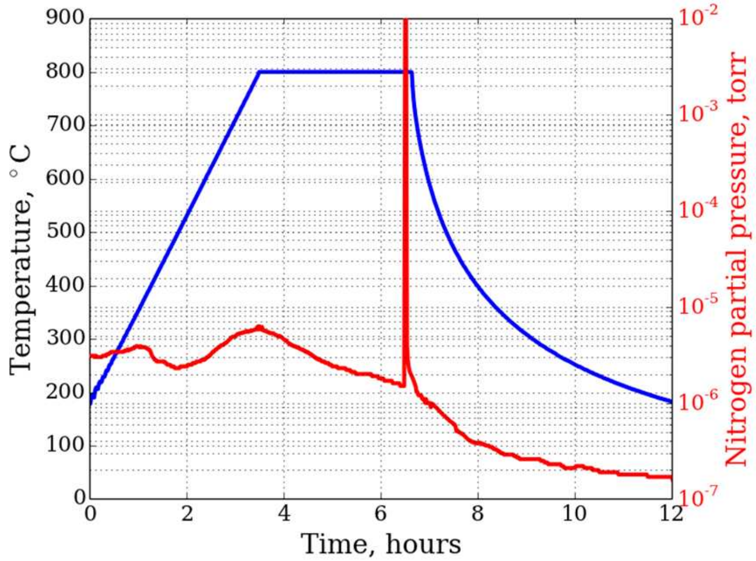

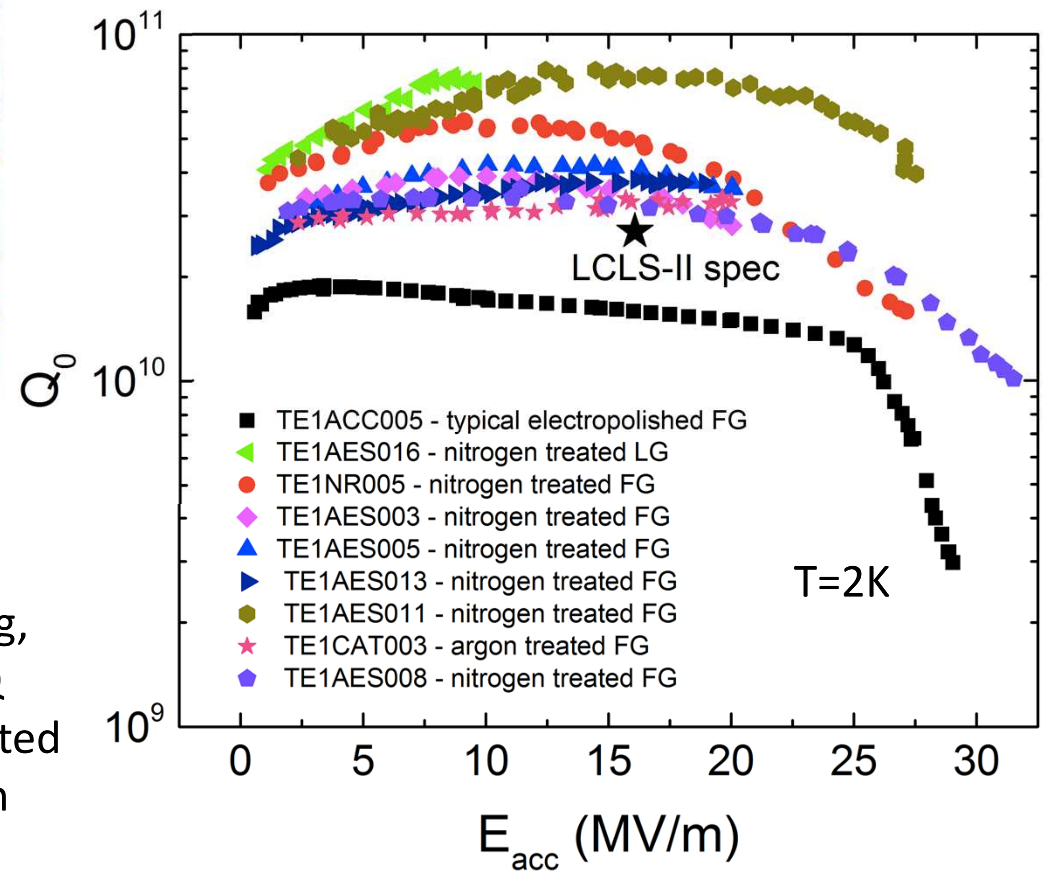

- Injection of small nitrogen partial pressure at the end of 800C degassing, followed by EP-> drastic increase in Q
- At present more than 40 cavities treated
- R&D program ongoing for LCLS-II with the goal of validating Q=2.7e10@2K, 16MV/m

A. Grassellino et al, 2013 Supercond. Sci. Technol. **26** 102001 (Rapid Communication) – selected for highlights of 2013

Surface Processing

Removal of "Damaged Layer"

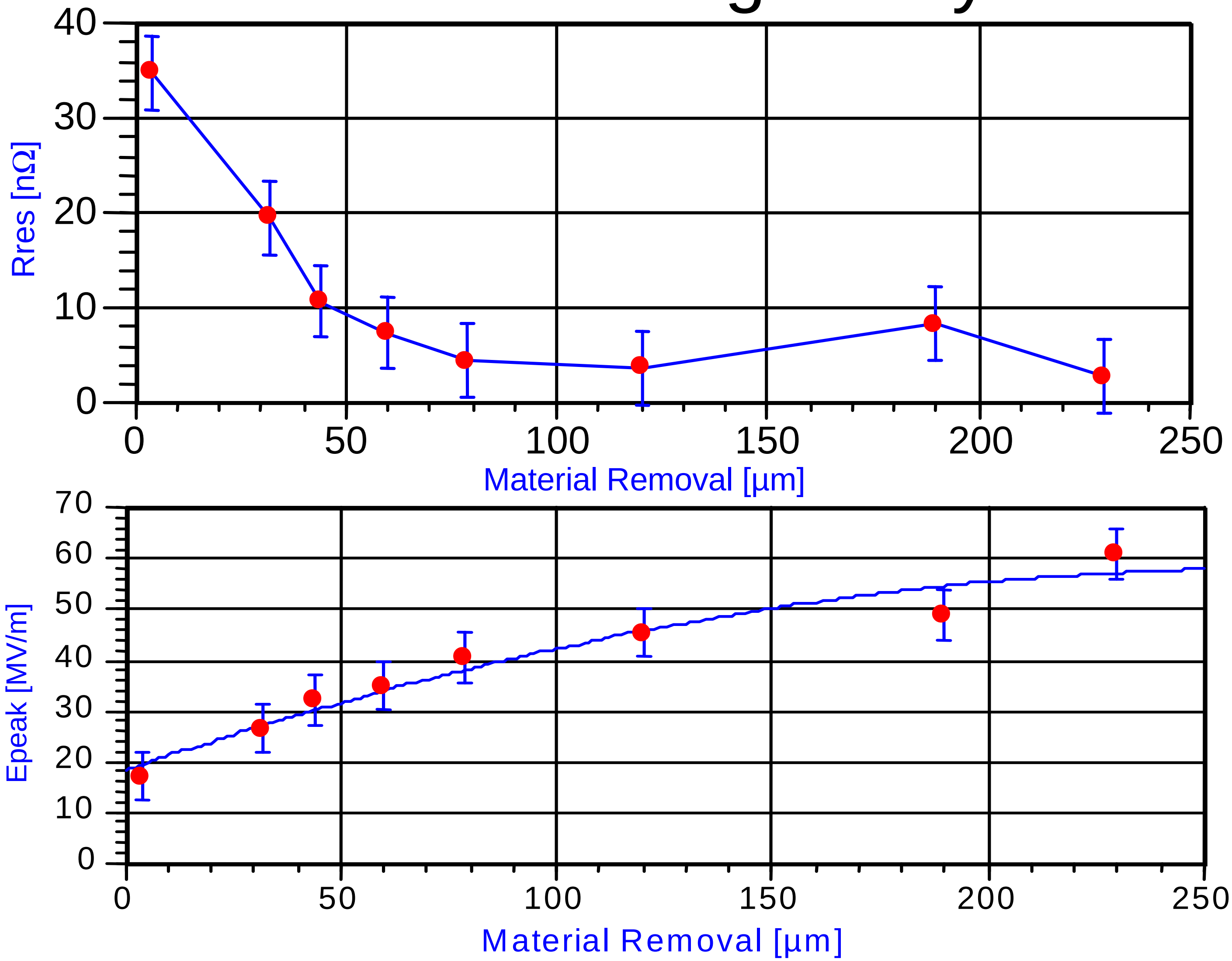

Cavity RF Surface

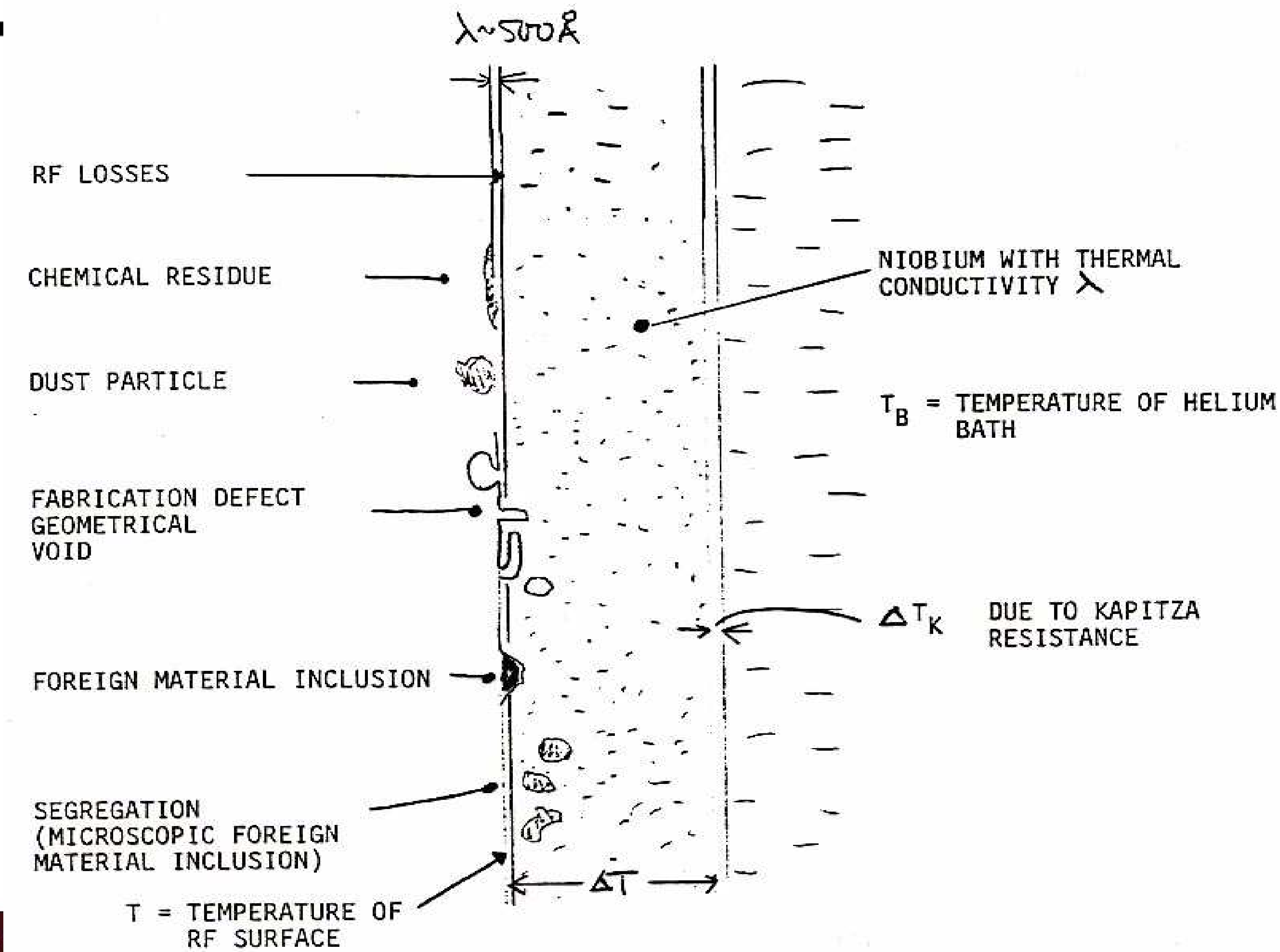

Buffered Chemical Polishing (BCP) Electropolishing (EP)

> **Chemical etching (BCP)** or **electro polishing (EP)**

	BCP	EP
	$HF : HNO_3 : H_3PO_4$	$HF : H_2SO_4$
volume ratio:	1 : 1 : 2	1 : 9
removal rate:	app. 1 µm/min	app. 0.4 µm/min

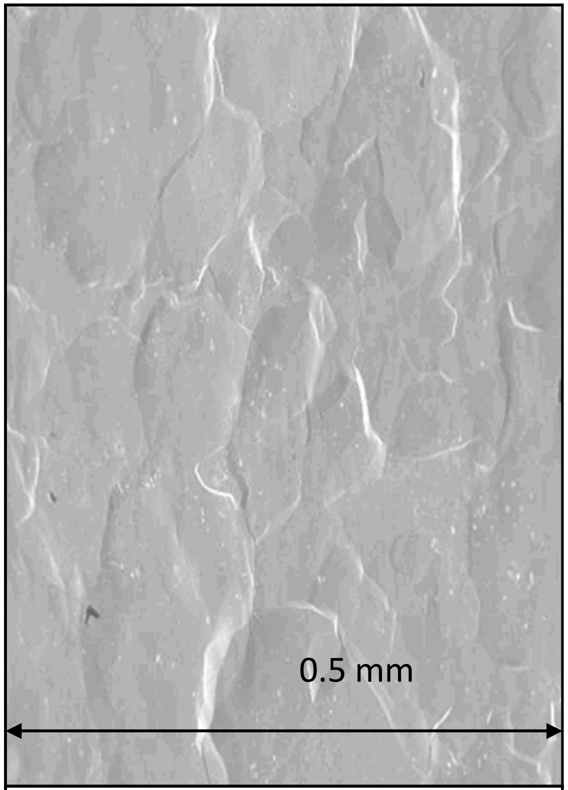

BCP Surface
(1µm roughness)

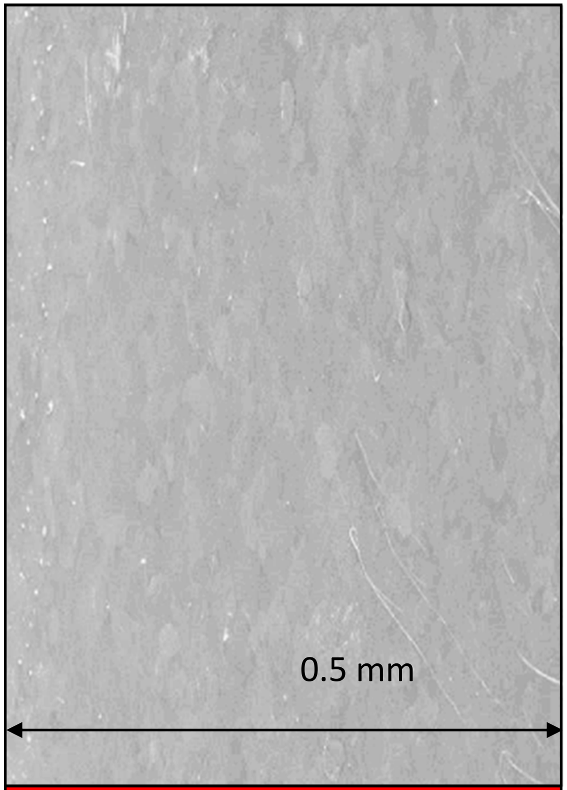

EP Surface
(0.1µm roughness)

BCP and EP System

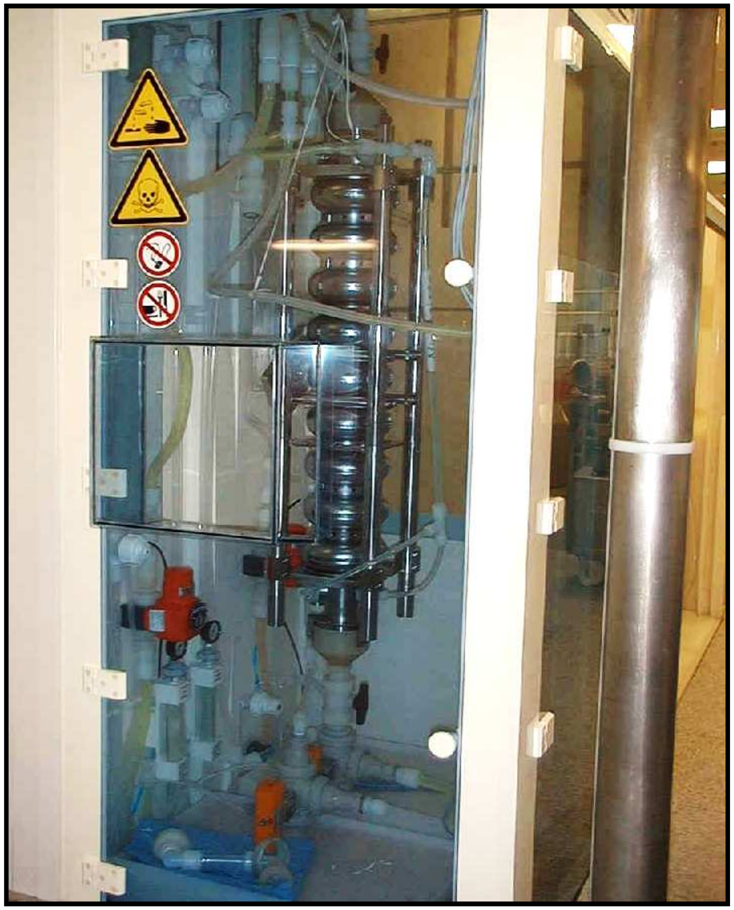

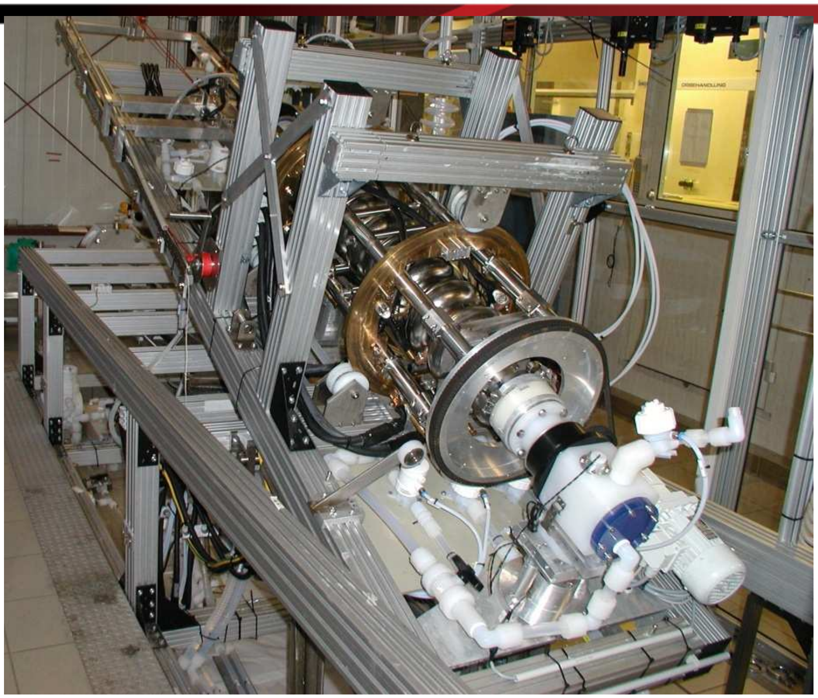

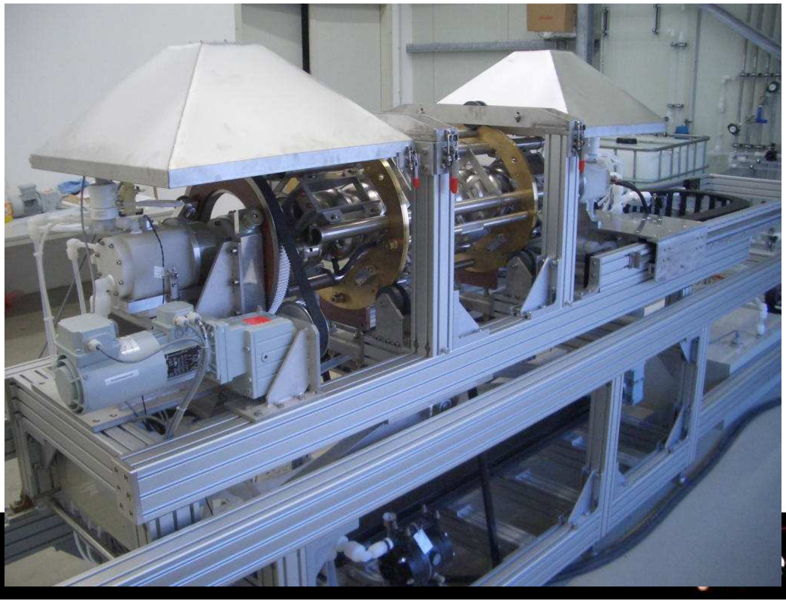

DESY BCP + EP,
Henkel Lohnpoliertechnik EP

High Pressure Rinse Systems

DESY-System

Jlab HPR Cabinet

KEK-System

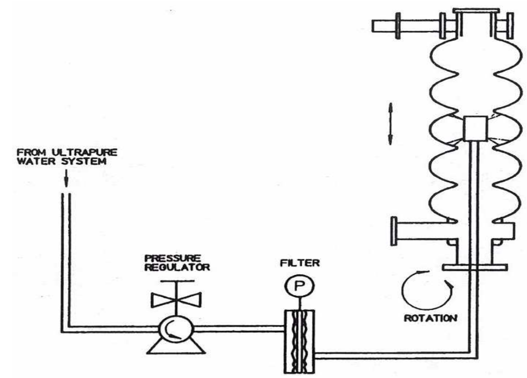

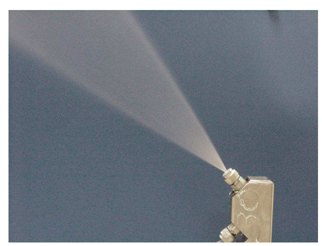

Clean Room Technology

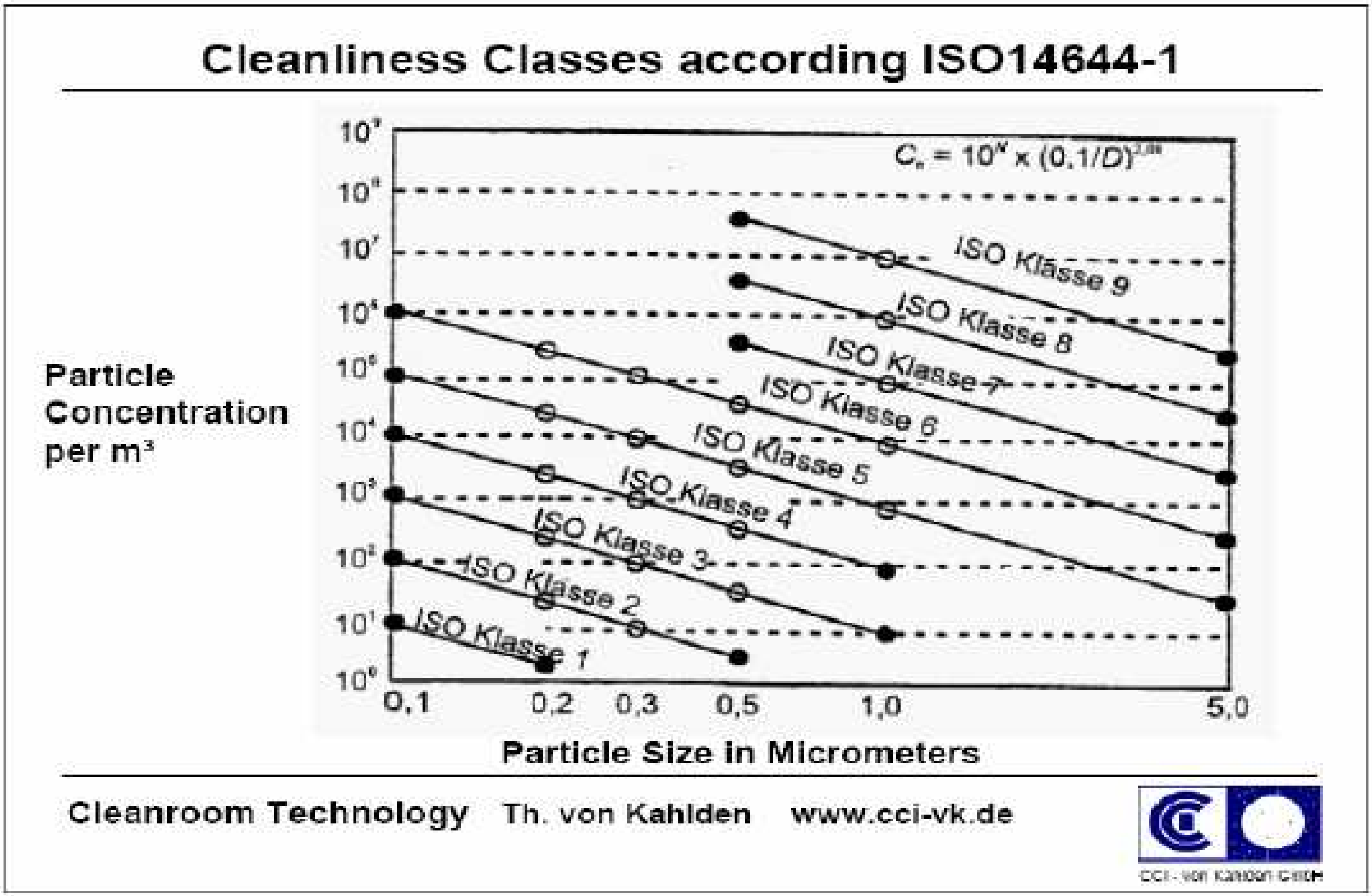

Clean Room: DESY

SRF Linac: CEBAF

SOUTH LINAC CRYOMODULES

SRF Linac: SNS

SRF Linac: ISAC-II

Figure 5: The ISAC-II superconducting linac.

Summary

- Steady progress has been made over the past decades in SRF science and technology
- SRF has become an enabling technology
- Still many exciting opportunities for future SRF technology
- Must advance understanding
- Innovation and creativity essential for continued success